OXYGEN AND CARBON ISOTOPES AND CORAL GROWTH IN THE GULF OF MEXICO AND CARIBBEAN SEA AS ENVIRONMENTAL AND CLIMATE INDICATORS

A Dissertation

by

AMY JO WAGNER

Submitted to the Office of Graduate Studies of
Texas A&M University
in partial fulfillment of the requirements for the degree of

DOCTOR OF PHILOSOPHY

December 2009

Major Subject: Oceanography

OXYGEN AND CARBON ISOTOPES AND CORAL GROWTH IN THE GULF OF MEXICO AND CARIBBEAN SEA AS ENVIRONMENTAL AND CLIMATE INDICATORS

A Dissertation

by

AMY JO WAGNER

Submitted to the Office of Graduate Studies of
Texas A&M University
in partial fulfillment of the requirements for the degree of

DOCTOR OF PHILOSOPHY

Approved by:

Chair of Committee,	Niall C. Slowey
Committee Members,	Benjamin Giese
	Ethan Grossman
	Thomas P. Guilderson
	Deborah J. Thomas
Head of Department,	Piers Chapman

December 2009

Major Subject: Oceanography

ABSTRACT

Oxygen and Carbon Isotopes and Coral Growth in the Gulf of Mexico and Caribbean Sea as Environmental and Climate Indicators. (December 2009)
Amy Jo Wagner, B.S., Texas A&M University at Galveston;
M.S., Texas A&M University
Chair of Advisory Committee: Dr. Niall C. Slowey

The Gulf of Mexico and Caribbean Sea comprise a sensitive and important region, both oceanographically and climatically. A better understanding of the history of climate and marine environmental conditions in this region provides valuable insight into the processes that affect climate globally. This dissertation furthers our understanding of these factors via investigations of the isotopes of corals and seawater, as well as coral growth. Results improve our understanding of how the isotope and coral growth records from the Gulf of Mexico and Caribbean Sea reflect recent environmental conditions, enhancing our ability to reconstruct the history of climate in this important region.

Analysis of the relationship between salinity and oxygen isotopic composition of seawater from the Texas/Louisiana continental shelf and Flower Garden Banks yield improved understanding of the relative contribution of the fresh water sources into the northern Gulf of Mexico, and also the oxygen isotopic composition of open-ocean seawater in this region.

Variations in the growth of long-lived coral cores from the Flower Garden Banks are compared to local and regional climate conditions, particularly winter air temperatures. During the latter half of the twentieth century, a close correlation has existed between slow coral growth and cold wintertime air temperatures along the Gulf Coast, which are due to a meridional orientation of the North American jet stream

(associated with the Pacific/North American climate pattern). Existing long coral growth records are too limited to assess this relationship during earlier years.

Knowledge of the marine radiocarbon (^{14}C) reservoir age is important for understanding carbon cycling and calibrating the radiocarbon ages of marine samples. Radiocarbon concentrations in corals from the Flower Garden Banks, Veracruz, and the Cariaco Basin are measured and used to determine the surface ocean ^{14}C reservoir ages for the Gulf of Mexico and Caribbean Sea. Results also indicate that the post-nuclear weapons testing $\Delta^{14}C$ values of the Gulf of Mexico and Caribbean Sea differ. This difference is attributed to the advection of ^{14}C-depleted surface water from the Southern Hemisphere into the Caribbean Sea.

The results reported in this dissertation provide valuable information for understanding the marine environment when using carbonate proxies to study and reconstruct past climate and marine conditions in the Gulf of Mexico and Caribbean.

DEDICATION

To my parents, Bob and Ruth Ann Wagner

ACKNOWLEDGEMENTS

I thank my committee chair, Dr. Slowey, and my committee members, Dr. Giese, Dr. Thomas, Dr. Grossman, and Dr. Guilderson for their patience, guidance and support throughout the course of this research.

I would like to extend my gratitude to the Department of Energy Global Change Education Program (GCEP) Graduate Research Environmental Fellowship (GREF) for funding my graduate work and the Texas Sea Grant for providing the funding for this research.

Much thanks goes to the crew of the M/V Fling; the Flower Garden Banks National Marine Sanctuary (FGBNMS) staff, E. Hickerson, G.P. Schmal, L. Kurjelja; the Florida Keys National Marine Sanctuary staff, J. Halas, B. Causey, A. Massey; U.S. Geological Survey staff, D. Hichey, C. Reicht; and S. Gittings, and S. Francis for all their help in making a successful coral drilling cruise. I would also like to extend thanks to those who collected water samples for me, E. Hickerson, D. Weaver, K. Deslarzes, S. Meyer-Franco, R. Long, and S. DiMarco.

I would also like to thank C. Schmit and R. Mortlock for performing salinity and oxygen isotope analyses.

Thanks goes out to my friends and colleagues from the Oceanography Department for making my time at Texas A&M University a great experience.

Finally, thanks to my family for their encouragement and never ending support. And thank you to Michael for being so patient and understanding. You have been my rock and I couldn't have done this without you.

TABLE OF CONTENTS

LIST OF FIGURES

FIGURE Page

LIST OF TABLES

CHAPTER I

INTRODUCTION

Understanding natural climate variability over the last several centuries, particularly annual to decadal variability, has become an important issue in the study of paleoclimate [e.g., *Crowley*, 2000]. To better characterize climate variability on these short time scales, high-resolution climate records are needed. Complicating the record of natural climate variability in the recent past (since the mid-1800s) is the addition of human-induced climate variability. To help disentangle the natural and anthropogenic variability, a high-resolution perspective that spans the time period from pre-industrial to today is needed. The data available from the modern instrumental record does not extend back far enough in time to do this, so one must turn to proxy records of climate. It is important to understand recent environmental conditions and how faithfully the proxies record these conditions in order to use them to reconstruct past climate. In this study, I will use isotope analyses of corals and seawater in conjunction with measurements of coral growth to better understand the marine environment and characterize natural climate variability in the Gulf of Mexico and Caribbean Sea.

The Gulf of Mexico and Caribbean Sea together form a marine environment that is an important region both oceanographically and climatically and is sometimes referred to as the "American Mediterranean". The Gulf of Mexico is the ninth largest body of water in the world and has a surface area of approximately 1,500,000 square kilometers. Over 20% of the gulf's area is underlain by the continental shelf (< 200 m water depth) [e.g., *Gore*, 1992]. One of the strongest ocean currents known, the warm Gulf Stream current, originates in the Gulf of Mexico as the Loop Current [see reviews by *Darnell and Defenbaugh*, 1990, and *Gore* 1992]. River drainage into the Gulf of Mexico is also quite extensive, with the Mississippi River contributing nearly 65% of the fresh water entering the gulf [*Moody*, 1967]. Surface waters enter the Gulf of Mexico from the

---

This dissertation follows the style of *Paleoceanography*.

Caribbean Sea to the south. The Caribbean gets water from both the northern and southern hemispheres and is one of the largest salt-water seas in the world with an area over 2,500,000 km^2 [*Darnell and Defenbaugh*, 1990; *Gore* 1992]. The low-latitude location of this region is conducive to a mild climate and warm sea surface temperatures.

Both oceanic and atmospheric circulation influence the climate of the Gulf of Mexico and Caribbean Sea, particularly the northern continental shelf along the Texas and Louisiana coasts. During the winter, shifts in the orientation of the strong American Jet Stream associated with the atmospheric Pacific/North American pattern can cause the milder, sub-tropical climate to be replaced by cold, Arctic air. In the summertime, southwesterly (upcoast) winds and currents replace the normal easterly (downcoast) flow, affecting the environmental conditions of the continental shelf.

Reef-building corals have proven to be very sensitive monitors of environmental conditions and potentially preserve a record of past climate. Analysis of the growth records and chemical composition of coral skeletal material has been shown to be a powerful approach to understanding climate prior to the instrumental record [e.g., *Dodge and Thomson*, 1974; *Buddemeier et al*., 1974; *Hudson et al*., 1976]. Coral skeletal material can preserve detailed records of past climate because they grow at a rate fast enough to provide a continuous, high-resolution record up to several centuries long, extending well beyond the availability of instrumental records. The coral reefs and banks in the Gulf of Mexico and Caribbean Sea may therefore provide valuable information about the past climate and environmental conditions in this region, but, the isotope geochemistry of the corals and seawater in which they grow needs to be better understood to take full advantage of corals as a proxy for past climate.

This dissertation is motivated by the need to characterize natural climate variability experienced in the Gulf of Mexico and Caribbean Sea over the past few centuries. It employs coral growth and isotope geochemistry to better understand climate in this important region during this time period. Several specific research questions will be addressed using various methods in the following chapters:

1. Using salinity and stable oxygen isotope values, can the relative contributions of the freshwater sources to the northern Gulf of Mexico be identified and determined? What is the open-ocean end member oxygen isotope value in the northern Gulf of Mexico?
2. Can a decadal pattern in coral growth rates of long-lived hermatypic corals collected at the Flower Garden Banks be identified? If so, is the pattern related to changes in local and regional climate? Does a relationship exist between changes in coral growth and broader atmospheric patterns such as the Pacific/North American pattern?
3. What is the reservoir age of surface ocean water in the Gulf of Mexico and Caribbean Sea based on coral radiocarbon measurements?
4. How does oceanic radiocarbon measured in coral skeletons differ between Gulf of Mexico and Caribbean sites? What are the possible mechanisms for these differences?

This document is organized to guide the reader through chapters based on the type of samples collected and the methods used to produce the data needed to answer the research questions outlined above. Chapter II provides detailed background information about the geographic setting of the sampling sites. The third chapter begins the discussion of the research completed during this study, exploring the relationship between salinity and oxygen isotope values in the north-central Gulf of Mexico and addressing research question #1. Chapter IV presents an analysis of the coral extension rates derived from newly collected coral cores from the Flower Garden Banks National Marine Sanctuary and considers question #2. Chapter V, the final research chapter, addresses questions #3 and #4 by presenting results of radiocarbon analyses in corals from the Gulf of Mexico and Caribbean Sea. The final chapter summarizes the results of this dissertation research and discusses how these results can support future studies of climate variability.

CHAPTER II

BACKGROUND AND SETTING

The region of focus in this study is the Gulf of Mexico and Caribbean Sea (Figure 2-1). While similar in some respects, each basin has its own unique oceanographic and atmospheric conditions. These similarities and differences will be discussed in the following sections. Samples of hermatypic, reef-building corals and water have been collected and analyzed for this study. The specific regions of coral collection are the Flower Garden Banks National Marine Sanctuary (FGBNMS), Veracruz, Mexico and the Cariaco Basin, off the coast of Venezuela. Water samples were collected at the FGBNMS and along the Texas/Louisiana continental shelf. The samples and specific sampling sites will be described in detail here. The reader will be referred back to this chapter on several occasions throughout the remainder of the text.

GULF OF MEXICO AND CARIBBEAN SEA

Stretching from Alabama down to the southern tip of Texas, the continental shelf in the northern Gulf of Mexico is generally broad with a gentle slope. West of the Mississippi Delta, the shelf broadens to nearly 200 km [*Boicourt et al*., 1998]. East of the Mississippi Delta to the Texas-Louisiana border, the shelf narrows to approximately 75 km wide. The winds over the Northern Gulf of Mexico shelf are greatly affected by the position and strength of the Bermuda high, particularly during the boreal summer months. During the spring and summer, the winds are predominantly out of the southeast and become more southerly along the south Texas shelf. Theses winds strongly favor seasonal upwelling along the northern Gulf of Mexico shelf [*Cochrane and Kelly*, 1986]. During the fall and winter, the shelf is regularly affected by strong cold air outbreaks from the north. Depending on the strength and duration, the entire shelf can be vertically mixed by these cold air outbreaks [*Nowlin and Parker*, 1974]. Except for the summer months, the mean nearshore flow is downcoast over most of the northern Gulf. Southerly winds that drive upwelling along the south Texas shelf in the

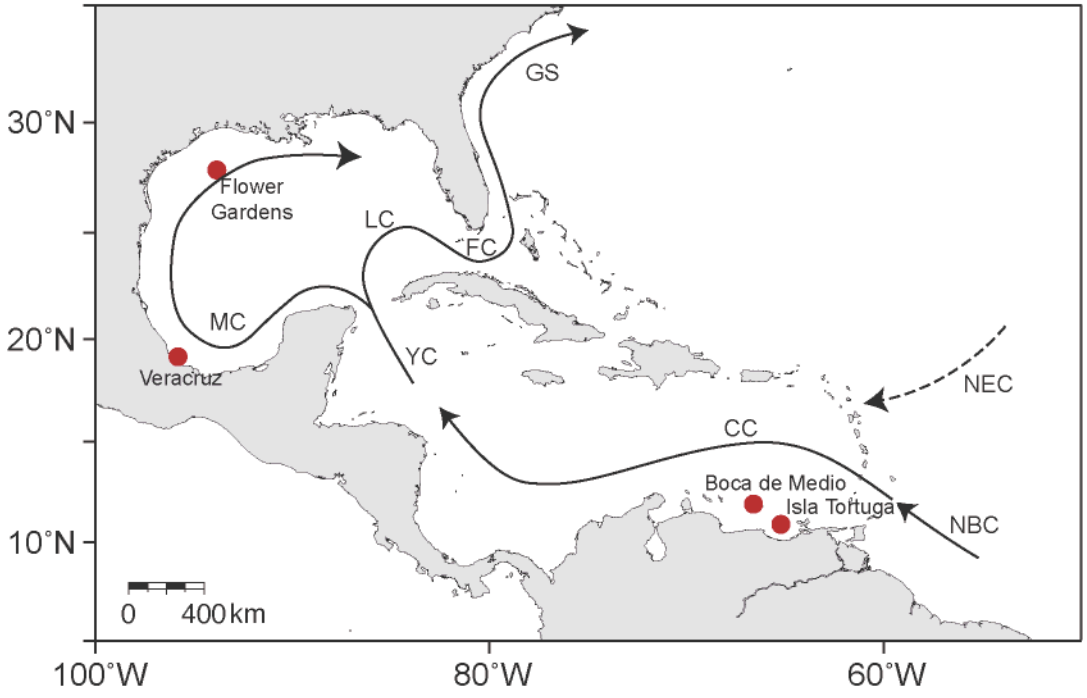

Figure 2-1. Map of the Caribbean Sea and Gulf of Mexico. Red dots indicate sites where coral samples were obtained. Black arrows represent surface currents. NBC – North Brazil Current; NEC – North Equatorial Current; CC – Caribbean Current; YC – Yucatan Current; MC – Mexican Current; LC – Loop Current; FC – Florida Current; GS – Gulf Stream. Seawater samples were collected on the continental shelf north of the Flower Garden Banks.

spring and summer force the flow back upcoast. This upcoast flow is observed all the way up to the Mississippi Delta [*Cochrane and Kelly*, 1986].

Surface circulation, coastal upwelling, and precipitation patterns that influence the southern Caribbean Sea are altered by the seasonal migration of the Intertropical Convergence Zone (ITCZ). Between January and March the ITCZ is south of the equator. Strong trade winds in the tropical north Atlantic cause a slow Ekman drift to the west and northwest, which helps to maintain the northwestward flow of the North Brazil and Guyana Currents toward the Caribbean. Trade winds blowing along the northern coast of Venezuela result in Ekman drift-induced upwelling [*Astor, et al.*, 2003; *Muller-Karger and Castro*, 1994; *Richards*, 1975]. In early summer (June/July), the ITCZ moves north to a position nearly over the Venezuelan coast. Trade winds die down, upwelling weakens, sea surface temperatures increase, and productivity falls [*Muller-Karger and Castro*, 1994].

SURFACE CURRENTS

The main surface currents in the Gulf of Mexico and Caribbean Sea are the Caribbean Current, Yucatan Current, Loop Current and the Florida Current [*Centurioni and Niiler*, 2003] (Figure 2-1). The surface circulation of the Caribbean Sea is dominated by the general east to west flow of the Caribbean Current which carries equatorial Atlantic water into the Gulf of Mexico and then to the north Atlantic as part of the meridional overturning circulation [*Fratantoni*, 2001].

Water flows into the Caribbean Sea in the southeast and flows westward as the Caribbean Current. Surface current velocities, as high as 70 cm s^{-1}, are highest along the coast of Venezuela and the Netherland Antilles [*Fratantoni*, 2001]. The Caribbean Current flows turns northwest past the Colombian Basin (80° W, 12° N) and is channeled through a trough southwest of Jamaica and then through the Yucatan Channel as the Yucatan Current [*Fratantoni*, 2001]. Water entering the Caribbean originates from both the North and South Atlantic Oceans [*Wilson and Johns*, 1997].

Once in the Gulf of Mexico, the Yucatan Current initially follows the continental shelf break from 21° N to 24.5° N and then changes direction to a northwesterly direction around 23.5° N, 87° W [*Molinari and Cochrane*, 1972]. There is a clockwise flow that extends northward into the Gulf of Mexico and joins the Yucatan Current and the Florida Current, which is known as the Loop Current. The position of the Loop Current is variable and can intrude into the Gulf of Mexico as an intense clockwise flow as far north as 29.1° N or it can flow in an almost direct path to the Florida Current [*Molinari et al.*, 1977; *Sturges and Evans*, 1983]. The Yucatan and Florida currents have been shown to be within 10% of each other's volume at any given time [*Molinari and Morrison*, 1988]. Therefore, variability in the Loop and Yucatan currents are expected to have a strong impact on the Florida Current. In addition to the Loop Current, *Sturges and Blaha* [1976] have suggested a western boundary current, the Mexican Current, in the far western Gulf of Mexico that stems from the Yucatan Current as it enters the Gulf of Mexico.

The primary surface current in the Gulf of Mexico is the Loop Current that brings warm waters from the Caribbean Sea through the Yucatan Strait into the Gulf of Mexico that hugs the North American coastline along Mexico and the United States. The water flows in a clock-wise direction and exits the gulf through the Florida Straits into the North Atlantic Ocean. During boreal winter, warm tropical waters from the Caribbean generally do not penetrate into the western and northern Gulf of Mexico; instead, they are typically limited to a narrow band in the southeastern Gulf of Mexico and reflected directly from the Yucatan Strait to the Florida Strait [*Poore et al.*, 2004]. During boreal summer, the northward migration of the ITCZ causes increased surface flow from the Caribbean Sea through the Yucatan Strait. The Loop Current penetrates deep into the Gulf of Mexico before exiting through the Florida Strait. As the Gulf Stream exits the Gulf of Mexico and moves north as the North Atlantic Western Boundary Current, it mixes horizontally but not vertically. Therefore, there is ample time for the surface water to equilibrate with the atmosphere. Considering the rate (24-30 Sv) at which the surface water is entering the Gulf of Mexico through the Yucatan

Channel and leaving through the Florida Straits, the residence time within the mixed layer is relatively short (on the order of two to three months).

ATMOSPHERIC CIRCULATION PATTERNS

One of the most prominent modes of interdecadal extratropical variability in the Northern Hemisphere is the Pacific/North American (PNA) pattern. The PNA pattern is most pronounced during the winter months and is characterized by synchronous changes in the strength of the high and low pressure centers over the North Pacific and North America [*Wallace and Gutzler,* 1981]. There are two distinct phases of the PNA pattern. The positive phase is dominated by more meridional (north/south) airflow associated with the jet stream due to an expanded ridge over western North America and deepened upper level troughs over the Aleutians and southeastern United States. During the positive phase, cold, dry Canadian air is brought down to the southern mid-continent and southeast portions of the US. This portion of the US experiences colder, wetter winters while the northwest US experiences warmer, drier winters and the eastern US experiences more frequent storms and more snowfall (Figure 2-2). A greater number of mid-latitude cyclones develop in the Gulf of Mexico during the positive phase of the PNA pattern as well [*Hardy and Henderson*, 2003]. During a negative phase of the PNA pattern, there is more zonal (east/west) airflow across the US and the south and southeast experiences warmer, drier winters while the northwest has cooler, wetter winters.

Winter climate in the southeast U.S. is intimately linked to the frequency and intensity of frontal passages across the region. The southern states typically experience relatively mild winters due to warm, moist air flowing in from the Gulf of Mexico. However, the minimum temperature can significantly drop due to the passage of cold fronts from the interior of North America. A strong correlation between below average minimum winter temperatures in New Orleans and the positive phase of the PNA pattern has been previously documented [*Erhardt,* 1990; *Leathers et al.,* 1991; *Slowey and Crowley,* 1995]. Since the southeast U.S. is very sensitive to changes in the phase of the PNA pattern, changes in the region's climate can be used to characterize the PNA

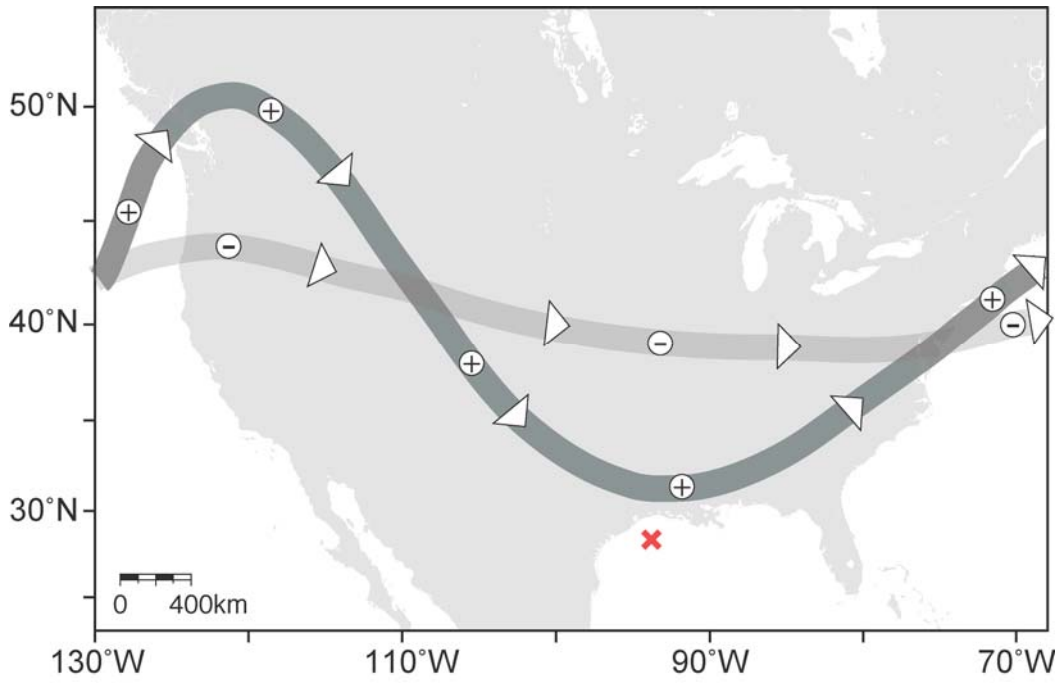

Figure 2-2. PNA schematic. Jet stream across the United States during the positive and negative phases of the PNA pattern. The red 'X' marks the location of the Flower Garden Banks National Marine Sanctuary.

[*Wallace and Gutzler,* 1981]. However, the atmospheric pressure measurements used to calculate the PNA index do not exist prior to the mid-1940s. To obtain a long-term record of the PNA pattern, we must therefore look to proxy indicators.

The Southern Oscillation Index (SOI) is one measure of air-pressure fluctuations between the western and eastern tropical Pacific [*Trenberth*, 1984; *Ropelewski and Jones*, 1987]. El Niño events occur during the negative phase of the SOI. Traditionally, the SOI has been calculated based on the differences in atmospheric pressure anomalies between Tahiti and Darwin, Australia. During a negative phase of the SOI, there is abnormally high atmospheric pressure over the western tropical Pacific (Darwin) and abnormally low air pressure over the eastern tropical Pacific (Tahiti). It has been suggested that a negative SOI (El Niño conditions) is correlated with a positive phase of the PNA pattern [*Niebauer*, 1988; *Vega et al*., 1998]. During an El Niño winter, the Gulf States experience wetter and colder than normal conditions and the region is more likely to have severe weather outbreaks.

The North Atlantic Oscillation (NAO) is associated with a substantial portion of Atlantic climate variability. The NAO index is based on sea level pressure differences between the Azores high and the Icelandic Low [*Barnston and Livezey*, 1987; *Hurrell*, 1995; *Hurrell et al*., 2003]. During the negative phase of the NAO, there is a weakening of the subtropical high and Icelandic Low, causing a decreased pressure gradient between the two pressure centers. The decreased pressure gradient produces weaker than average westerly winds across the mid-latitudes of the Atlantic Ocean, which results in colder winters in northern Europe, and warmer, wetter winters in the Mediterranean and the northwest Atlantic. The east coast of the United States typically experiences more cold air outbreaks and harsher winter conditions than usual during the negative phase of the NAO.

SAMPLE SITES

Situated approximately 180 km south of the Texas/Louisiana border at 27.9°N, 93.7°W, the Flower Garden Banks National Marine Sanctuary (FGBNMS) is the

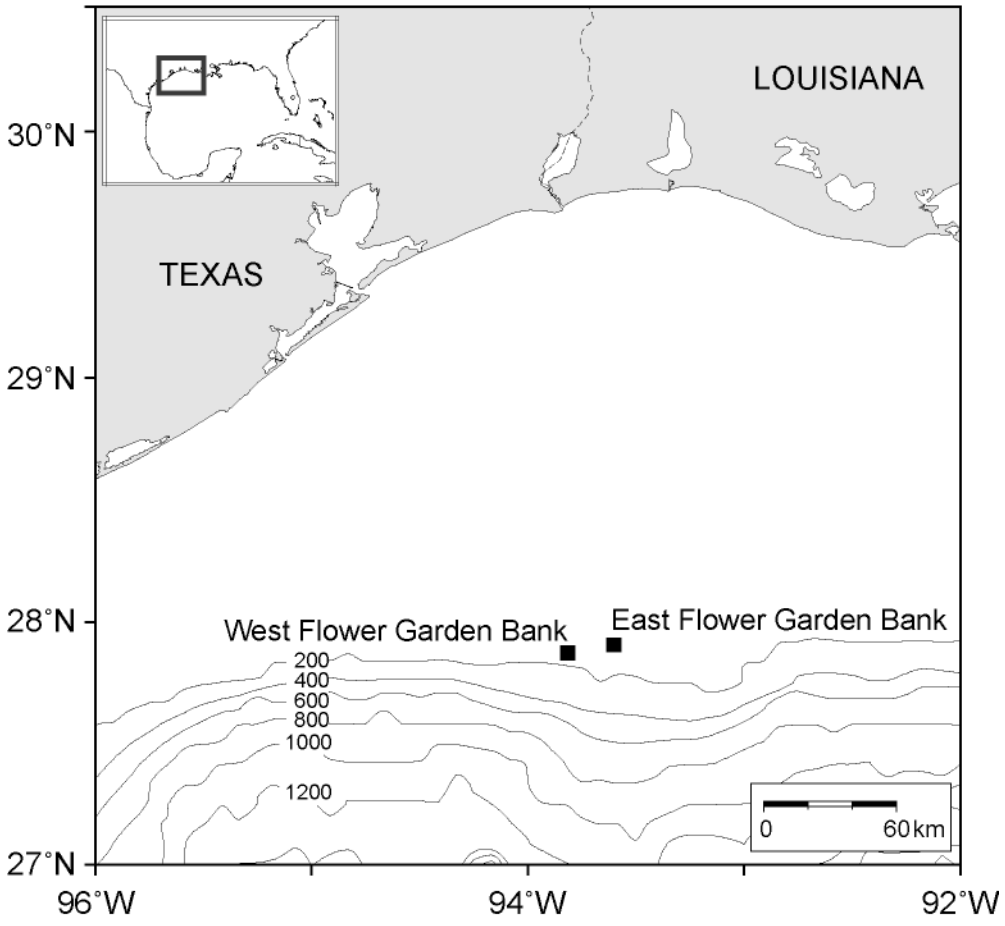

Figure 2-3. Map of the north-central Gulf of Mexico showing the location of the Flower Garden Banks.

northernmost hermatypic coral reef on the North American continental shelf (Figure 2-3). The Flower Garden Banks lie at the shelf edge, in the region of maximum continental shelf width, where water temperatures range seasonally from 18-30°C [*Hagman and Gittings,* 1992]. There are two distinct banks at the Flower Garden Banks, East Flower Garden Bank (EFG) and West Flower Garden Bank (WFG). The banks lie 17 - 49 m below the sea surface. The two banks are approximately 19 km apart and East Bank is slightly larger and shallower than West Bank (300 acres and 100 acres, respectively). Strong cold fronts can result in significant cooling of the waters at the Flower Garden Banks [*Nowlin and Parker*, 1974]. During the winter months, the mean surface current in this part of the Gulf of Mexico is in the southwesterly direction. In the summer months, a shift in winds causes the current to reverse direction and flow to the northeast [*Cochrane and Kelly*, 1986]. Coral cores from both banks were used in this study.

Veracruz, Mexico is located on the east coast of Mexico in the Bay of Campeche (southwestern Gulf of Mexico). There are approximately 25 named reefs in the Veracruz Reef System (VRS) in the southwestern Gulf of Mexico (Figure 2-4). The reefs in the VRS grow in a naturally turbid environment. During the summer rainy season, when several rivers that discharge near the reef system transport high concentrations of sediment, visibility can be less than one meter [*Horta-Puga*, 2003]. During the winter months, like at the Flower Garden Banks, the position of the mid-latitude jet stream over the North American continent can bring cold, polar air masses as far south as Veracruz, which decreases seawater temperature and increases turbidity. The VRS can be divided into two subgroups, the northern and southern groups. The northern group is located off the city of Veracruz and is nearer to the city's sewage treatment plant and the port docks [*Horta-Puga*, 2003]. The southern group of reefs is located off the fishing village of Anton Lizardo [*Tunnell*, 2007] and is the region from which the coral samples used in this study were collected (one coral core from Chopas Reef and one from Santiaguillo Reef were used).

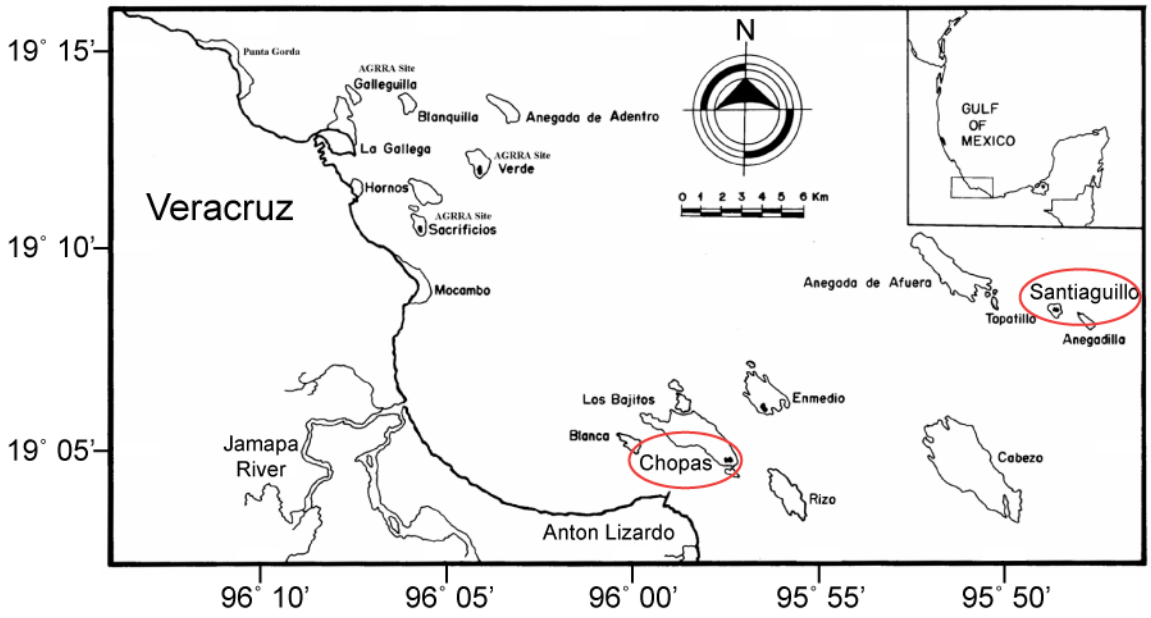

Figure 2-4. Map of the Veracruz Reef System (VRS) off the coast of Veracruz, Mexico. Figure from *Horta-Puga* [2003]. Red ovals show the locations of the reefs where coral cores were collected.

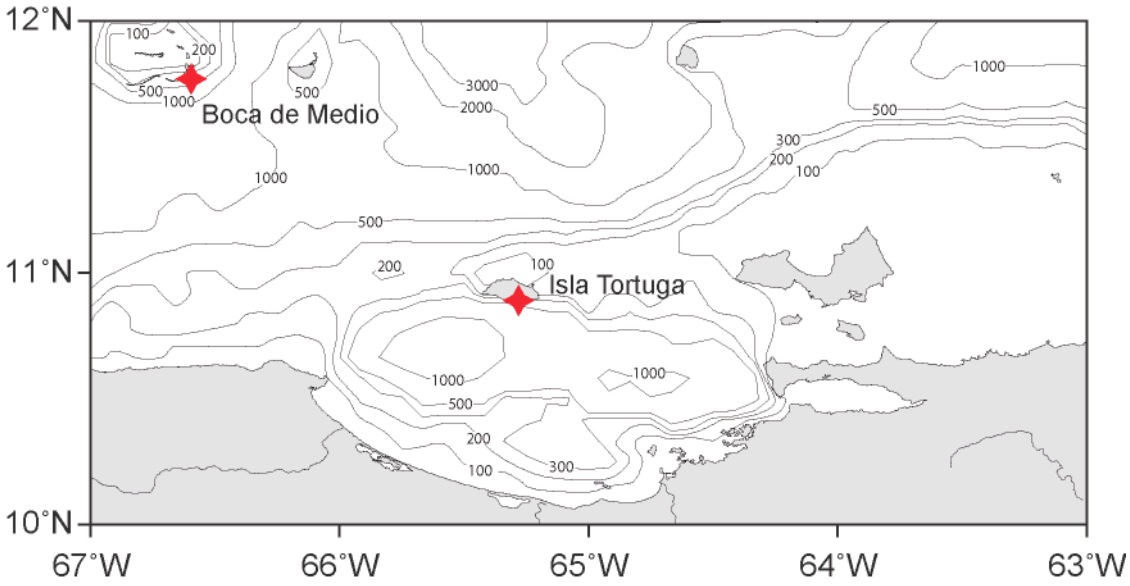

Figure 2-5. Map of the Cariaco Basin. Boca de Medio and Isla Tortuga reef sites are noted by the red stars.

The Cariaco Basin is located off the northern coast of Venezuela in the Caribbean Sea between 10° - 11° N and 64° - 66° W. It is made up of two small sub-basins, each approximately 1400 m deep. A 900 m deep sill separates the two basins. The entire basin is enclosed by the 200 m contour and is connected to the Caribbean Sea through two shallow channels (< 150 m) to the west and north [*Schubert*, 1982]. The Cariaco is anoxic below approximately 300 m, therefore there is little to no bioturbation of the sediments. Coral cores were collected at two locations in the Cariaco Basin, Isla Tortuga and Boca de Medio (Figure 2-5).

The Cariaco Basin sits at the northern boundary of the Intertropical Convergence Zone (ITCZ) during the northern hemisphere summer months of June through August (Figure 2-6). This causes an increase in precipitation over Venezuela, weak surface winds, little upwelling, and high sedimentation from local river runoff [*Muller-Karger et al.*, 2001]. The increase in rainfall and fluvial discharge from rivers directly affect the Cariaco Basin and southern Caribbean [*Hastenrath*, 1990; *Muller-Karger et al.*, 1988; *Nobre and Shukla*, 1996]. During the winter months of November through February, the ITCZ lies to the south of the Cariaco basin and causes high surface winds that induce increased upwelling and production. This pattern leads to annual varved sediment layers [*Astor et al.*, 2003; *Muller-Karger et al.*, 2001]. Seasonal changes in sea surface temperatures in the Cariaco Basin range from 6-12°C and are associated with wind-driven upwelling and thermal stratification cycles [*Goñi et al.*, 2006].

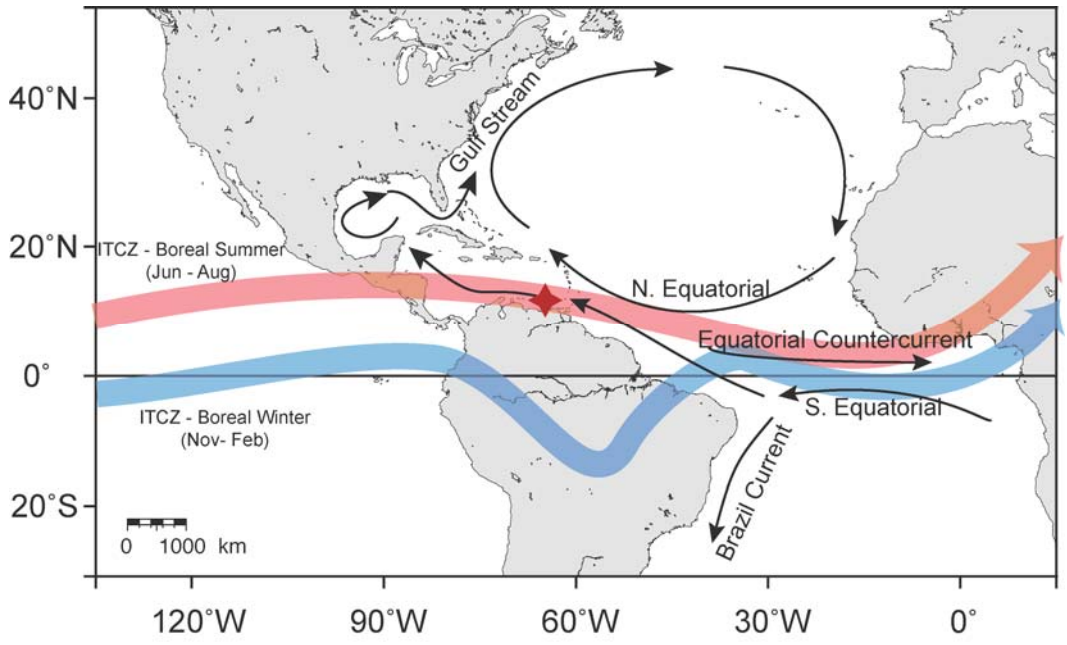

Figure 2-6. Location of the ITCZ during boreal summer (red) and boreal winter (blue) and surface currents in relation to the Cariaco Basin (red star).

CHAPTER III

OXYGEN ISOTOPES IN SEAWATER

INTRODUCTION

Variations of the salinity and temperature of seawater are generally good indicators of the mixing of water masses from two different sources (such as fresh river water and seawater). In situations where there are more than two possible sources of water, or temperature is not a conservative tracer, the oxygen isotope ratio[1] of a parcel of seawater in combination with its salinity can provide an effective indicator of the water's origin [*e.g., Craig and Gordon 1965*]. Salinity-$\delta^{18}O$ relationships have proven to be especially valuable for understanding the mixing and circulation of seawater in coastal areas and marginal seas [e.g., *Torgersen*, 1979; *Fairbanks*, 1982; *Khim et al*., 1997]. The temperature of shelf waters along the Texas/Louisiana coast behaves in a conservative manner during the winter months but is not a useful tracer during the summer when the shelf can be highly stratified [*Rabalais et al*., 2001; *Rowe*, 2001]. Therefore, knowledge of the salinity-$\delta^{18}O$ relationships of these shelf waters is needed to understand their origin and distribution.

Studies of the circulation and mixing of waters along the northern continental shelf and slope of the Gulf of Mexico have yet to focus upon analysis of salinity-$\delta^{18}O$ relationships. The oxygen isotopic compositions of fresh waters reflect the different latitudes and temperatures of the source areas of the water due to fractionation of meteoric water [e.g., *Craig,* 1961; *Dansgaard,* 1964; *Rozanski et al*., 1993; *Clark and Fritz*, 1997]. Because of this, the waters entering the Gulf of Mexico via rivers have different oxygen isotopic signatures depending on the location of the rivers' drainage basins [e.g*., Kendall and Coplen*, 2001]. A limited number of oxygen isotope measurements have been used to study the hydrology of Texas coastal areas [*Zerai*, 2001; *Hyeong and Lawrence,* 2003] and water chemistry in Florida estuaries [*Surge and*

[1] Oxygen isotope ratio δ notation: $\delta^{18}O = ({}^{18}O/{}^{16}O_{sample} - {}^{18}O/{}^{16}O_{standard})/({}^{18}O/{}^{16}O_{standard})\text{-}1000$ where the standard for water samples is Vienna Standard Mean Ocean Water (VSMOW).

Lohmann, 2002]. Furthermore, a vertical profile of measurements was made at Stetson Bank (the northernmost reef in the Flower Garden Banks National Marine Sanctuary), which is located near the edge of the shelf [*Gentry et al*., 2008]. Though estimates of the $\delta^{18}O$ value of waters from the open-ocean Gulf of Mexico exist, this value has yet to be determined by direct measurement. No published studies have used salinity-$\delta^{18}O$ relationships to study the circulation and mixing of river waters and open ocean seawater along the Texas-Louisiana continental shelf and slope. The objectives of this study are to (1) evaluate the relative contributions of the different freshwater sources on the northern Gulf of Mexico continental shelf using salinity and stable oxygen isotope values and (2) to establish the open ocean end member oxygen isotopes value using samples from the Flower Garden Banks on the edge of the shelf/slope break.

STUDY AREA

The area of focus for this study is the continental shelf of the northern Gulf of Mexico along the Texas and Louisiana coasts. Several large rivers flow into this part of the Gulf of Mexico, including the Mississippi, Atchafalaya, Sabine, Trinity, Brazos, and Colorado Rivers (Figure 3-1). Average fluxes and $\delta^{18}O$ values for these rivers are listed in Table 3-1. For a detailed description of the area, including wind and current information, refer to Chapter II.

The Mississippi and Atchafalaya Rivers drain approximately 3.2 million km^2 of the Midwestern United States [*Dunn*, 1996] and are the primary source of freshwater to the northern Gulf of Mexico with an annual average flux of approximately 4.88×10^{11} m^3/yr and 2.1×10^{11} m^3/yr, respectively. The influx of fresh water from the Mississippi and Atchafalaya river systems varies seasonally with the average peak flux of 30000 m^3/s in the spring and minimum flux of 5000 m^3/s in the fall [*Murray*, 1997].

Water from the Mississippi River is diverted into the Old River overflow channel and joins the Red River to form the Atchafalaya River [*McPhee*, 1989; *Roberts*, 1998]. The Red River originates in the Texas Panhandle and, therefore, drains only a small, southern part of the country compared to the drainage basin of the Mississippi River.

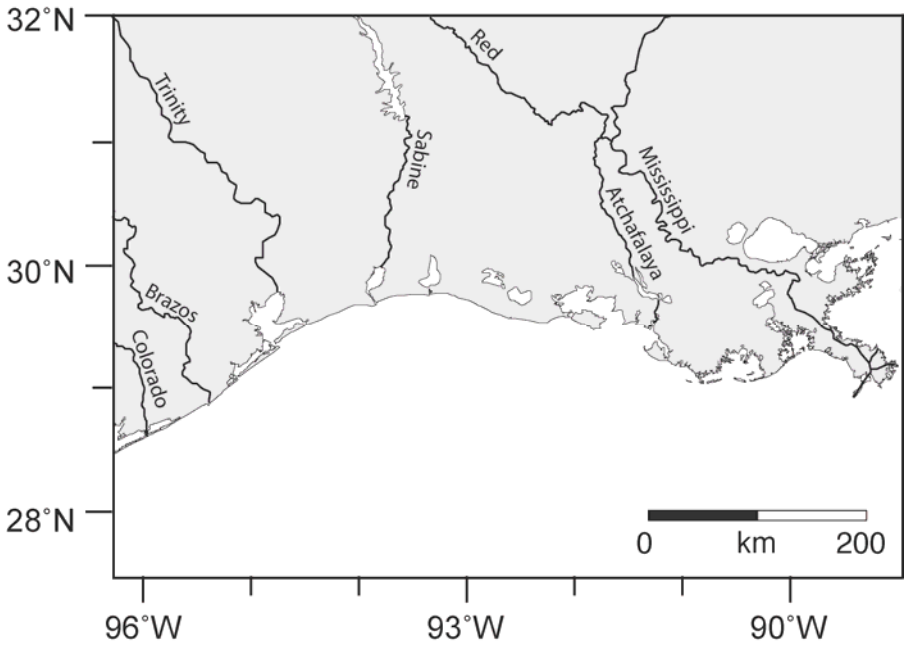

Figure 3-1. Map showing major rivers that drain into the northern Gulf of Mexico.

Table 3-1. Average river discharge and $\delta^{18}O$ for the major rivers draining into the north-central Gulf of Mexico.

	Mississippi[2]	Atchafalaya[3]	Brazos[4]	Sabine[5]	Trinity[6]	Colorado[7]
Jan	15957	3713	285	346	567	86
Feb	17077	4237	288	388	554	96
Mar	19453	4987	341	403	603	87
Apr	21893	5163	275	319	551	76
May	20361	4471	326	263	608	98
Jun	16536	4282	339	209	626	130
Jul	11604	3378	169	189	526	74
Aug	8108	2030	95	142	396	27
Sep	7607	1825	107	129	427	49
Oct	7718	1935	157	92	617	59
Nov	8946	2382	199	123	606	82
Dec	16034	3021	240	244	510	77
Average monthly flux (m^3/s)	14275	3452	235	237	549	79
$\delta^{18}O$ (‰)	-6.6[8]	-5.8[8]	-2.5[9]	-2.9[9]	-2.2[9]	-2.3[9]

[2] USGS National Water Information System (http://waterdata.usgs.gov/nwis) Site 07374000 Mississippi River at Baton Rouge, LA. Monthly averages of daily data from 1970 through 1983 and 2004 through 2008.
[3] USGS NWIS Site 07381600 Lower Atchafalaya River at Morgan City, LA. Averages of monthly means October 1995 through September 2008.
[4] USGS NWIS Site 08116650 Brazos River near Rosharon, TX. Averages of monthly means 1970 through September 2008.
[5] USGS NWIS Site 08030500 Sabine River near Ruliff, TX. Averages of monthly means 1970 through 2008.
[6] USGS NWIS Site 08067000 Trinity River at Liberty, TX. Averages of monthly means 1970 through September 2008.
[7] USGS NWIS Site 08162500 Colorado River near Bay City, TX. Averages of monthly means 1970 through 2008.
[8] C. Kendall, unpublished USGS data, 2008.
[9] *Coplen and Kendall* [2000].

Since 1977, the amount of water diverted from the Mississippi River into the Atchafalaya is adjusted such that the Atchafalaya flow is approximately 30% of the combined Red River flow and the total Mississippi flow above the Old River overflow channel [R. Huff, personal communication, 2009]. This ratio is maintained by the U.S. Army Corps of Engineers as part of their effort to control the amount of water flowing down the Mississippi River. Depending on the flux of the Red River, between 20% and 30% of the total Mississippi River flow is diverted into the Atchafalaya. As a consequence, the flux of water down the Atchafalaya River as well as the Red River contribution varies significantly on both seasonal and annual bases [*Bratkovich et al*., 1994].

The annual hydrographic regime along the Texas-Louisiana continental shelf is a down-coast flow (toward west southwest), except for the summer months when the flow reverses and flows up-coast from the Texas/Mexico border toward the Mississippi River Delta. River discharge from the major Texas and Louisiana rivers is also at a minimum during the summer months. The distribution of sea surface salinity reflects the direction of the surface flow [*Li et al*., 1997]. During the winter and spring when there is a steady offshore wind and down-coast flow, surface salinity increases as the distance south from shore increases. In the summer, the winds reverse direction, which causes pile-up of fresh water near the mouths of the Mississippi and Atchafalaya Rivers. Figure 3-2 shows seasonal averages of sea surface salinity along the Texas-Louisiana shelf. Although increased evaporation during the summer removes water enriched in ^{16}O from the sea surface, the sum of precipitation minus evaporation in this part of the Gulf of Mexico yields a precipitation surplus [*Turner*, 2003] so it is unlikely to be a factor in shelf water $\delta^{18}O$ values.

The area of the Mississippi River drainage basin is the third largest in the world, only behind the watersheds of the Amazon and Congo Rivers, draining 41% of the 48 contiguous states [*Dunn*, 1996]. A large percentage of the drainage originates in the northern half of the country, with very little runoff coming from southern states. This northern origin of Mississippi River water drives the oxygen isotope ratio of the river

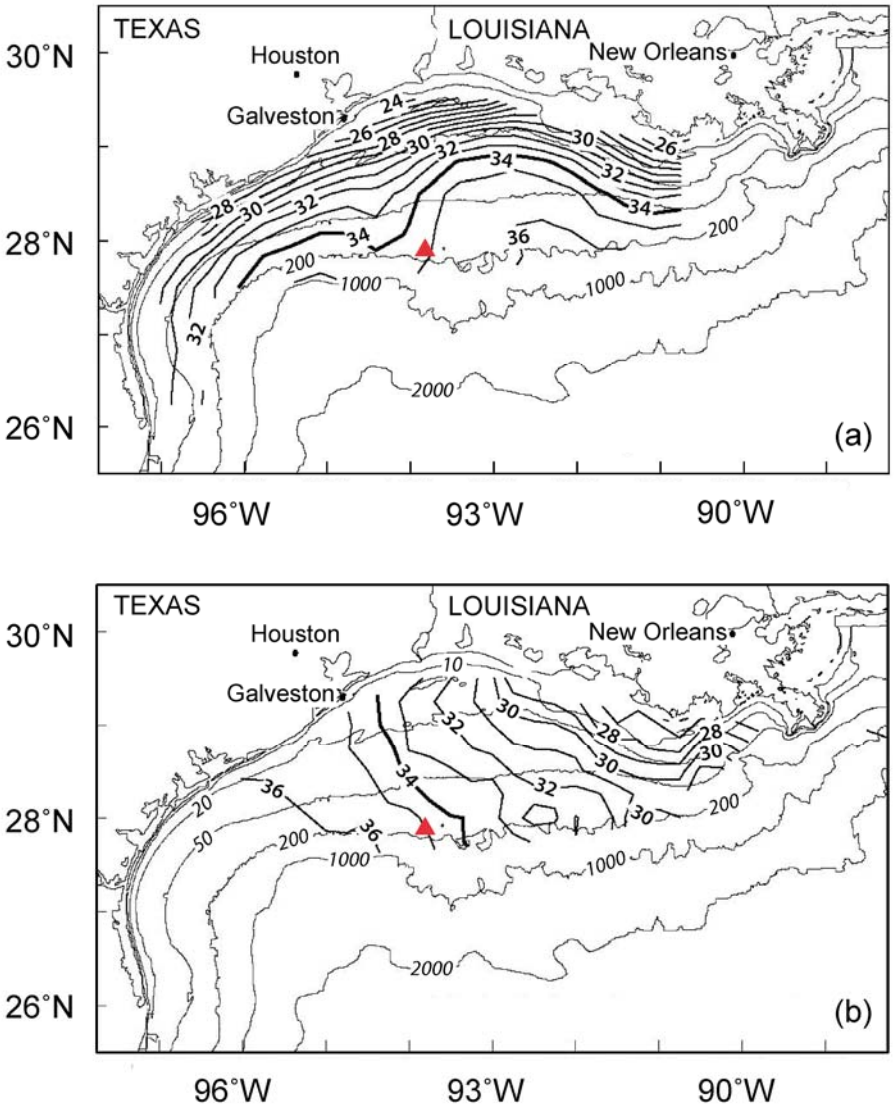

Figure 3-2. Average sea surface salinity. Averages for (a) eight May cruises and (b) seven July-August cruises along the Texas/Louisiana continental shelf. Bold numbers and contours indicate sea surface salinity; Italic numbers and fine contours indicate seafloor depths (m); Red triangles mark the location of the Flower Garden Banks. Figure adapted from *Li et al.* [1997].

water to be more negative because of the inverse relationship between latitude and $\delta^{18}O$ of precipitation [*Bowen and Wilkinson,* 2002; *Dutton et al.,* 2005]. While the majority of the Atchafalaya River water comes from the Mississippi River, the remaining is supplied from the Red River, which originates in the Texas panhandle. The proportion of Mississippi water to Red River water in the Atchafalaya is highly variable from season to season and from year to year.

Compared to the volume of freshwater contributed to the northern Gulf of Mexico, Texas rivers contribute relatively little to the shelf (Table 3-1). While the flux of freshwater from these rivers is a fraction of that of the larger Mississippi and Atchafalaya Rivers, their average $\delta^{18}O$ values are significantly more positive (ranging from -2.9‰ to -2.2‰) [*Lawrence*, 1993; *Coplen and Kendall*, 2000; *Hyeong and Lawrence,* 2003], primarily due to the southern source region of the Texas rivers.

Samples collected for river water oxygen isotope analysis between 1997 and 2004 from the Mississippi and Atchafalaya by the United States Geological Survey (USGS) exhibit seasonal variability in $\delta^{18}O$ of the river water entering the northern Gulf of Mexico. The average $\delta^{18}O$ value for the Mississippi River water at St. Francisville, LA is -6.6‰ with a range of values from -8.6‰ to -5.0‰. Atchafalaya River water samples were collected at Melville, LA and have an average $\delta^{18}O$ value of -5.8‰ and a range from -7.2‰ to -3.7‰ [C. Kendall, unpublished USGS data, 2008]. In comparison, the approximate $\delta^{18}O$ of open ocean surface water in the Gulf of Mexico has been estimated to be about 0‰ or 1‰ when salinity is 35 (*Hyeong and Lawrence* [2003] and *Lawrence* [1993], respectively).

SAMPLE COLLECTION AND ANALYTICAL METHODS

Seawater samples for salinity and $\delta^{18}O$ analyses were collected from the Texas-Louisiana continental shelf during two research cruises, one in August 2005 immediately prior to the passage of Hurricane Katrina, and the other in May 2006. Additional seawater samples from the Gulf of Mexico were collected at the Texas-Louisiana shelf/slope break at the Flower Garden Banks (FGB) National Marine Sanctuary. Divers

collected individual bottle samples at the surface and down to the reef top of the Flower Garden Banks, at depths of approximately 20 m, to determine whether there are seasonal changes in salinity and/or $\delta^{18}O$. The samples from the Flower Garden Banks were taken at different times of the year during cruises of opportunity beginning in September 2004 and ending in September 2006. The Gulf of Mexico can have rough weather during the winter and spring, so diving and sample collection opportunities during these times of the year were very limited. Figure 3-3 shows the sample locations from the two cruises and the location of the Flower Garden Banks.

Salinity was measured at the Geochemical and Environmental Research Group laboratory at Texas A&M University using a Guildline 8400B Autosal salinometer with an accuracy better than 0.002 Equivalent PSU. Oxygen isotope analyses of the water samples were performed at the Lamont-Doherty Earth Observatory using the CO_2-water equilibration method of *Epstein and Mayeda* [1953] with a Multiprep automated preparation system (Multiprep) on a VG Prism III stable isotope ratio mass spectrometer. Oxygen isotope ratios were determined as the per mil deviation of the sample from that of a lab standard that was calibrated to the VSMOW, GISP, and SLAP standards. Results reported here are averages of replicate analyses and relative to VSMOW. Based on repeated analysis of the lab standards, the analytical precision of an individual sample was 0.03‰ (1 σ). The mean difference of duplicate runs was 0.04‰ with a standard deviation of 0.03‰. If any set of replicates had a difference of greater than 0.067‰, it was rerun. The results of the oxygen isotope ratios and salinity analyses of the samples used in this study are listed in Appendix A. All values reported are from sea surface samples unless otherwise noted.

RESULTS AND DISCUSSION

The first set of samples was collected in August 2005 along the Louisiana shelf from west of the mouth of the Mississippi River west to the Texas-Louisiana border (Figure 3-3). The average river discharge in August is relatively low (approximately 8100 m^3/s for the Mississippi and 2000 m^3/s for the Atchafalaya, see Table 3-1) and the

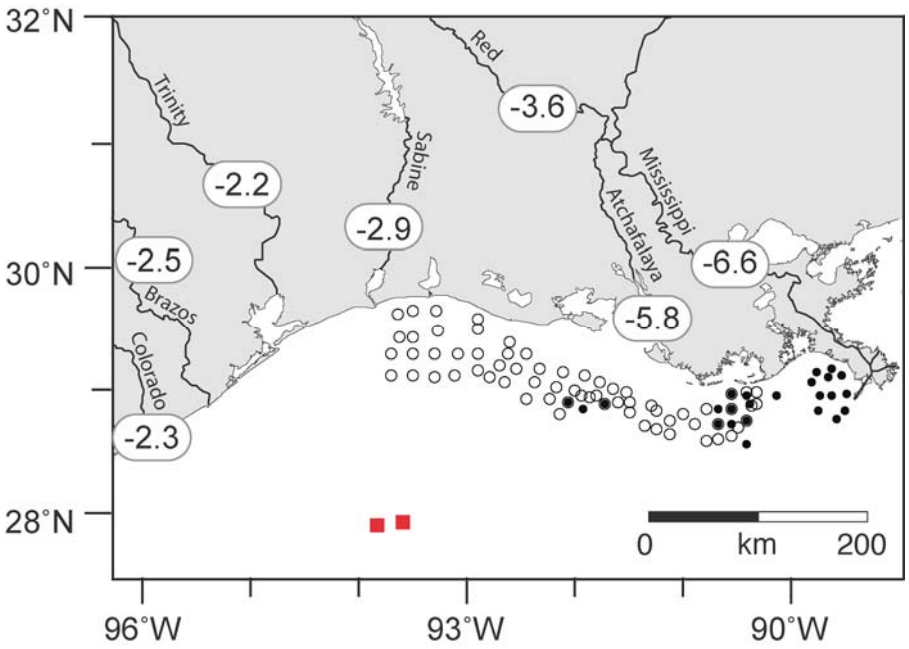

Figure 3-3. Locations of seawater sampling sites. Filled circles indicate May 2006 samples; Open circles show August 2005 samples; Red squares indicate the Flower Garden Banks. Values in white ovals are average $\delta^{18}O$ (‰) of river samples (data from C. Kendall [unpublished USGS data, 2008] and *Coplen and Kendall* [2000]).

water on the continental shelf is typically highly stratified during this time of the year. When the samples were taken in 2005, the discharge of both the Mississippi and Atchafalaya Rivers (5600 m^3/s and 1000 m^3/s, respectively) were considerably below the long-term August averages. The oxygen isotope values for samples from this cruise range from -1.0‰ to 0.3‰ and the salinities ranges from 23.7 to 31.5 with fresher water close to the coast and mouths of the Mississippi and Atchafalaya Rivers.

In contrast to the August 2005 sampling cruise, the May 2006 cruise occurred shortly after the peak river discharge. While discharge was much greater than during the August 2005 cruise, discharge rates were still below the long-term means (16300 m^3/s compared to 20400 m^3/s for the Mississippi River and 4100 m^3/s compared to 4500 m^3/s for the Atchafalaya River). The majority of the samples were taken near the mouth of the Mississippi River and west along the Louisiana coast just past the mouth of the Atchafalaya (Figure 3-3). The water on the Texas-Louisiana continental shelf during this time of year is well mixed and the current flows down coast in the westward direction. The oxygen isotope values for these samples range from -1.3‰ to 1.1‰ and the salinity range is 24.5 to 36.4. The freshest, most negative $\delta^{18}O$ values are found at the easternmost sample sites, close to the mouth of the Mississippi River, and the saltiest, most positive $\delta^{18}O$ values are from the western sample sites.

Compared to the inner shelf samples, the water samples from the Flower Garden Banks show a much more narrow range of salinity (35.7 to 36.6) and $\delta^{18}O$ (1.0 to 1.2‰) values. For 50 samples, the average salinity and $\delta^{18}O$ values are 36.1 (σ = 0.3) and 1.1‰ (σ = 0.05‰), respectively. This average salinity at the Flower Garden Banks is representative of average open-ocean Gulf of Mexico salinity [*Antonov et al.*, 2006]. The average Flower Garden Banks $\delta^{18}O$ value reported here establishes the salinity and $\delta^{18}O$ values that we take to be generally representative of open ocean waters in the northern Gulf of Mexico.

Figure 3-4 shows $\delta^{18}O$ plotted as a function of salinity for all water samples. The salinity and $\delta^{18}O$ values on the Texas-Louisiana continental shelf west of the mouth of the Mississippi appear to vary seasonally with the amount of freshwater input into this

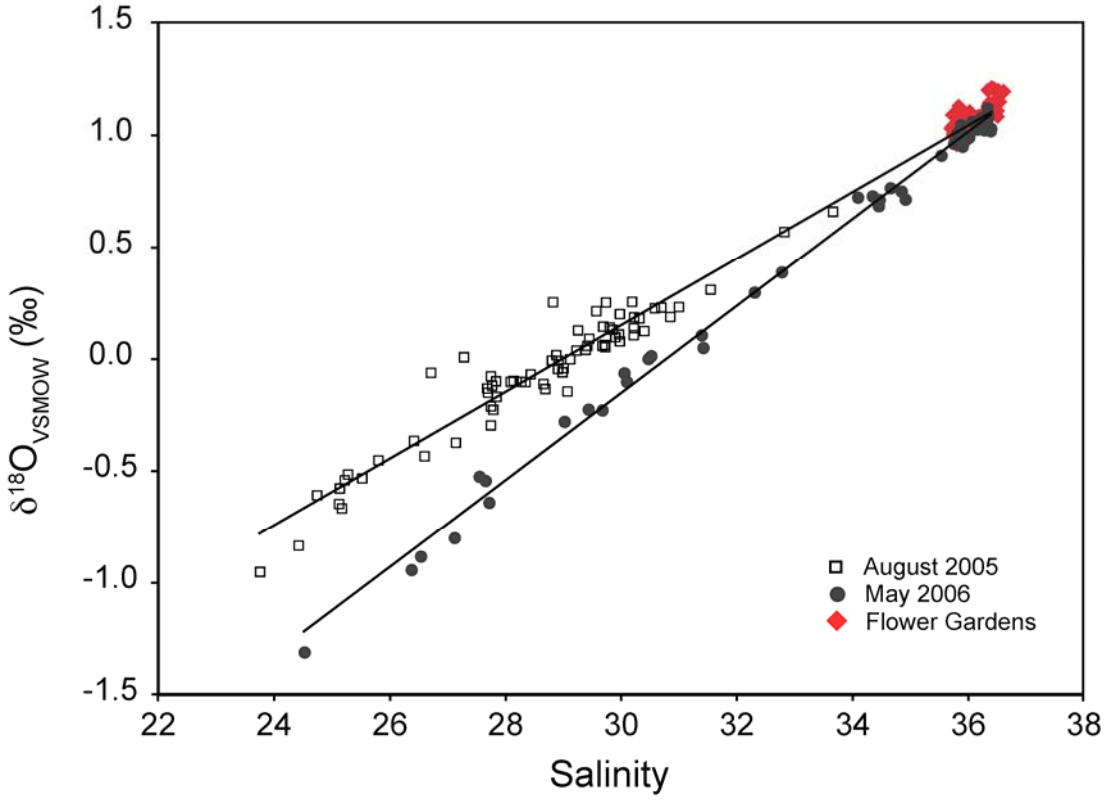

Figure 3-4. Salinity vs. $\delta^{18}O_{sw}$ for all samples. Water samples from the Flower Garden Banks were taken at various times of the year over a period of two years. When the fit lines for August 2005 and May 2006 data are extrapolated to a salinity of zero, the corresponding $\delta^{18}O$ values are -4.3‰ and -6.0‰, respectively.

area. The regression line for the data from each cruise, when extrapolated to a salinity value of zero, yields the $\delta^{18}O$ value (y-intercept of the line) of the predominant freshwater end member of the shelf waters at the time of collection. During August 2005, the $\delta^{18}O$ of the freshwater end member was approximately -4.3‰, while that for May was -6.0‰, indicating a more ^{18}O-depleted source of freshwater along the coast at that time. Some of the same sites were sampled during both the August 2005 and May 2006 cruises and the salinity-$\delta^{18}O$ relationships at these sites varied in a fashion that is consistent with the salinity-$\delta^{18}O$ relationships of the other samples, confirming that the difference in $\delta^{18}O$ of the freshwater end member indicated by the data is a real temporal variation (not an artifact of spatial differences in sample sites).

The salinity-$\delta^{18}O$ data corresponding to the Flower Garden Banks samples were not used during the process of fitting the two lines shown in Figure 3-4. It is therefore noteworthy that the lines converge and intersect the cluster of data points for the Flower Garden Banks, providing confirmation that the average salinity and $\delta^{18}O$ values of this cluster are representative of the open-ocean end member.

The $\delta^{18}O$ value of -6.0‰ for the fresh water end member during May 2006 falls within the ranges of oxygen isotopic compositions reported by the USGS for both Mississippi and Atchafalaya River waters, so the source of the waters cannot be determined with certainty from the existing salinity-$\delta^{18}O$ data alone. However, based on consideration of several other factors, we suggest that the freshwater end member for waters on the Texas-Louisiana shelf at this particular time does have a Mississippi River character and may well have reached the shelf via the mouth of the Mississippi. It is the time of year when the peak discharges of the rivers occur due to the spring runoff and, consequently, when the greatest flux of Mississippi water into the Atchafalaya River occurs and the relative contribution of Red River water to the Atchafalaya River is least [*Bratkovich et al*., 1994]. Therefore, the oxygen isotope values for the Mississippi and Atchafalaya River waters should be similar in value. In addition, winds and currents at this time of year are conducive to the east to west flow of waters along the shelf, so the

sample sites adjacent to the western edge of the Mississippi Delta are likely to be in the path of waters that flow onto the shelf from the mouth of the Mississippi River.

Samples analyzed from August 2005 indicate a fresh water end member with a $\delta^{18}O$ value of -4.3‰, which falls within the range of oxygen isotopic compositions reported by the USGS for Atchafalaya River waters, but is too positive to be within the range of compositions reported by the USGS for Mississippi waters. The predominant source of the freshwater end member for the shelf waters at this particular time should therefore be the Atchafalaya River. This interpretation is consistent with several other factors. During this time of the year, the discharges of both the Mississippi and Atchafalaya Rivers are greatly reduced. While the discharge of the Red River is also reduced, its relative contribution to the Atchafalaya may nevertheless increase [*Bratkovich et al*., 1994], causing the Atchafalaya to have a more positive $\delta^{18}O$ value. It is also during the summer that the winds along the Texas-Louisiana shelf reverse so shelf waters flow along the coast from Texas toward the Mississippi River Delta and tend to pile up along the Louisiana shelf. Given this flow pattern, waters from the Atchafalaya are more likely to occur at the sample sites.

Given this summer pattern of continental shelf circulation, an additional consideration might be that ^{18}O-enriched fresh water derived Texas rivers might be transported into the continental shelf into the study area.

SUMMARY AND IMPLICATIONS

From seawater samples collected at the Flower Garden Banks, the open ocean end member $\delta^{18}O$ value for the northern Gulf of Mexico shelf has been established to be 1.1‰. Knowledge of this value is important when trying to understand the mixing of fresh river water and open ocean seawater along the northern Gulf of Mexico shelf, and in particular the Texas-Louisiana shelf and slope.

Seawater samples analyzed for salinity and oxygen isotopic composition from two cruises along the Louisiana continental shelf during summer and spring (August 2005 and May 2006) indicate the ability to estimate the relative contributions of the

different freshwater sources on the northern Gulf of Mexico shelf. During August, when river discharge is at its lowest and the wind and currents have reversed from their usual east to west flow, samples indicate a fresh water end member oxygen isotope value of -4.3‰, which suggests a strong influence of Atchafalaya River water on the shelf at this time. In May, when river discharge is near its peak and the isotopic compositions of the Atchafalaya and Mississippi are expected to be close together, a fresh water end member oxygen isotope value of -6.0‰ suggests strong Mississippi River signature on the shelf waters.

In addition to knowing the $\delta^{18}O$ of the seawater end member, understanding the relative contributions of the fresh water sources is crucial when studying the circulation and mixing on the shelf, and other related processes such as hypoxia [*Rabalais et al*., 2001; *Rowe*, 2001]. Using river and shelf salinity-$\delta^{18}O$ data, it has been shown in this study that the relative contributions of the major rivers flowing into the Texas-Louisiana shelf area, the Mississippi and Atchafalaya Rivers, have a large amount of seasonal and annual variability. In addition to variability in the percent contribution of each river, the oxygen isotope values of the rivers also vary seasonally because of changes in the $\delta^{18}O$ of the river sources. Therefore, depending on the relative contributions, it can be difficult to distinguish between the two primary sources using the oxygen isotope values.

Further analysis of water samples from along the Texas-Louisiana shelf during peak and minimum discharge seasons would help with understanding the source of water in the northern Gulf of Mexico and the seasonal effect wind-driven circulation has on the shelf in transporting freshwater offshore, including the relative importance of discharge from Texas rivers. Because of the high degree of seasonal and annual variability in the fresh water discharge and source of the river waters, more river water $\delta^{18}O$ measurements, particularly from the Mississippi, Atchafalaya, and Red Rivers, are greatly needed.

Better understanding of the $\delta^{18}O$-salinity relationships of waters on the shelf can contribute to improved reconstructions of past environmental conditions using $\delta^{18}O$ of carbonates from the northern Gulf of Mexico. Previously the oxygen isotope

compositions of the skeletons of reef building corals at the Flower Garden Banks have been used as a proxy for water temperature changes in the past few decades [*Smith*, 2001], a more recent a study has used $\delta^{18}O$ and Sr/Ca measurements in *Conus* gastropod shells from Stetson Bank to investigate water temperature and salinity [*Sosdian et al*., 2006; *Gentry et al*., 2008], and there are ongoing studies utilizing the $\delta^{18}O$ of foraminifera shells, corals, and mollusks. However, if the $\delta^{18}O$ of the seawater varies by season due to changes in the ratio of freshwater present, the results of using proxies such as these could be affected. The seasonal range of salinity and $\delta^{18}O$ observed at the Flower Garden Banks from 2004 through 2006 are 0.9 and 0.17‰, which corresponds to an approximate potential uncertainty in temperature estimates from measurements of calcium carbonate coral skeletons at the Flower Garden Banks [e.g., *Grossman and Ku*, 1986] of ±0.4°C. Further study to define the seasonal $\delta^{18}O$-salinity relationships along the shelf of the northern Gulf of Mexico is important if past water temperatures are going to be faithfully reconstructed from the oxygen isotopic compositions of corals, mollusks, and other calcium carbonate materials.

CHAPTER IV

CORAL GROWTH AND CLIMATE VARIABILITY

INTRODUCTION

Society is strongly affected by interannual and decadal climate change. Tropical climate events, such as the El Niño/Southern Oscillation (ENSO) phenomenon, are well known for their impact on fisheries, agriculture, marine life and weather across the tropical Pacific [*Barber and Chavez*, 1986; *Philander*, 1990; *Adams et al*., 1999]. However, the influence of climate change is not only felt in the tropics, but in all regions of the world [*Ropelewski and Halpert*, 1986; *Glynn*, 1990]. To better cope with these climate events, it is necessary to identify and understand the character of both natural climate variability and any human-induced climate change. Our ability to characterize the natural climate variability would greatly benefit from long climate records, which would enhance our understanding of climate change and its regional effects. To identify the nature of climate change, it is essential to have a long history of climate that extends beyond the Industrial Revolution and to understand the processes and mechanisms that link tropical and extratropical climate. Several climate reconstructions using proxy data have been created for the tropics [*Cole et al.,* 1993; *Dunbar et al.,* 1994; *Guilderson and Schrag,* 1999; *Linsley et al.,* 2000; *Urban et al.,* 2000]. However, very few annually resolved long-term records of extratropical climate are available.

Reef-building corals have proven to be very sensitive monitors of environmental change. Variations in the annual extension rate and skeletal material deposited through time have been shown to preserve long, detailed records of past climate [e.g., *Dodge and Thomson,* 1974; *Buddemeier et al.,* 1974; *Hudson et al.,* 1976; *Barnes and Lough,* 1989; *Dunbar and Cole,* 1993]. A strong correlation generally exists between water temperature and the growth of reef building corals [*Buddemeier and Kinzie,* 1976; *Dodge and Vaisnys,* 1980].

The Flower Garden Banks are located at the edge of the continental shelf, rising up to within 20 m of the sea surface but surrounded by water depths of nearly 200 m.

Nowlin and Parker [1974] showed that the passage of cold fronts during the winter, such as those associated with a positive phase of the PNA pattern, could result in significant cooling of the waters on the continental shelf as far offshore as the Flower Garden Banks. They documented a case when the passage of one wintertime cold front across the northern Gulf of Mexico continental shelf decreased surface water temperature 1-2°C as far as 250 km offshore, demonstrating that the effects of these cold fronts could easily extend out to the Flower Garden Banks, which are 180 km from shore. Water temperatures on the shelf can approach the lower limit of acceptable water temperatures for coral growth during the winter months when severe or repeated cold-air outbreaks occur [*Highsmith*, 1979]. Because the corals grow faster during the winter [*Hudson*, 1981; *Cruz-Piñón et al*., 2003; *Carricart-Ganivet*, 2004], coral growth and extension rates will be particularly sensitive to changes in winter climate at the Flower Garden Banks.

While the response of corals to many environmental factors is not clearly understood, the temperature of the water in which the coral is growing has been shown to elicit one of the strongest responses in extension rates and deposition of skeletal material. Were they available, long temperature reconstruction records that reflect extratropical climate would greatly enhance our understanding of past climate change (both natural and anthropogenic) and their effects. This chapter aims to discuss the relationship between coral growth (as annual extension rates) from corals in the north and west Gulf of Mexico and wintertime temperature trends in the southeastern United States.

METHODS

Several long cores of the calcium carbonate skeletal material of *Montastraea faveolata* corals were collected in May 2005 at the Flower Garden Banks National Marine Sanctuary by a team of divers from Texas A&M University, the Florida Keys and Flower Garden Banks National Marine Sanctuaries, and the US Geological Survey. Cores of *M. faveolata* were collected from the East and West Flower Garden Banks. The corals were drilled using an underwater hydraulic drill with a 4-inch outer diameter

Table 4-1. Coral core collection information. Reef, date, water depth and core length information about the coral cores for which extension rates were calculated in this study.

Core ID	Reef	When	Water Depth (m)	Length of core (m)	Years
EFG1	East Flower Garden Bank	May 2005	18.3	2.1	2004 – 1839
EFG2	East Flower Garden Bank	May 2005	18.3	1.59	2004 -1940
WFG2	West Flower Garden Bank	May 2005	23.8	1.48	2004 - 1844
VC5	Chopas Reef, Veracruz	1991	4.3	1.57	1990 - 1882
VC7	Santaguillo Reef, Veracruz	1991	5.8	2.17	1990 - 1785

stainless steel, diamond-tipped drill bit. The cores were returned to Texas A&M University where each core segment was cut into approximately 8 mm thick slabs, cleaned, dried and digitally X-radiographed at the Texas A&M University Large Animal Hospital.

Coral cores of *M. faveolata* previously collected from reefs off the coast of Veracruz, Mexico were also examined. Extension rates were recalculated from existing X-radiographs using the methods outlined below. The primary focus will be on the extension rates of the corals from the Flower Garden Banks and the results from the Veracruz, Mexico corals will be used for comparison. See table 4-1 for a list of coral cores analyzed for this study and details about their collection.

Two distinct types of high-density bands are visible in the X-radiograph images of the coral skeletons (see Figure 4-1). In the Gulf of Mexico and Caribbean, corals of the species *Montastraea faveolata* deposit high-density growth bands seen as dark, horizontal lines, which are formed during the warmest months of the year (typically June through September), so one year of growth (high-density band to high-density band) is assumed to represent August through the following July [*Buddemeier et al*., 1974; *Hudson et al*., 1976]. Less dense bands are formed during the remainder of the year [*Knutson et al.,* 1972; *Dodge and Thomson,* 1974; *Hudson et al.,* 1976]. The exact reason for why high-density bands, and likely slower growth, are deposited during the summer months is not entirely known. Available light and water temperatures have been suggested as the controlling factors of the formation of these high-density bands during the summer months [*Buddemeier et al*., 1974] or metabolic energy may be being redirected from colony growth to sexual reproduction during this time of the year [S. Gittings and K. Deslarzes, personal communication]. Intermediate high-density bands can also be formed on a sub-annual basis and are seen as thinner, less distinct dark bands between annual growth bands. These bands are typically deposited during the winter months and are termed stress bands. These high-density stress bands are most likely to have formed during unusually cold winters, as these corals generally do not grow well when water temperatures are below about 18°C and temperatures less than

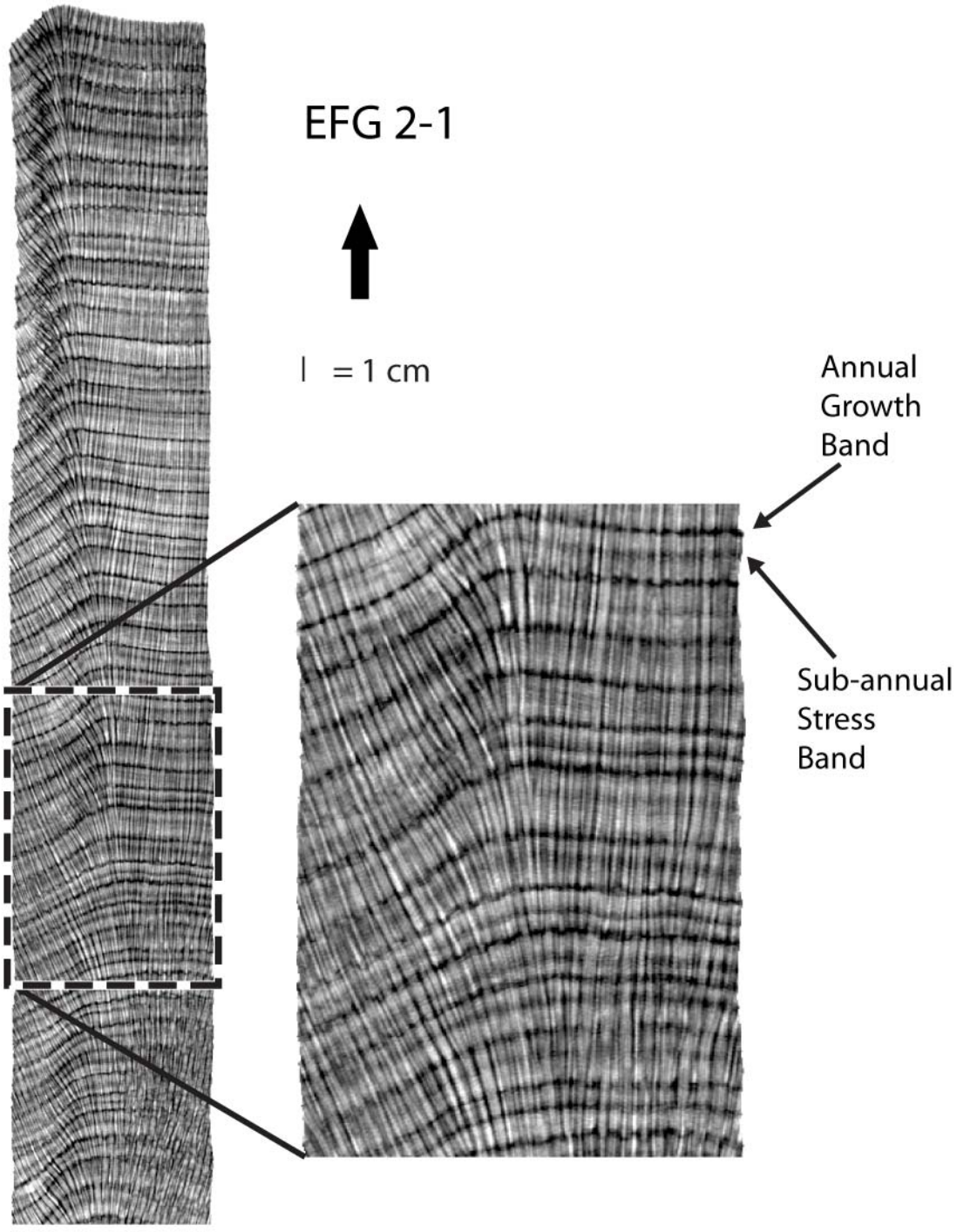

Figure 4-1. X-radiographic negative image of coral slab. Note the difference between annual high-density growth bands and sub-annual stress bands.

approximately 16°C can be deadly [*Buddemeier and Kinzie,* 1976; *Dodge and Vaisnys,* 1980]. Variations in skeletal density caused by variations in extension rate and calcification over the course of the year result in the formation of high and low density band couplets.

Coral core chronologies were determined by counting backwards from the most recently deposited high-density band. Extension rates were determined by measuring the distance between each annual high-density growth band by grey-scale analysis. The grey-scale analysis was completed using CoralXDS software [*Helmle et al*., 2002] from Nova Southeast University (available at http://www.nova.edu/ocean/coralxds/). Calculated extension rates are listed in Appendix B. The year is listed as the year the growth ended (i.e., growth from August 1979 to August 1980 is listed as 1980).

Several factors were taken into consideration when selecting coral heads to be cored and sampled. The first was the location of the coral core relative to the maximum growth axis of the coral colony. For mounding, or hemispherically shaped coral colonies, growth generally decreases with the distance from the central growth axis of the colony [*Dodge and Thomson*, 1974; *Weber et al*., 1975]. The angle of the drill orientation can also be a factor. If the drilling angle is not parallel to the growth axis, measured apparent extension rates may be larger than the actual extension rates. To minimize bias associated with these factors, prior to drilling, the coral head was inspected for evidence of growth hiatuses or changes in the growth axis orientation and then the core was drilled in the center of the coral head. When cores were cut into slabs, the slab orientation was chosen to be as close as possible to perpendicular to the direction of growth in the top core section. Each slab was cut to maintain a constant growth axis orientation and provide a continuous record the entire way down the core. A line perpendicular to the high-density bands was carefully chosen using the X-ray images in an effort to avoid measuring extension in areas of the coral slab that appeared to have unusual growth. Nevertheless, it becomes much more difficult to maintain a good orientation of the coral core/slab relative to the central growth axis and direction of coral growth the longer the coral core (i.e., in the older portion of the coral skeletal

material) since one cannot tell what the internal skeletal structure looks like until the core has been drilled. Additional coral cores were collected as part of the coral drilling project but when the cores/slabs were inspected, they were clearly off the central growth axis or the orientation of the core was not perpendicular to the growth and they were not included in this study. It is also difficult to look at individual years and/or events further back in the coral cores because the chronology of the core becomes less certain. More confidence is therefore placed in the recent part of the coral growth record. The 9-pt smoothed curve is useful in identifying decadal events rather than single-year events in the older part of the cores.

Coral reef communities are complex ecosystems and contain living, biological organisms in a changing environment, sensitive to many external environmental factors. Therefore, it cannot be assumed that changes in coral growth occur solely in response to changes in the temperature of the surrounding water. It is important to focus on the larger signals and not the individual or random variations associated with each coral core. To identify signals that are consistent among all the corals and minimize bias due to differences in extension rates between coral colonies, the individual growth records were normalized with z-score normalization. The z-score normalization is calculated by subtracting the mean of a given coral core record from each individual measurement from that record and then dividing by the standard deviation to normalize both the mean and the variance of the coral record. This was done for each individual coral record and then all the normalized records were stacked to produce a single composite record of average annual growth. A 9-point weighted average is overlaid on the time series to minimize annual variability and highlight decadal signals in the coral extension records.

Air temperature, 500-mb geopotential height, and sea surface temperature values are all used in the analysis of the coral growth results. Sea surface temperature and 500-mb geopotential height are derived from the NCEP/NCAR Reanalysis [*Kalnay et al*., 1996] provided by the National Oceanic and Atmospheric Administration (NOAA)/ Oceanic and Atmospheric Research (OAR)/Earth Systems Research Laboratory (ESRL) Physical Sciences Division (PSD) in Boulder, Colorado from their website at

http://www.cdc.noaa.gov. Average minimum winter air temperature as recorded in New Orleans is from the United States Historical Climatology Network (USHCN) [*Williams et al*., 2007] provided by the Carbon Dioxide Information Analysis Center in Oak Ridge, Tennessee from their website at http://cdiac.ornl.gov/epubs/ndp/ushcn/newushcn.html. Absolute minimum winter air temperature at 31°N, 90°W is from *Erhardt* [1992]. Note that winter is defined as December through February in this study and is listed for the year winter ends. Also remember that the coral growth is expressed as annual extension rate and integrates an entire year of growth while many of the other variables discussed are only for the winter.

RESULTS AND DISCUSSION

The East and West Flower Garden Bank cores collected for this study are among the longest records for this region, extending back to the 1840s. Annual extension rates were determined for the three coral cores collected at the Flower Garden Banks and are plotted as time-series in Figure 4-2. Both cores sampled from the East Flower Garden Bank (EFG1 and EFG2) were collected at 19 m water depth while the coral core from the West Flower Garden Bank (WFG2) was collected from almost 23 m water depth. The average extension rate for EFG1 is 10.41 mm/year (σ = 1.48, n=167); EFG2 has an average of 9.54 mm/year (σ = 1.31, n = 65) and the average for WFG2 is 8.01 mm/year (σ = 1.21, n = 161). The difference in water depth between the East Flower Garden Bank and West Flower Garden Bank is the probable reason the average extension rate for the WFG2 core is 1.5 mm/year to 2.4 mm/year less than the EFG1 and EFG2 average extension rates. The calcification of reef corals, such as the species discussed here, is directly correlated with the photosynthetic activity of their zooxanthallae [*Goreau and Goreau*, 1959]. An increase in water depth decreases the amount of light available for photosynthesis.

There is a large amount of variability between the individual growth records of cores collected at the same bank and cores collected at different banks. There are several reasons why a high amount of variability is present and expected. Corals are

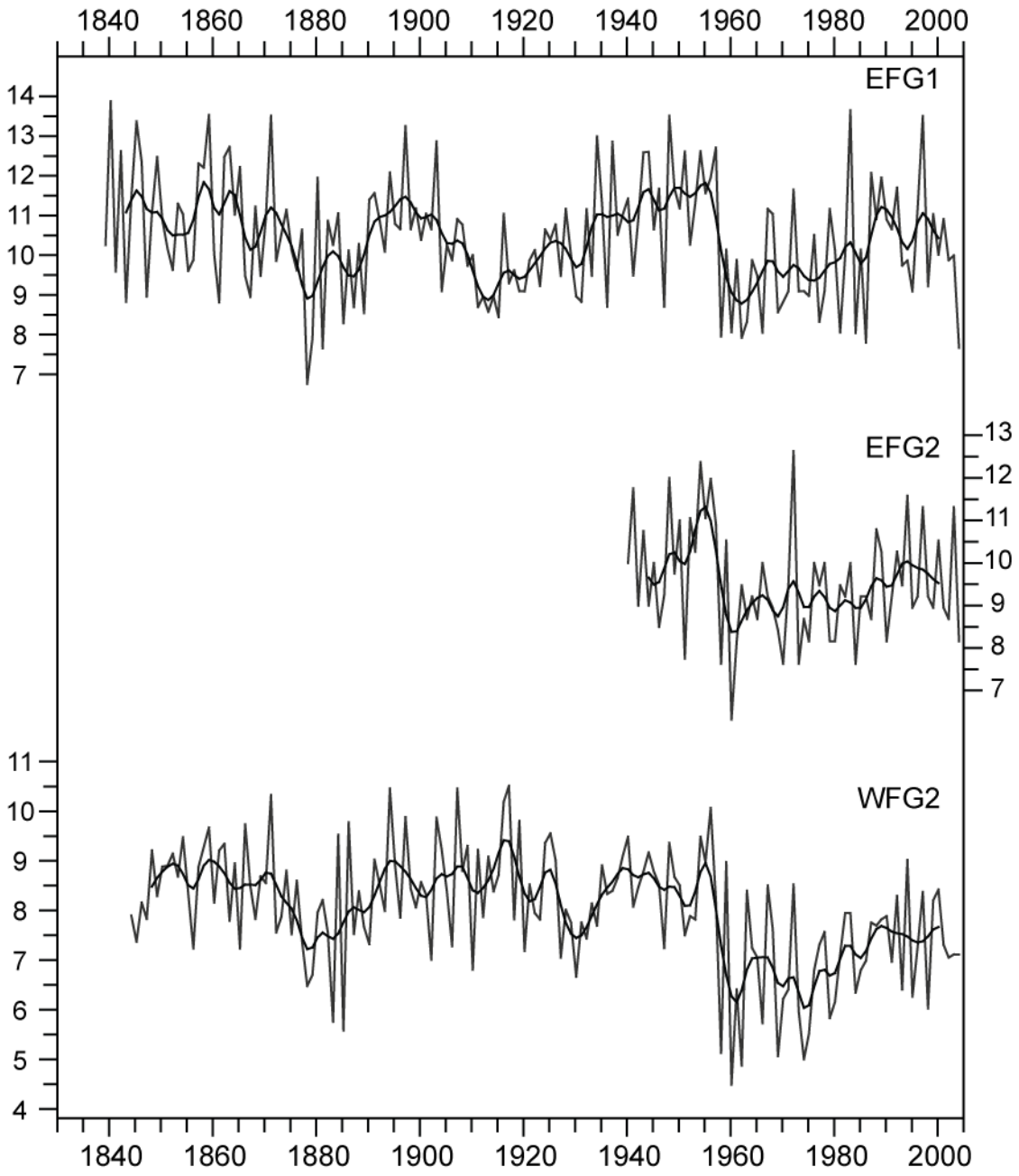

Figure 4-2. Flower Garden Banks coral extension rates. Extension rates (mm/year) of the three corals from the Flower Garden Banks that were collected and analyzed for this study. Bold lines are 9-pt moving averages for individual time series.

Table 4-2. All coral cores used for growth rate analysis.

Core ID	Location	Years	Reference
EFG1	East Flower Garden Bank	2004 – 1838	This study
EFG2	East Flower Garden Bank	2004 – 1939	This study
WFG2	West Flower Garden Bank	2004 – 1843	This study
VC5	Chopas Reef Veracruz, Mexico	1990 – 1871	This study
VC7	Santaguillo Reef Veracruz, Mexico	1990 – 1784	This study
KD WFG1	West Flower Garden Bank	1989 – 1910	*Deslarzes* [1992]
KD WFG2	West Flower Garden Bank	1989 – 1910	*Deslarzes* [1992]
KD EFG1	East Flower Garden Bank	1989 – 1910	*Deslarzes* [1992]
KD EFG2	East Flower Garden Bank	1989 – 1910	*Deslarzes* [1992]
HR1	East Flower Garden Bank	1979 – 1913	*Hudson and Robbin* [1980]
HR2	East Flower Garden Bank	1979 – 1891	*Hudson and Robbin* [1980]
HR3	East Flower Garden Bank	1979 – 1911	*Hudson and Robbin* [1980]
HR4	East Flower Garden Bank	1979 – 1922	*Hudson and Robbin* [1980]
HR5	East Flower Garden Bank	1979 – 1903	*Hudson and Robbin* [1980]
HR6	East Flower Garden Bank	1979 – 1917	*Hudson and Robbin* [1980]
HR7	East Flower Garden Bank	1979 – 1920	*Hudson and Robbin* [1980]
HR8	East Flower Garden Bank	1979 – 1945	*Hudson and Robbin* [1980]
HR9	East Flower Garden Bank	1979 – 1886	*Hudson and Robbin* [1980]
HR10	East Flower Garden Bank	1979 – 1902	*Hudson and Robbin* [1980]
HR11	East Flower Garden Bank	1979 – 1902	*Hudson and Robbin* [1980]
HR12	East Flower Garden Bank	1979 – 1907	*Hudson and Robbin* [1980]

complex, biological organisms responding to their external environment. Even different colonies at the same reef, which are exposed to essentially the same hydrographic conditions, can respond in different ways due to their individual nature and other stresses experienced by each colony. Other factors that could cause variability between coral cores are the location of the coral core relative to the maximum growth axis of the coral colony and the angle of the drill orientation. These factors were taken into account as much as possible during drilling, slabbing, and the calculation of extension rates (see Methods).

One feature that is consistent between the extension rates of the three coral cores from the Flower Garden Banks is a sharp decrease in extension rate between the years of 1956-57 and 1957-58. In addition to an approximate 2.5 mm/year decrease in growth since this event in the late 1950s, growth remained below the long-term average for several years but appears to be gradually increasing. A concern regarding this event seen in the extension rates is that in two of the three cores (EFG1 and WFG2), this event is at or near the core break point between two drilled sections of the core. To verify that this decrease is not merely an artifact of a break in the core sections, extension rates calculated for the three new Flower Garden Banks cores were compared with those previously published [*Hudson and Robbin*, 1980; *Deslarzes*, 1992] (Table 4-2). The normalized time series of each individual coral core are averaged together for each study. Figure 4-3 shows all normalized coral extension rate data sets from each study and also all cores stacked together into one composite record with the 9-pt weighted average overlaid. A plot of the number of individual coral core records averaged together for each year is included (note: there is a sharp drop off in the number of corals prior to 1910 and after 1990).

In each of the previously published data sets [*Hudson and Robbin*, 1980; *Dodge and Lang*, 1983; *Deslarzes*, 1992; *Slowey and Crowley*, 1995] and in each of the three new coral cores described here (Figure 4-2) the decrease in extension rates between 1956-57 and 1957-58 is the prominent feature. Among the Flower Garden Banks corals analyzed in this study, extension rates are relatively uniform in WFG2 from the 1890s

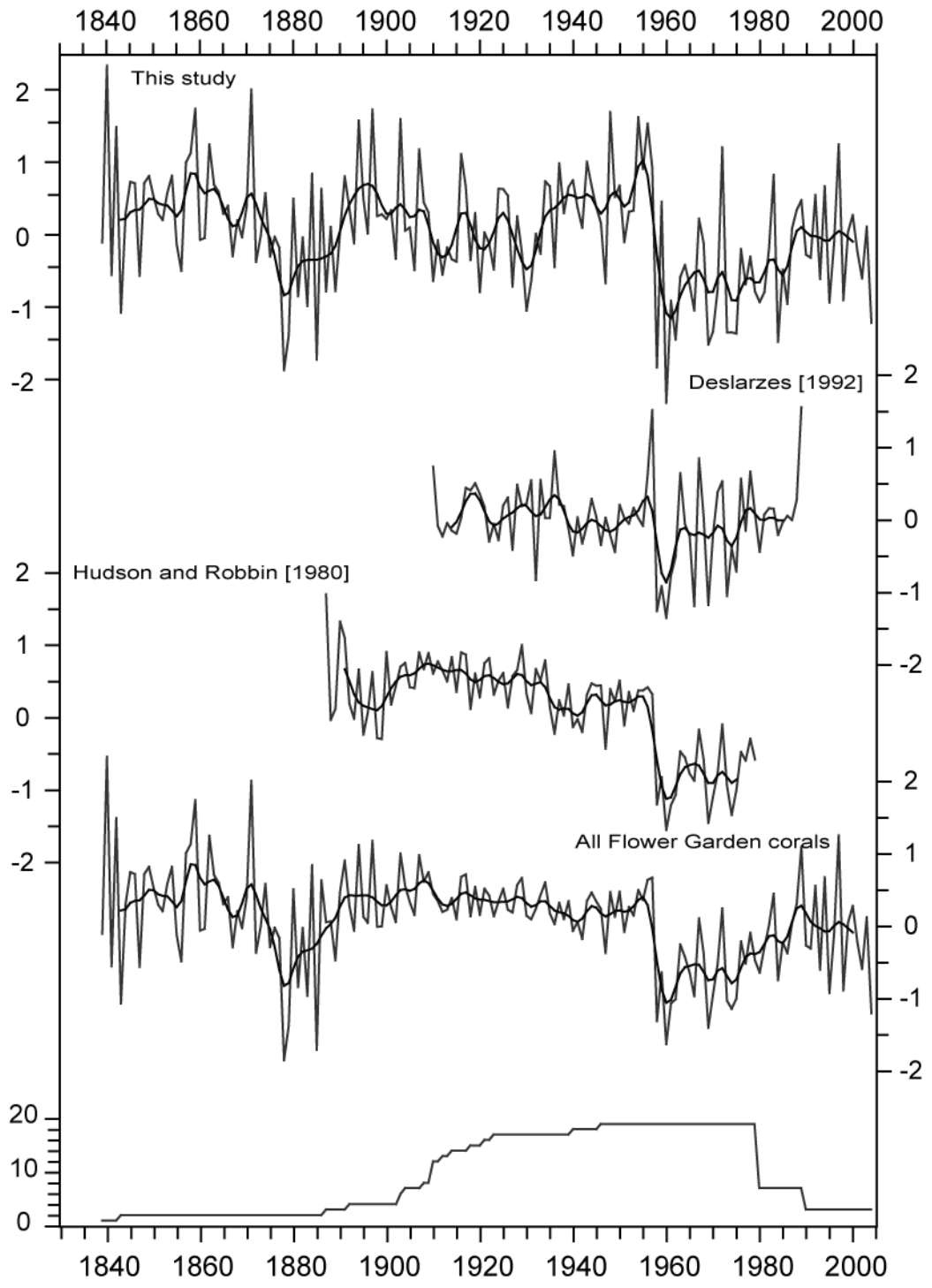

Figure 4-3. New and previously published coral extension rates. Z-score normalized extension rates (mm/year) and total number of coral cores used for the stacked record. Bold lines are 9-pt moving averages for individual time series.

until 1957-58. EFG1 does not have the same stability during this time period. This could be due to the variability between individuals as a result of environmental forces on the particular coral colony or because of the location of the core in respect to the central growth axis and orientation of the drilling apparatus.

Why does the winter of 1957-1958 shows up as such a strong anomaly in the extension rates of nearly all the records discussed? Previous studies have suggested an increase in reef depth due to sub-seafloor salt movement [*Rezak and Bright*, 1981], an increase in freshwater outflow from the Atchafalaya River [*Dodge and Lang*, 1983] and a decrease in water temperature associated with a shift in winter climate [*Slowey and Crowley*, 1995]. This study favors the explanation put forth by *Slowey and Crowley* [1995]. The corals in this region, and especially *M. faveolata*, are more sensitive to wintertime weather. The winter of 1957-58 was one of the most severe in the south-eastern U.S. in many years [e.g., *Dickson and Namias*, 1976], causing a disastrous citrus freeze in Florida [*Downton and Miller*, 1993; *Rogers and Rohli*, 1991]. Figure 4-4 shows the average minimum winter (DJF) temperature recorded at New Orleans, Louisiana, the 500-mb geopotential height anomaly, sea surface temperature anomaly and the normalized Flower Garden Banks extension record. The New Orleans temperature record shows that the winter of 1957-58 was, on average, the coldest winter recorded between 1889 and 2006 [*Williams et al*., 2007]. The 500-mb geopotential height anomaly shows a much lower pressure during the winter of 1957-58 compared to other years. This is consistent with more frequent and stronger low-pressure cold fronts passing through this area. The sea surface temperature record [*Kalnay et al*., 1996] shown in Figure 4-4 does not show a significant cooling at this time. However, because of the coarse resolution (2.5° by 2.5°) and smoothed nature of this temperature reconstruction, it may not be able to capture high frequency, small spatial scale temperature changes that occur on the Texas/Louisiana shelf.

To determine the spatial impact of the 1957-58 event, coral cores from other reefs in the Gulf of Mexico were compared to those from the Flower Garden Banks. *Hudson et al*. [1976] presented X-ray images of several coral cores off the lower

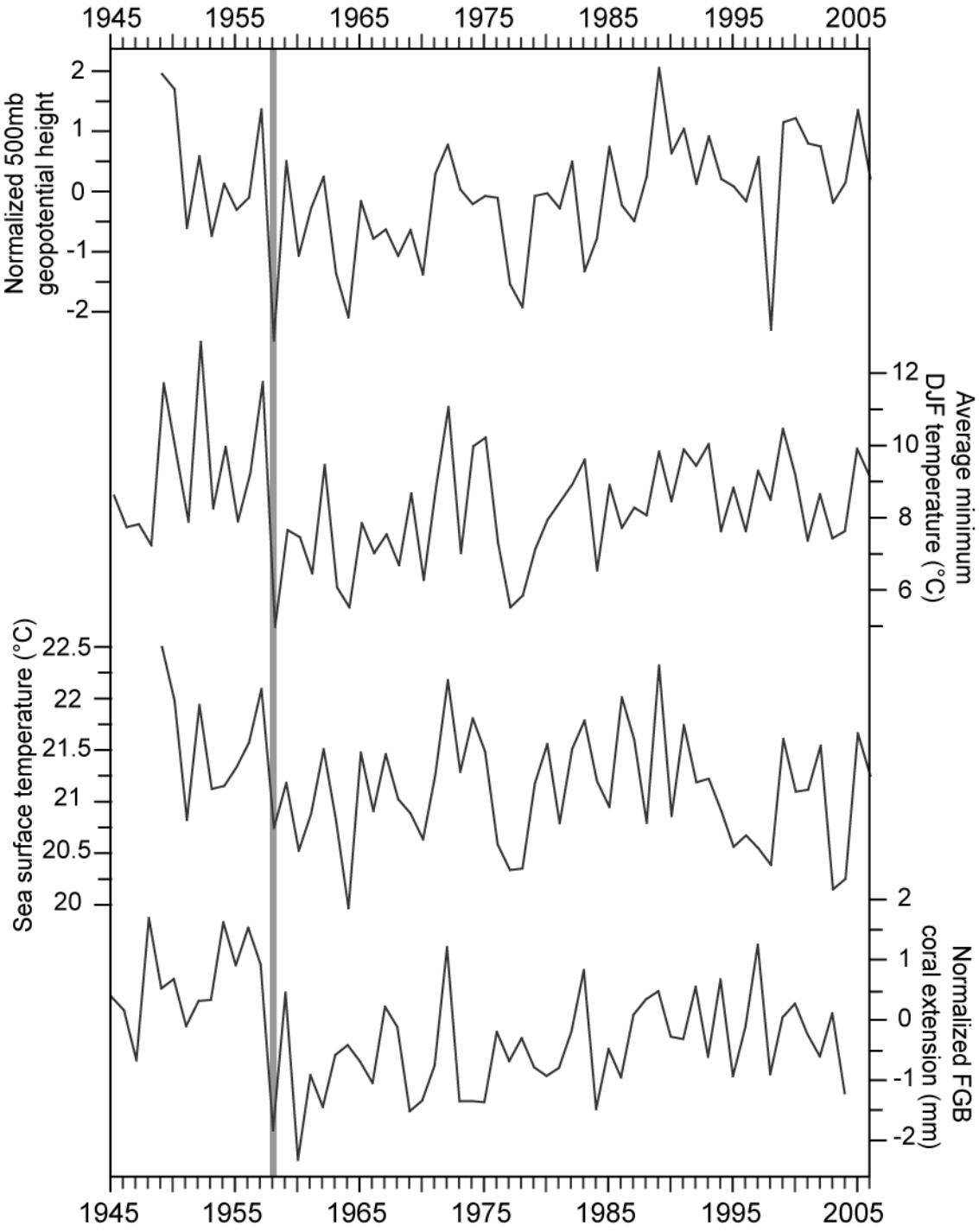

Figure 4-4. Gulf coast time series (1945 – 2006). Normalized 500-mb geopotential height at 30°N, 90°W [*Kalnay et al*., 1996]; average minimum winter air temperature as recorded in New Orleans [*Williams et al*., 2007]; winter sea surface temperature at 26.7°N and 93.7°W [*Kalnay et al*., 1996]; normalized Flower Garden Banks coral extension record. Shaded vertical line marks 1957-58.

southeastern Florida coast (Florida Keys) and correlated the presence of stress bands in these cores with unusually cold winters in Key West, Florida. He reported an unusually cold winter at Key West and clear stress bands in several of the coral cores in 1957-58, indicating the effects of the event were seen as far south as the Florida Keys.

The 1957-58 event can also be seen in the extension rate record of a coral core from the western Gulf of Mexico. The Veracruz, Mexico corals are sensitive to local climate patterns in the southwest Gulf of Mexico, including the "El Norte" winter storms that originate to the northwest and carry cold air masses to the Veracruz region. For more information about the Veracruz Reef System and the individual reefs used for this study, refer to Chapter II. The "El Nortes" are similar to the cold fronts that pass through the southern United States and the Flower Garden Banks in the northern Gulf of Mexico during the winter months. The coral growth record of corals from Veracurz are more likely to reflect environmental changes associated with local climate variability in the western Gulf of Mexico then regional North American climate variability, and therefore, would require a larger, more regional climate signal to be apparent in corals from both Veracruz and the Flower Garden Banks.

Figure 4-5 shows the extension rates of the Veracruz coral cores and the stacked Flower Garden Banks record for comparison. The average extension rate for VC5 is 8.3 mm/year (σ = 1.25, n = 118) and the average for VC7 is 9.07 mm/year (σ = 1.39, n = 206). Although some of the local stresses on these corals are much different than those on the corals at the Flower Garden Banks, the decrease in extension rate between 1956-57 and 1957-58 is seen as a significant feature in the VC7 coral core. The signal is absent in the VC5 core but this is not surprising because of the proximity of the reef to land and high amounts of river runoff. However, the presence of a large change in extension rate in the VC7 core indicates a broader spatial extent of the anomalous 1957-58 event beyond the northern Gulf of Mexico.

Downton and Miller [1993] hypothesized that variations in the frequency of freezes in the southeast United States is related to variations in the three atmospheric circulation patterns that affect this region the most: the Pacific/North American (PNA)

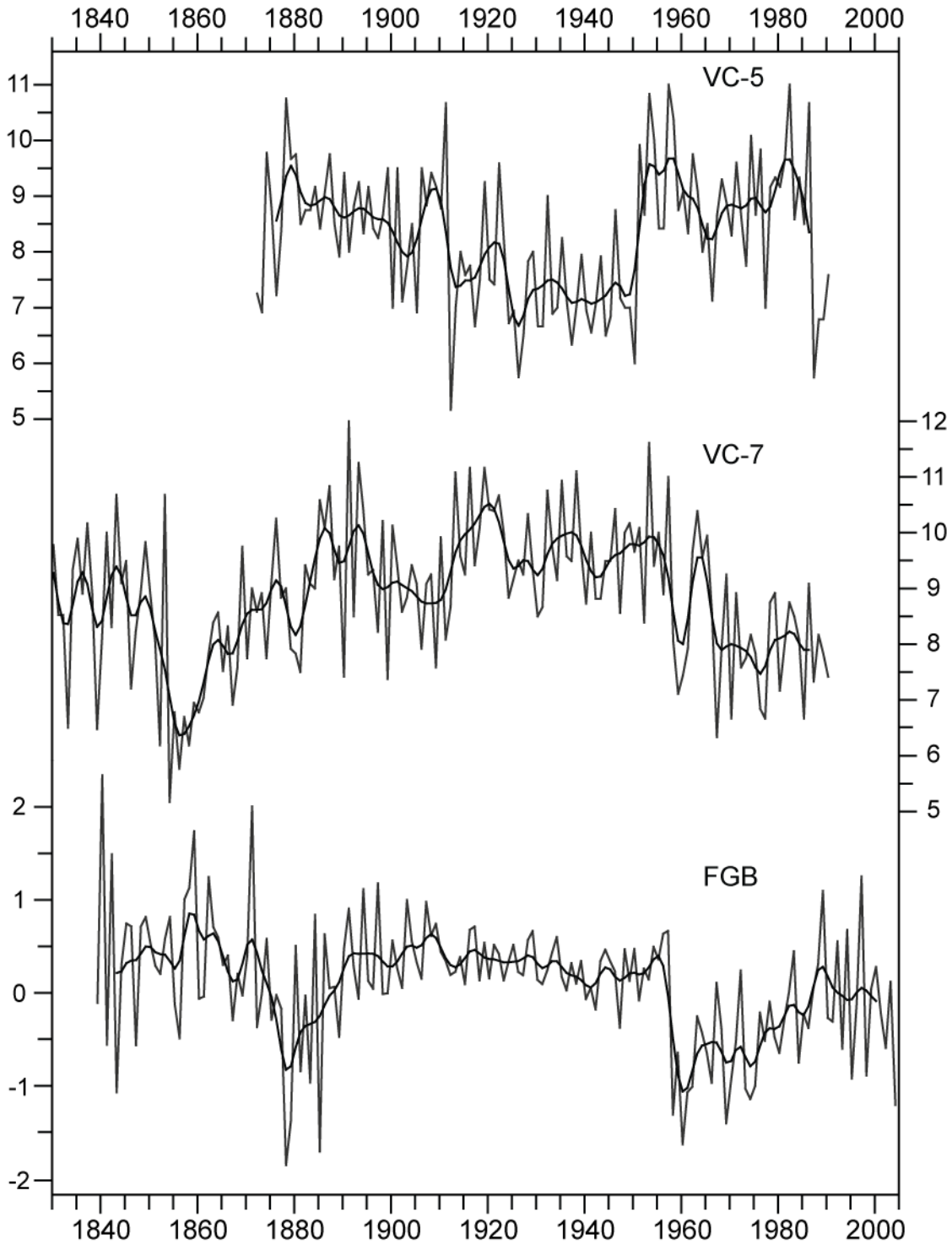

Figure 4-5. Additional coral extension rates. Veracruz extension rates (mm/year) and stacked Flower Garden Banks coral extension record. Bold lines are 9-pt moving averages for individual time series.

pattern, the Southern Oscillation Index (SOI) and the North Atlantic Oscillation (NAO). More detail on each of these patterns is found in Chapter II. A negative SOI is associated with El Nino events and wetter, cooler winters in the southeast and Gulf Coast. A negative phase of the NAO is associated with harsher winter conditions and more cold air outbreaks along the east coast of the United States. Figure 4-6 shows the PNA, SO, and NAO indices for the winter months and the normalized coral extension record. While all three atmospheric circulation patterns have been shown to have an effect on winter climate in this region, the PNA pattern tends to be the most influential in regards to winter temperatures in the south and southeastern United States. A strong negative correlation between the PNA pattern and winter air temperature in the southeast U.S. exists. A positive phase of the PNA pattern generally results in cooler minimum winter temperatures and the passage of more cold, arctic fronts through the region. The phase of the PNA pattern and occurrence of these cold frontal systems has been linked to freezes of the citrus crop in Florida [*Rogers and Rohli*, 1991; *Downton and Miller*, 1993]. Since the PNA pattern has the strongest correlation with winter temperatures in the south and southeastern U.S., and the index is derived from extratropical observations, understanding the PNA beyond the scope of the instrumental record could be useful in understanding more about tropical/extratropical climate interactions. *Slowey and Crowley* [1995] have previously suggested that the phase of the PNA pattern could be linked to extension rates of the corals at the Flower Garden Banks. The path of wintertime storms is directly determined by the orientation of the jet stream across North America. A more zonal flow of the jet stream is associated with a negative phase of the PNA pattern while a southward dip in the jet stream that pulls cold, arctic air into the south and southeastern United States is associated with a positive phase of the PNA pattern. A positive phase of the PNA pattern is more likely to encourage stronger and more frequent winter cold fronts into the south and southeast. *Rogers and Rohli* [1991] documented how the time period from 1947 to 1956 was a period when relatively few significant fronts brought cold Arctic air massed to the southeastern U.S. This time

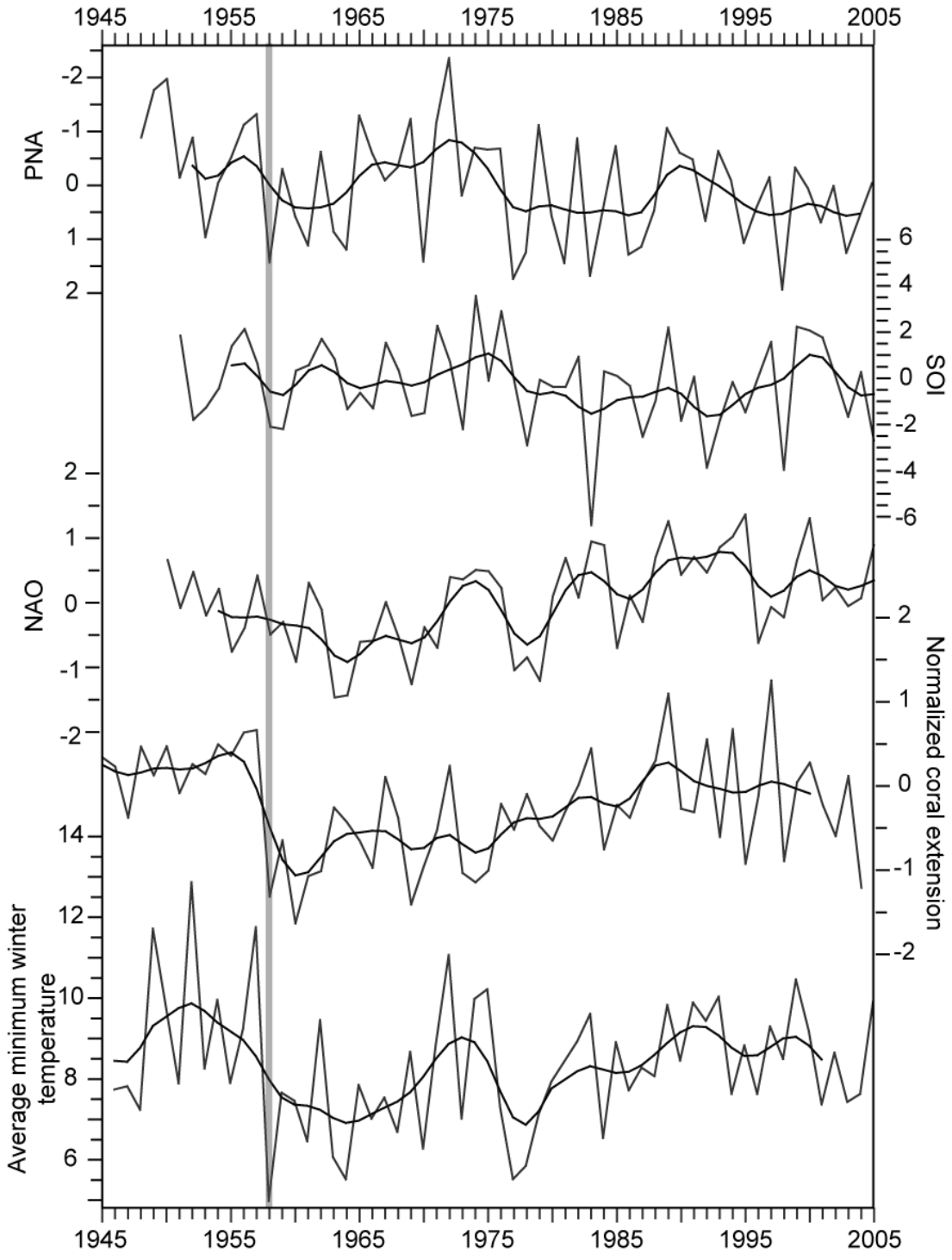

Figure 4-6. Atmospheric circulation indices. The PNA index (note reversed y-axis), SOI, NAO. Normalized coral extension record and average minimum winter temperature at New Orleans are shown for comparison.

period also correlated with a negative phase of the PNA pattern. Extension rates of the corals at the Flower Garden Banks are also quite stable during this time period.

The remainder of the coral extension record for corals at the Flower Garden Banks shows there are some other interesting features. A plot of the average minimum winter air temperatures as recorded in New Orleans, Louisiana [*Williams et al*., 2007] and absolute minimum temperatures at 31˚N and 90˚W [*Erhardt*, 1990] (Figure 4-7) shows a good correlation between winter temperature in the southeastern United States and extension rates of corals at the Flower Garden Banks.

During the winter of 1899, one of the strongest and worst winter storms in American history occurred. The storm affected most of the country and in particular the southeast U.S. [*Erhardt,* 1992]. However, the winter of 1899 does not appear as an anomalously cold winter in the New Orleans average minimum winter temperature record likely because the rest of the winter was relatively mild [*Rogers and Rohli*, 1991].

To what extent is the extreme cold event of the winter of 1899 reflected in the coral growth record? This particular winter event is not apparent in the new coral records that extend back that far. This is likely due to the storm being an isolated event and not causing seawater to cool to the point that it would affect the corals, as it usually requires repeated events to cool the waters at the Flower Garden Banks [*Nowlin and Parker* 1974] significantly and so to impact coral growth. *Hudson and Robbin* [1980] reported an average low extension rate in 1899; however, there is large inter-core variability between the twelve cores they used. *Dodge and Lang* [1983] suggest the minimum average may be an artifact of the fact that only two of the twelve cores extended back that far, which could have introduced a bias in extension rates if all twelve coral cores were not equally weighted. The normalized extension rates for *Hudson and Robbin* [1980] do show a negative extension rate in the late 1890s, but it is not seen in the stacked record since it is not apparent in the new Flower Gardens cores (Figure 4-3). (Note: the normalization process may also introduce a bias to the extension rate records.) *Slowey and Crowley* [1995] use the averaging method of *Hudson and Robbin* [1980] and also report a minimum in extension rate in 1899.

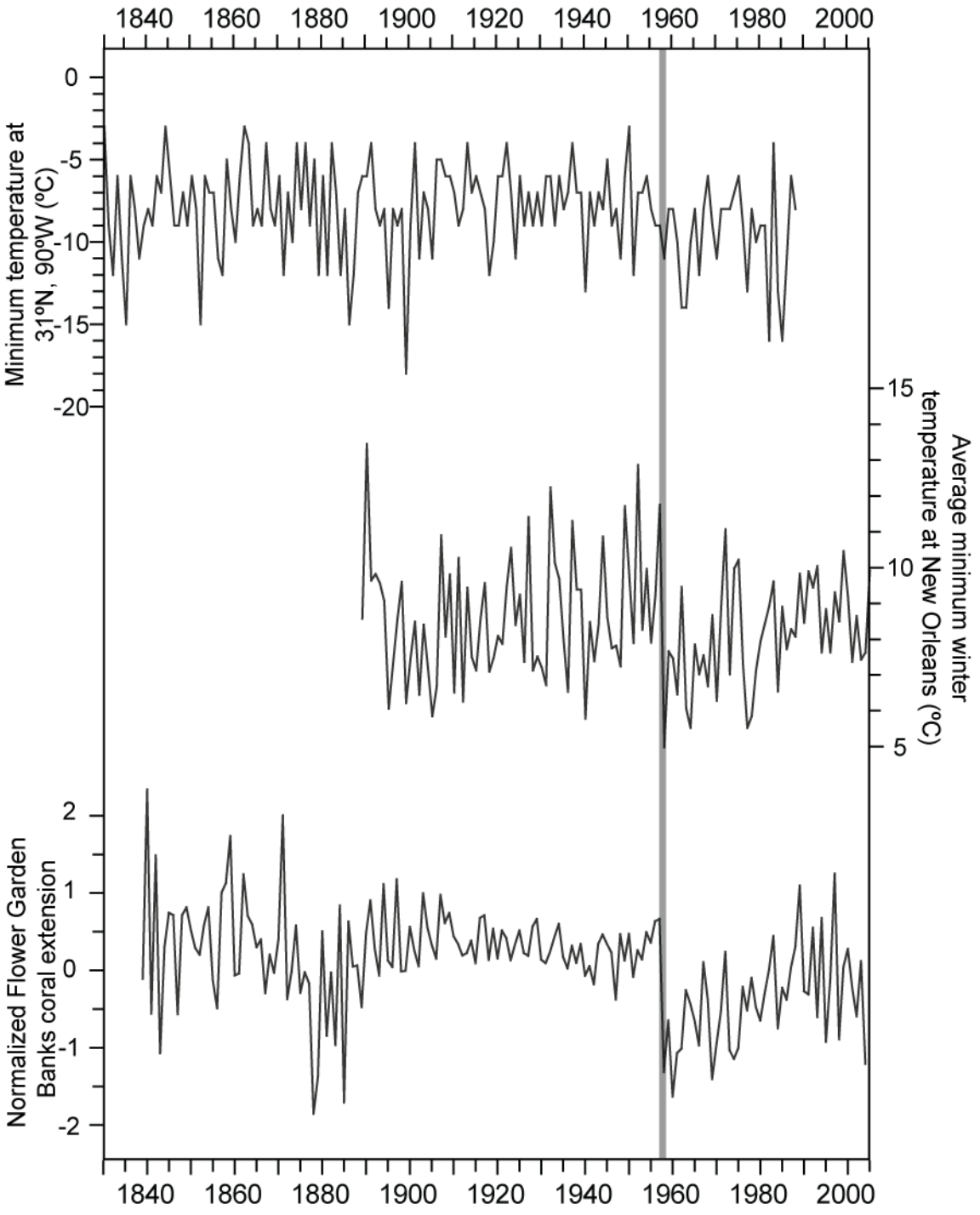

Figure 4-7. Comparison of winter temperatures and coral growth. Average winter minimum temperature at New Orleans, overall minimum temperature at 31°N, 90°W, and normalized Flower Garden Banks coral extension rate.

Another interesting feature seen in the new coral extension records is an extended period of lower extension rates from approximately 1875 to 1890. Low extension is seen in both of the new long extension records described here (EFG1 and WFG2), which extend as far back as 1875 (Figure 4-2). As discussed in the "Methods" section, there are reasons to be cautious when interpreting older portions of long extension records. Nevertheless, there is remarkable agreement between the two records from 1875 to 1890, which is also apparent in the 9-pt smoothed curve. Interestingly, this period has been suggested to be a time of increased ENSO activity [i.e., *Kiladis and Diaz*, 1986; *Urban et al*., 2002] that could also indicate a period of more years when the PNA was positive.

One would expect to see stress-bands in the X-rays of the Flower Garden Banks corals during years of unusually cold winters and when there are repeated passages of cold fronts (i.e., during the positive phase of the PNA pattern). Such repeated passage of cold fronts is associated with a meridional flow of the jet stream and causes vertical mixing of the water column along the shelf, mixing cold surface water down to the coral reef. A stress band is visible in each of the three new coral slabs in the year 1957-58. In fact, during the period between 1957-58 and 1969-1970 there are numerous stress bands in the corals, suggesting a series of years that were stressful to the corals. During the winters of 1952-53, 1957-58, 1960-61, 1963-64, 1969-70, 1976-77, 1977-78, 1980-81, 1982-83, 1985-86, 1986-87, 1994-95, 1997-98, and 2002-03 the phase of the PNA pattern was positive and more winter storms and colder temperatures occurred. Table 4-3 shows the presence of visible stress-bands in the X-radiographs of the coral core slabs. For every winter between 1952-53 and 1977-78 when there was a significantly positive PNA pattern, at least two of the coral cores exhibited a stress band. However, between 1980-81 and 1994-95, during years of a positive PNA pattern, either none of the newly sampled corals exhibit a stress band or only one of three does.

During the same time period, between 1952 and the present, there were many years in which a stress band occurred and the PNA was not significantly positive or was negative. The period between 1948 and 1957 has been suggested to have a more zonal

Table 4-3. Years that coral stress bands occur.

Year	EFG1	EFG2	WFG2	Year	EFG1	EFG2	WFG2
2003		x	x	1968		x	x
2002		x		1967		x	
2001		x		1966	x	x	x
2000				1965	x	x	x
1999				1964	x	x	x
1998	x	x		1963	x	x	x
1997				1962		x	
1996	x	x	x	1961	x	x	x
1995		x		1960	x	x	x
1994		x		1959	x	x	x
1993				1958	x	x	
1992				1957			
1991		x		1956		x	
1990	x			1955		x	x
1989	x	x	x	1954		x	x
1988		x		1953		x	x
1987		x		1952			
1986				1951		x	x
1985			x	1950			
1984		x	x				
1983			x				
1982		x					
1981							
1980							
1979		x	x				
1978	x	x	x				
1977		x	x				
1976		x	x				
1975	x						
1974							
1973	x	x	x				
1972							
1971		x					
1970	x	x	x				
1969		x	x				

path of the North American jet stream and very few years in which the PNA was in a positive phase. However, in cores WFG2 and EFG2 there is a stress band almost every year. Core EFG1 does not exhibit any stress bands during this time interval. A period of major freezes in the southeast U.S. since 1977 was also linked to an increase in the number of winters when the PNA pattern was positive [*Rogers and Rohli*, 1991]. However, very few of these years show a correlation with stress bands in the corals. While the presence of winter high-density stress bands in the coral skeletal record can be a good indication of periods of unusually cold winters in the southeastern U.S. and particularly the northern Gulf of Mexico, there are periods when the correlation does not hold up (i.e., periods with cold winters and the absence of stress bands or periods with more mild winter conditions frequent stress bands) and suggests that water temperature is not the only environmental factor that causes stress bands in the corals. It also suggests that although the PNA is in a positive phase, the jet stream may not be oriented as to divert strong enough and frequent enough cold fronts into the northern Gulf of Mexico to cool shelf waters enough to stress the corals.

CONCLUSIONS AND IMPLICATIONS

Variations in coral growth (as annual extension rates) derived from long-lived corals at the Flower Garden Banks correspond to variations in local and regional climate conditions, particularly winter air temperature. A clear feature seen in the new coral cores described in this study is a significant decrease in the extension rate of the corals at the Flower Garden Banks between the winters of 1956-57 and 1957-58, which is in agreement with results of previous studies of corals at this site [*Hudson and Robbin*, 1980; *Dodge and Lang*, 1983; *Deslarzes*, 1992; *Slowey and Crowley*, 1995]. This decrease in coral extension is correlated with an unusually cold winter in the southeastern U.S. and a positive phase of the PNA pattern, which reflects a meridional orientation of the winter flow of the jet stream over North America. Examination of the variations in the growth of corals from Veracruz, Mexico shows that the effects of this 1957-58 shift in wintertime climate extended to the westernmost Gulf of Mexico as well.

Since corals in southern Florida also show this event [*Hudson et al*., 1976], the effects of the climate event were extremely widespread and included the entire northern Gulf of Mexico. The gulf-wide occurrence of 1957-58 effects on coral growth is consistent with a broadly operative driving mechanism being the cause of the change in coral growth. Thus, it is more likely that coral growth variations at the Flower Garden Banks are controlled by winter climate effects on water temperature [*Slowey and Crowley*, 1995] than by regionally restricted drivers such salt-movement related changes in reef depth [*Rezak and Bright*, 1981] or variations in Mississippi/Atchafalya River discharge [*Dodge and Lang*, 1983].

Slowey and Crowley [1995] proposed that the use of long-lived coral growth records could provide information about the Pacific/North American (PNA) pattern prior to the acquisition of instrumental data currently used to measure variations of atmospheric pressure and the orientation of the jet stream over North America. Given the data here, it is as yet unclear if this will be possible. Changes in coral growth and the occurrence of stress bands clearly do correspond to certain climate signals, such as the 1957-1958 cold climate event and the occurrence of severe winters during the latter half of the twentieth century. However, the correspondence between variations in the coral growth records presented here and climate is less certain during the later half of the nineteenth century and the first half of the twentieth century. Because differences exist between growth records obtained from different corals and the reliability of any individual long coral growth record decreases in the older portions of the record, the number of available long coral growth records is as yet insufficient to evaluate the correspondence between changes in coral growth and climate during these earlier times. With additional long coral records to include with existing long records, individual coral variations can be suppressed and the common patterns will be emphasized. Therefore, it will be necessary to collect additional long records of coral growth before a clear correlation between changes in coral growth and climate can be determined.

CHAPTER V

RADIOCARBON IN CORALS*

INTRODUCTION

Due to the rapid mixing rates in the atmosphere, terrestrial organisms typically exhibit $^{14}C/^{12}C$ concentrations in equilibrium with that of the atmosphere (once corrected for mass dependent fractionation using the discrimination between ^{13}C and ^{12}C). Alternately, marine organisms generally deposit their carbonate shells close to isotopic equilibrium with the seawater in which they are living (deriving carbon from the DIC of the surrounding water). Because of the large carbon reservoir of the oceans and the rates in which carbon mixes across the ocean-atmosphere boundary and across the interface between the ocean's surface mixed layer and underlying waters, the surface mixed layer of the ocean is depleted in ^{14}C relative to the atmosphere. This causes marine organisms to exhibit an apparent ^{14}C age greater than their contemporaneous terrestrial counterparts. It is therefore necessary to apply a correction in order to compare marine and terrestrial samples. This correction is termed the marine reservoir age, R, [*Stuiver et al.*, 1986] and is the difference in years between the measured ^{14}C age of a marine organism's carbonate shell and the atmospheric ^{14}C age at the time as reported in the terrestrial calibration curve, IntCal04 [*Reimer et al.*, 2004]. Additionally, a regional correction designated as ΔR [*Stuiver and Braziunas*, 1993] is needed to adjust for the difference between the regional reservoir age and the nominal average global marine reservoir age for surface ocean waters, as modeled, using a one dimensional ocean-atmosphere box diffusion model [*Oeschger et al.*, 1975]. Due to temporally and spatially varying oceanographic processes that can influence surface water ^{14}C, the regional reservoir age can differ greatly from the global marine average. Therefore, it is

---

* Part of this chapter is reprinted with permission from "Pre-bomb surface water radiocarbon of the Gulf of Mexico and Caribbean as recorded in hermatypic corals" by A.J. Wagner, T.P. Guilderson, N.C. Slowey, and J.E. Cole, 2009, *Radiocarbon*, *50*, in press, Copyright 2009 by the Arizona Board of Regents on behalf of the University of Arizona.

important to know the regional correction (ΔR) when calibrating marine samples with the internationally ratified marine calibration curve, Marine04 [*Hughen et al.*, 2004a]. At present, only a few studies have computed the reservoir age and ΔR in the Caribbean, and there have been no studies within the Gulf of Mexico.

The large amount of bomb-produced radiocarbon (^{14}C) introduced into the atmosphere during the 1950s and 1960s by the atmospheric testing of nuclear weapons led to elevated ^{14}C levels in atmospheric CO_2 that reached a peak in 1963 [*Nydal and Loveseth*, 1983] and has since gradually declined as this 'pulse' of 'bomb' $^{14}CO_2$ has been exchanged with the ocean and terrestrial reservoirs. Oceanic uptake of the bomb-^{14}C pulse by the transfer of carbon between the atmosphere and surface waters of the ocean as $^{14}CO_2$ provides a valuable tracer of the air-sea $^{14}CO_2$ exchange over the last half-century. Exchange of $^{14}CO_2$ between the atmosphere to the surface ocean and from the surface to subsurface waters is important because it reflects fundamental oceanic processes and provides insight into the oceanic fate of CO_2 produced by the burning of fossil fuels. The extent to which ^{14}C can be employed as an oceanographic tracer depends upon our understanding of the $\Delta^{14}C$ of surface waters and how this value has varied through time. Bomb radiocarbon in surface ocean dissolved inorganic carbon (DIC) shows high spatial variability in the $\Delta^{14}C$ values of different water masses because of the large ocean/atmosphere gradient in $\Delta^{14}C$. ^{14}C enters the ocean through gas exchange with the atmosphere with an equilibration time of seven to ten years [*Broecker and Peng*, 1982; *Mahadevan*, 2001; *Sweeney et al.*, 2007]. One would expect to see the bomb-^{14}C maximum in the surface ocean delayed by approximately that amount of time with respect to that in the atmosphere.

Direct measurements of radiocarbon in the atmosphere and the ocean are rather limited. Atmospheric $\Delta^{14}C$ measurements have documented the rapid increase of radiocarbon in the atmosphere due to nuclear weapons testing in the mid-20th century [*Nydal and Loveseth*, 1983; *Levin et al.*, 1985; *Manning et al.*, 1990; *Levin and Kromer*, 1997], including a large hemispheric difference in the timing and amplitude of the bomb radiocarbon peak. Since these measurements are non-existent prior to the mid-1950s

and limited since, atmospheric ^{14}C proxy data are required in order to study the history of ^{14}C. Understanding of past $\Delta^{14}C$ of the atmosphere comes largely from the $\Delta^{14}C$ measurements of tree-rings [*Stuiver and Quay*, 1981; *Stuiver et al*., 1998; *McCormac et al*., 2004]. $\Delta^{14}C$ measurements in the ocean are very sparse in both space and time [e.g. *Nydal*, 2000]. Data were collected during GEOSECS and WOCE cruises; however, these data only provide a one time snap-shot at each location. Prior to GEOSECS, there are very few synoptic studies of the distribution of radiocarbon in the ocean. The spread of bomb produced ^{14}C through the oceans since the 1950s has provided a unique opportunity to study the circulation of different water masses in the oceans and air-sea interactions. However, to explore the ocean dynamics and spatial distribution, time-series of the changes in ocean ^{14}C content are needed to best utilize this tracer.

While direct $\Delta^{14}C$ measurements of this kind do not exist, proxy records, such as the ^{14}C content of coral skeletal material, can be used to estimate how the $\Delta^{14}C$ of the ocean has changed over time. Coral $\Delta^{14}C$ is a good water mass tracer due to the fact that corals incorporate seawater DIC into their carbonate skeletons. Many pre- and post-bomb coral $\Delta^{14}C$ records for the surface waters of the Atlantic, Pacific, and Indian Oceans have been previously reported [*Nozaki et al*., 1978; *Druffel*, 1987; *Guilderson et al*., 1998; *Guilderson et al*., 2000; *Druffel et al*., 2004; *Grumet et al*., 2004]. These records have yielded important information about ocean circulation, ocean ventilation, upwelling, and air-sea exchange of CO_2. However, few records exist in the Caribbean Sea and Gulf of Mexico [e.g., *Druffel*, 1980; *Guilderson et al*., 2005].

Radiocarbon measurements on coral skeletal material from four sites are presented here. The first half of the study will present ^{14}C reservoir age and ΔR estimates based on pre-bomb $\Delta^{14}C$ in marine carbonates from four localities in the Caribbean and Gulf of Mexico. These values are important in calibrating the radiocarbon ages of carbonate samples from the Gulf of Mexico and Caribbean Sea. The second half will address the pre- to post-bomb ^{14}C signature in the surface waters of the Caribbean and Gulf of Mexico and what this may imply about the air-sea interaction and the origin of the surface water. These data at the four sites span the pre- to post-bomb period when

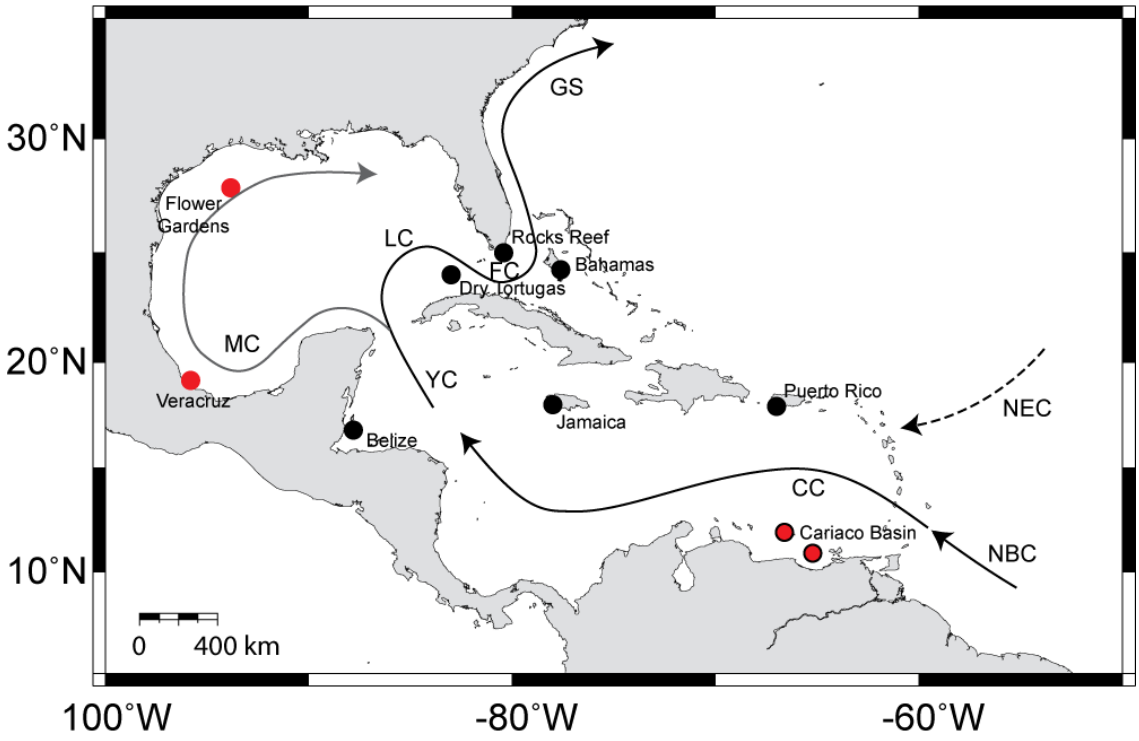

Figure 5-1. Radiocarbon sites in the Caribbean Sea and Gulf of Mexico. Existing sites are in black and new sites from this study are in red. Some major surface currents are labeled (CC - Caribbean Current, FC - Florida Current, GS - Gulf Stream, LC - Loop Current, MC - Mexican Current, NBC - North Brazil Current, NEC - North Equatorial Current, and YC - Yucatan Current).

$\Delta^{14}C$ increased due to the input of radiocarbon into the atmosphere as a result of nuclear weapons testing. These data are compared with previously published data from the Caribbean, Atlantic, and eastern Gulf of Mexico (Figure 5-1). All data show a similar $\Delta^{14}C$ pattern from the pre- to post-bomb period when $^{14}CO_2$ was exchanged between the atmosphere and ocean. This paper puts modern radiocarbon signatures in a context to understand past variability.

BACKGROUND

The bulk of nuclear weapons testing occurred during the late 1950s and early 1960s in the northern hemisphere, which caused a difference in the amplitude and timing of the peak $\Delta^{14}C$ curve between the Northern and Southern Hemispheres. $\Delta^{14}C$ in the Northern Hemisphere reaches a maximum almost 150% greater than that seen in the Southern Hemisphere, and reaches that maximum a year and a half earlier. A similar pattern is expected in the ocean (Figure 5-2), with the predicted post-bomb peak approximately a decade after the atmospheric $\Delta^{14}C$ maximum.

Radiocarbon in the surface ocean can be used as a water mass tracer due to the age of water and how long since it has interacted with the atmosphere. The two primary processes that affecting the $\Delta^{14}C$ of the surface ocean are (1) the rate at which the surface water equilibrates with the atmosphere (which is related to the residence time of the water at the surface where gas exchange occurs) and (2) the hydrographic regime of the area (i.e. the origination of the source water). This chapter discusses the relative importance of these processes in regards to the $\Delta^{14}C$ of surface water in the Atlantic Ocean.

Hydrographic conditions of individual areas impact the surface ocean $\Delta^{14}C$. Surface water in the subtropical gyres of the Atlantic Ocean has long residence times and high rates of gas exchange with the atmosphere leading to (comparatively) higher $\Delta^{14}C$. In contrast, surface water in equatorial regions is subject to vertical mixing with ^{14}C-depleted water that is upwelled from depths and has lower $\Delta^{14}C$. The lower $\Delta^{14}C$ of deeper waters is due to the water being out of contact from the atmosphere for a long

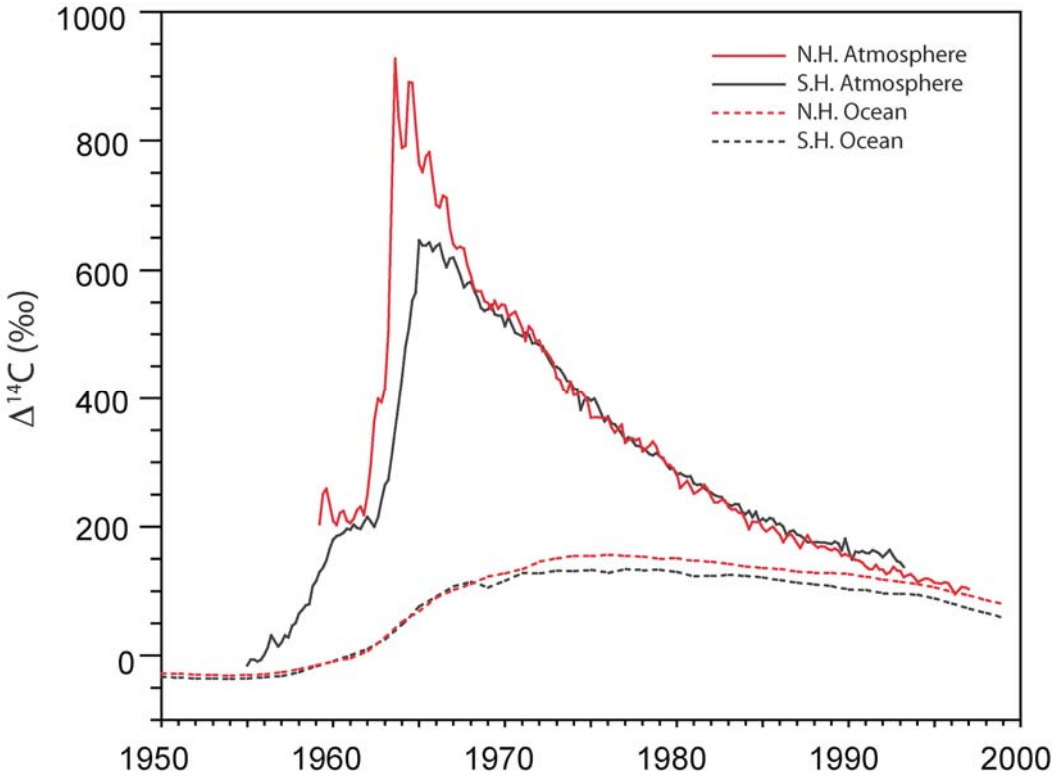

Figure 5-2. Atmospheric and modeled ocean $\Delta^{14}C$. Solid red line – northern hemisphere atmospheric $\Delta^{14}C$ [*Nydal and Loveseth*, 1983]; solid grey line – southern hemisphere atmospheric $\Delta^{14}C$ [*Manning et al*., 1990]; dashed red line – northern hemisphere modeled ocean $\Delta^{14}C$ [*Rodgers et al*., 1999]; dashed grey line – southern hemisphere modeled ocean $\Delta^{14}C$ [*Rodgers et al*., 1999].

enough time for ^{14}C decay to decrease the ^{14}C content in the water. Direct oceanic ^{14}C measurements by *Broecker and Olson* [1961] showed that the $\Delta^{14}C$ difference between the North Atlantic gyre and south equatorial region was approximately 10‰ prior to the effect of bomb radiocarbon on the surface ocean.

Understanding South Atlantic circulation is important to place the ^{14}C signal found in the coral records from the Caribbean and Gulf of Mexico in a larger context. The source of Benguela Current is thought to be from three primary sources: The South Atlantic Current (the southern limb of the South Atlantic subtropical gyre), the Agulhas Current coming from the Indian Ocean around the southern tip of South Africa, and sub-Antarctic water from the Antarctic Circumpolar Current [*Gordon et al.*, 1992; *Garzoli and Gordon*, 1996]. The Benguela Current begins as a northward flow off the southern tip of South Africa and bends toward the northwest and separates from the African coast around 30°N. The prevailing south and southeasterly winds drive offshore surface drift and coastal upwelling of cold, nutrient-rich water. The Benguela Current then feeds into the broad South Equatorial Current that flows westward toward the eastern coast of South America where it bifurcates into the North Brazil Current and the Brazil Current [*Peterson and Stramma*, 1991]. More of the water from the South Equatorial Current goes into the North Brazil Current and continues into the northern hemisphere which partially accounts for the net transport of upper-level water from the South Atlantic into the Northern hemisphere. The Benguela Current transports approximately 21 Sv north toward 32°S where it begins to turn northwestward, carrying about 18 Sv of surface water across 28°S. Approximately 4 – 5 Sv of Antarctic Intermediate Water is observed to flow northward with the Benguela Current. Near 28°S, most of the current turns to the west while approximately 3 Sv drifts to the north. At 15°S the surface flow is primarily to the west [*Stramma and Peterson*, 1989].

The Industrial Effect (or Suess Effect, as it is called after it was first reported by Hans Suess in the 1950s) is caused by the addition of ^{14}C-free CO_2 to the atmosphere due to the burning of fossil fuels [*Suess*, 1955]. Fossil fuels are devoid of ^{14}C due to the age of the materials used to produce fossil fuels (i.e. coal and petroleum). Thus, CO_2

emitted by the combustion of fossil fuels is free of ^{14}C and, in effect, diluted the atmospheric radiocarbon signal since the late 19th century until the large input of radiocarbon to the atmosphere due to nuclear weapons testing in the late 1950s and early 1960s [*Stuiver and Quay*, 1981].

METHODS

Coral cores were collected from live corals using diver-operated underwater hydraulic drilling equipment. All specimens are of the species *Montastrea faveolata,* a common Caribbean reef-building hermatypic coral that exhibits regular annular banding [*Goreau*, 1959; *Hudson et al*., 1976; *Fairbanks and Dodge*, 1979, *Dodge and Lang*, 1983]. Two coral cores each from the Gulf of Mexico and the Cariaco Basin were used in this study (Figure 2-1). The first was collected in May 1990 from the Flower Garden Banks National Marine Sanctuary (93°50'W, 27°52'N) in approximately 20 m of water. The second specimen from the Gulf of Mexico is from Santiaguillo Reef (95°48.5'W, 19°08.3'N), which is located approximately 20 km off the coast of Veracruz, Mexico in the western Gulf of Mexico. The coral grew in approximately 6 m of water and was drilled in 1991. The two coral cores from the Cariaco Basin (Figure 2-5) used in this study are from Boca de Medio Island (66°36'W, 11°55'N) and Isla Tortuga (65°21'W, 10°53'N). Boca de Medio is located in the Los Roques archipelago, outside of the Cariaco Basin proper. The sample was drilled in July 1998. Isla Tortuga is located at the northern margin of the Cariaco Basin. The coral core was collected from the southern coast of the island in March 1996 in water depth of approximately 2 m. For a more detailed description of the sampling sites, see Chapter II.

The cores were cut into ~10 mm slabs, cleaned and air-dried. Coral slabs were X-rayed to determine the high and low density band couplet. Ages were assigned using the density bands and counting back from the top of the core. Based on published literature, high-density bands were assumed to have formed during the boreal summer season [e.g., *Hudson et al*., 1976; *Fairbanks and Dodge*, 1979], typically during the warmest months of July, August and September. The age model for the samples is

assumed to be accurate within one year, except for the Isla Tortuga core. There is more uncertainty in the age model for this core due to breaks in the slab and difficulty in piecing together the X-ray images. A break in the coral slab during the late 1950s was adjusted using the radiocarbon peak compared to the timing of the peak from the Boca de Medio coral core. This coral core had very clear annual bands and there was no difficulty in determining the chronology for this core, which is why it was used to adjust the Isla Tortuga core. Samples were micromilled from the respective slabs to obtain calcium carbonate from the corals for radiocarbon analysis. Annual samples for years 1945 – 1954 were chosen for analysis in this study because of the years of overlap between the individual coral cores prior to atmospheric nuclear weapons testing. Radiocarbon measurements were made at the Center for Accelerator Mass Spectrometry (CAMS) at the Lawrence Livermore National Laboratory [*Davis et al*., 1990]. Annual samples of approximately 10 mg were placed in individual vacutainers, evacuated, heated and acidified with orthophosphoric acid at 90°C. The resultant CO_2 was then converted to graphite in the presence of an iron catalyst [*Vogel et al*., 1987]. Radiocarbon results are reported as age-corrected $\Delta^{14}C$ (‰) as defined by [*Stuiver and Polach*, 1977] and include a background and $\delta^{13}C$ correction. Reproducibility of results is better than ±3.5‰ (1σ) based on an in-house coral process standard. All radiocarbon data are listed in Appendix C.

Coral radiocarbon measurements are compared to the internationally approved marine radiocarbon calibration curve known as Marine04 [*Hughen et al*., 2004a]. Marine04 estimates the global ocean ^{14}C ages between 0 and 26 cal kyr BP. From 0 to 10.5 cal kyr BP, the Marine04 curve is derived from the IntCal04 tree-ring based curve [*Reimer et al*., 2004] that is estimated by a random walk model (RWM) [*Buck and Blackwell*, 2004] and then used as input into a global ocean-atmosphere box diffusion model [*Stuiver and Braziunas*, 1993] to predict ocean mixed-layer ^{14}C ages. The model is forced with a prescribed atmospheric $\Delta^{14}C$ and pCO_2 and then uses an average air-sea exchange coefficient to 'flux' $^{14}CO_2$ between the ocean and atmosphere. The coefficients were tuned to yield a pre-bomb surface $\Delta^{14}C$ of -50‰ and $\Delta^{14}C$ consistent with

the deep Pacific as documented during GEOSECS. Output from the global ocean-atmosphere box diffusion model are combined with coral and foraminiferal ^{14}C data (for 10.5 to 26 cal kyr BP) using the RWM to derive the Marine04 curve [*Hughen et al.*, 2004a]. Regional surface excursions from this predicted "global" average are due to oceanographic processes, as previously discussed [*Stuiver et al.*, 1998]. To calibrate marine ^{14}C ages using Marine04, it is necessary to know ΔR for the region of interest.

PRE-BOMB RESULTS AND DISCUSSION

Coral $\Delta^{14}C$ pre-bomb data from this and previous studies are shown in Figure 5-3. The average $\Delta^{14}C$ of the four new records from this study during the time period 1945 – 1954 is -52.9 ± 0.5‰ (n = 32). Prior to nuclear weapons testing, the $\Delta^{14}C$ variability in the atmosphere was relatively stable. The atmospheric $\Delta^{14}C$ average was approximately -6.5‰ between 1850 and 1900 and there is little difference between the northern and southern hemisphere (approximately 5‰) [*Nydal and Loveseth*, 1983; *Manning et al.*, 1990]. Direct surface ocean ^{14}C measurements between July 1955 and December 1957 by *Broecker and Olson* [1961] showed the $\Delta^{14}C$ difference between the North Atlantic gyre and south equatorial region was approximately 8‰ (-47‰ and -55‰ respectively) prior to the effect of bomb radiocarbon on the surface ocean. As seen in Figure 5-3, coral data from samples in the Gulf of Mexico, Caribbean, and Florida show little difference from each other during the pre-bomb period. However, there is much greater variability than that seen in atmospheric $\Delta^{14}C$ indicating that processes other than gas exchange affect the $\Delta^{14}C$ of the ocean. The few pre-bomb coral measurements available from southern hemisphere Brazilian corals (average $\Delta^{14}C$ of -58.7 ± 1.0‰ [*Druffel*, 1996]) fall within the range of the northern hemisphere Atlantic coral measurements and indicate a small hemispheric difference between $\Delta^{14}C$ in corals from the northern and southern hemispheres exists. During the years that the records overlap (1945 - 1954) and prior to the atmospheric nuclear weapons testing, all four new records show similar $\Delta^{14}C$ values (Table 5-1). The mean Flower Garden Banks $\Delta^{14}C$ is

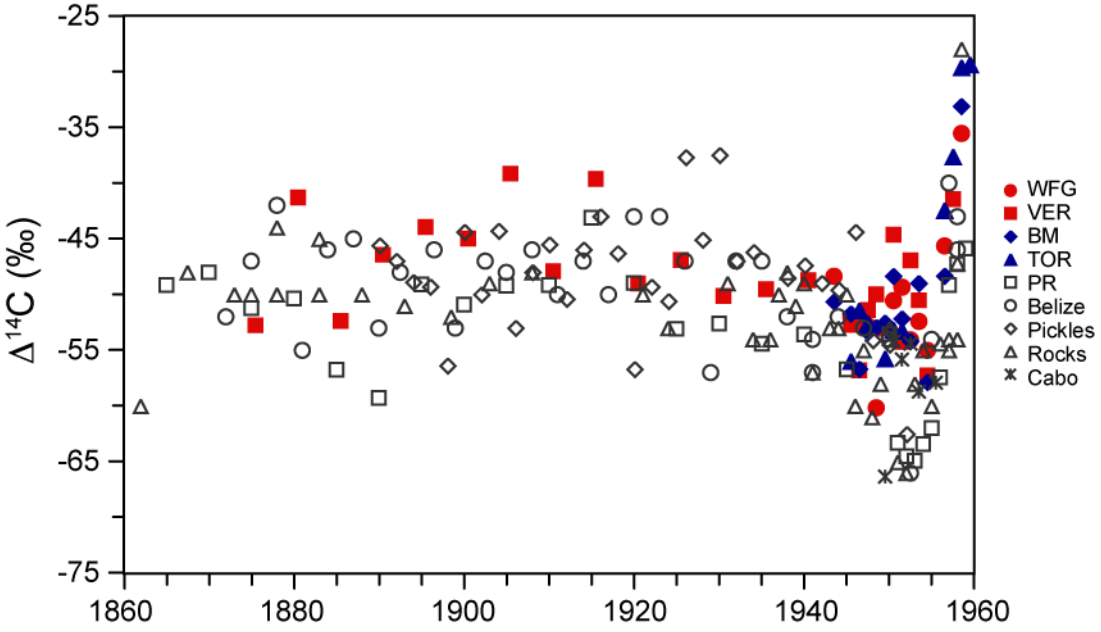

Figure 5-3. $\Delta^{14}C$ data for all coral cores during the pre-bomb period. Solid, colored symbols are from this study (WFG – West Flower Garden Bank; VER – Veracruz, Mexico, BM – Boca de Medio, Cariaco Basin, TOR – Isla Tortuga, Cariaco Basin) and open, black symbols are previously published data (PR – Puerto Rico [*Kilbourne et al*., 2007], Belize [*Druffel*, 1980], Pickles Reef, Florida [*Druffel*, 1997], Rocks Reef, Florida [*Druffel and Linick*, 1978; *Druffel*, 1982], Cabo Albrohos, Brazil [*Druffel*, 1996]).

Table 5-1. Radiocarbon information for coral samples used in this study. Age corrected $\Delta^{14}C$, conventional ^{14}C age of sample, computed reservoir age and computed ΔR. $\Delta^{14}C$ and ^{14}C ages are calculated using weighted average of individual data points. Variance is weighted mean measurement error.

Site	Midpoint (year)	$\Delta^{14}C$ (‰) (age corrected)	^{14}C Age (conventional)	Reservoir Age (years)	ΔR (years)
Flower Garden Banks	1950 (n=9)	-53.2 ± 1.0	439 ± 9	240 ± 13	-30 ± 26
Veracruz, Mexico	1950 (n=10)	-51.9 ± 1.1	428 ± 10	229 ± 13	-41 ± 26
Gulf of Mexico Avg	1950 (n=19)	-52.6 ± 0.7	434 ± 7	235 ± 11	-36 ± 25
Boca de Medio	1950 (n=10)	-53.2 ± 1.0	438 ± 9	239 ± 13	-31 ± 26
Isla Tortugas	1950 (n=3)	-53.9 ± 1.5	447 ± 14	248 ± 17	-22 ± 28
Caribbean Avg	1950 (n=13)	-53.4 ± 0.8	441 ± 8	242 ± 12	-28 ± 25
Veracruz, Mexico	1885 (n=5)	-47.6 ± 1.5	456 ± 14	354 ± 15	-13 ± 27

-53.2 ± 1.0‰ (n = 9), the Veracruz, Mexico average $\Delta^{14}C$ is -51.9 ± 1.1‰ (n = 10), the average Boca de Medio $\Delta^{14}C$ is -53.2 ± 1.0‰ (n = 10), and the Isla Tortuga mean $\Delta^{14}C$ is -53.9 ± 1.5‰ (n = 3). The two Gulf of Mexico records combined have an average $\Delta^{14}C$ of -52.6 ± 0.7‰ (n = 19) and the two Cariaco Basin records have an average $\Delta^{14}C$ of -53.4 ± 0.8‰ (n = 13).

The $\Delta^{14}C$ of samples from the Veracruz, Mexico coral core were measured to 1875. The pre-bomb average for the Veracruz, Mexico coral samples from 1875 through 1940 is -47.0 ± 0.9‰, Belize is -48.2 ± 0.7‰ [*Druffel*, 1980], Rocks Reef is -49.5 ± 1.0‰ [*Druffel and Linick*, 1978; *Druffel*, 1982], Pickles Reef is -47.3 ± 0.6‰ [*Druffel*, 1997], Bermuda is -43.9 ± 0.5‰ [*Druffel*, 1989; *Druffel*, 1997], and Puerto Rico is -51.7 ± 0.8‰ [*Kilbourne et al*., 2007]. There are a few pre-bomb samples from the Cariaco Basin reported in *Guilderson et al*. [2005] that are within the average range of other Caribbean coral $\Delta^{14}C$. These are compared to the internationally ratified calibration curve, Marine04, which has an average of -50.6 ± 0.7‰ [*Hughen et al.*, 2004a].

The $\Delta^{14}C$ of the Northern Hemisphere atmosphere in 1950 as recorded in tree rings is -24.5 ± 1.1‰ [*Reimer et al.*, 2004] and the $\Delta^{14}C$ of the global ocean as derived from the Marine04 model is -56.7 ± 2.8‰ [*Hughen et al*., 2004a]. These results yield average reservoir ages of 235 ± 11 years (ΔR of -36 ± 25 years) and 242 ± 12 years (ΔR of -28 ± 25 years) in the Gulf of Mexico and Cariaco Basin, respectively. Surface water $\Delta^{14}C$ in the Gulf of Mexico and Cariaco Basin are so similar due to the rapid transport between the basins with relatively little modification of the surface water masses. Because of the rapid surface circulation of the region, it is reasonable to combine the Caribbean and Gulf of Mexico data to obtain values representative of the entire region. The average reservoir age and ΔR for the entire Gulf of Mexico/Caribbean Sea region are 238 ± 10 years and -32 ± 25 years, respectively. These values compare well to an average reservoir age of 280 ± 44 years and ΔR of 10 ± 49 years for all previously published data from the region (Table 5-2).

Table 5-2. All previously reported reservoir ages and ΔR values for the Gulf of Mexico and Caribbean Sea.

Site	Year	Reservoir Age	ΔR	Reference	Material
Bahamas	1950	229 ± 43	-40 ± 42	*Broecker and Olsen* [1961]	Gastropod
Bahamas	1885	423 ± 59	56 ± 59	*Broecker and Olsen* [1961]	Gastropod
The Rocks, FL Keys	1950	281 ± 21	11 ± 31	*Druffel* [1980]	Coral
The Rocks, FL Keys	1850	405 ± 18	33 ± 16	*Druffel and Linick* [1978]; *Druffel* [1982]	Coral
Tortugas, FL	1884	482 ± 52	114 ± 51	*Lighty et al.* [1982]	Coral
Golden Cay, Bahamas	1912	493 ± 66	146 ± 66	*Lighty et al.* [1982]	Coral
Gulf of Honduras, Belize	1950	259 ± 20	-11 ± 30	*Druffel* [1980]	Coral
Jamaica	1884	323 ± 42	-44 ± 41	*Broecker and Olsen* [1961]	Gastropod
Jamaica	1930	273 ± 43	-30 ± 42	*Broecker and Olsen* [1961]	Gastropod
La Parguera, Puerto Rico	1950	306 ± 14	36 ± 26	*Kilbourne et al.* [2007]	Coral
La Parguera, Puerto Rico	1885	402 ± 13	35 ± 26	*Kilbourne et al.* [2007]	Coral
Cariaco Basin, Venezuela	1935	336 ± 61	33 ± 60	*Hughen et al.* [2004b]	Foraminifera
Cariaco Basin, Venezuela	1910	361 ± 50	12 ± 50	*Hughen et al.* [2004b]	Foraminifera
Isla Tortuga, Venezuela	1941	264 ± 41	-22 ± 40	*Guilderson et al.* [2005]	Coral
Isla Tortuga, Venezuela	1906	290 ± 41	-70 ± 40	*Guilderson et al.* [2005]	Coral
Boca de Medio, Venezuela	1945	256 ± 42	-18 ± 41	*Guilderson et al.* [2005]	Coral
Los Testigos, Venezuela	1940	285 ± 43	-1 ± 42	*Guilderson et al.* [2005]	Coral

The sample from Veracruz, Mexico extends before the time of significant industrialization and the derived $\Delta^{14}C$ reconstruction lacks any visible Suess Effect in its earliest years. A similar lack of a visible Suess Effect is seen in data from Puerto Rico [*Kilbourne et al*., 2007] and Bermuda [*Druffel*, 1997]. Therefore, we do not make any attempt to correct for the Suess Effect.

The small ΔR values for the Caribbean and Gulf of Mexico region imply good agreement with the 1-D marine model and the atmospheric curve used to derive the Marine04 curve and estimate the "global" marine surface water ^{14}C age. This implies common source waters and similar residence times of the source waters feeding this region. This also implies that the source waters that feed the Caribbean and Gulf of Mexico and the air-sea exchange of CO_2 in this region are close to the global average. Therefore, for the pre-bomb period the global marine model can be used to provide a reasonable estimate of the ^{14}C age of marine samples for the Caribbean and Gulf of Mexico for modern times (i.e., when boundary conditions in the area are as they are today).

For times in the past when different climatic/oceanographic regimes existed, one cannot make this same assumption. For example, a change in the relative proportions of surface water from the North and South Atlantic would have an impact on the reservoir and ΔR ages of the region. The ΔR calculated from a coral off southern Puerto Rico is 36 ± 26 years [*Kilbourne et al*., 2007] compared to -32 ± 25 years for the Caribbean. The difference between the values is likely due to the difference in source water to the areas (Northern Atlantic via the North Equatorial Current versus equatorial waters via the North Brazilian Current).

POST-BOMB RESULTS AND DISCUSSION

$\Delta^{14}C$ time histories in the Atlantic rose from pre-bomb values of -50‰ to values in excess of 120‰ following the peak in nuclear weapons testing. However, time series curves of $\Delta^{14}C$ from corals at different locations in the tropical Atlantic show variations in the shape, amplitude and timing of the surface ocean radiocarbon post-bomb peak.

Consistent with the signal being a direct response to atmospheric $^{14}CO_2$ exchange [e.g., *Mahadevan*, 2001], beginning in the late 1950s the $\Delta^{14}C$ measured in tropical and subtropical Atlantic corals began to rapidly increase. During this period the gradient between the $\Delta^{14}C$ of the ocean and atmosphere is at a maximum and the $\Delta^{14}C$ of the surface water, and therefore that of the corals bathed in the water, is significantly influenced by gas exchange with the atmosphere. However, the difference between the Gulf of Mexico corals and those sampled from the Cariaco Basin off the coast of Venezuela is greater than 30‰ (Figure 5-4). In comparison to previous studies, the maximum values at the Flower Garden Banks (158.4 ± 3.5‰) and Santiguillo Reef (159.4 ± 4.1‰) are similar to those seen at the Rocks Reef in Florida [*Druffel and Linick*, 1978; *Druffel*, 1982] and Belize [*Druffel*, 1980] with values of 152.4‰ and 151.3‰, respectively. Interestingly, the maximum $\Delta^{14}C$ values determined for the Cariaco corals (127.0 ± 3‰ and 127.0 ± 4‰ for Boca de Medio and Isla Tortuga, respectively) are close to the value reported by *Druffel* [1996] for Cabo Albrohos off the coast of Brazil (137.8 ± 2.3‰).

Why is the gradient between the northern hemisphere ocean and southern hemisphere ocean so great during the post-bomb interval? The surface water in the south equatorial current is subject to vertical mixing with ^{14}C-depleted water that is entrained into the Benguela current from the Indian Ocean and has a reservoir age on the order of 600 years [*Southon et al*., 2002] which is then transported across the Atlantic. Sub-surface water is older and therefore has a lower $\Delta^{14}C$ value than water that has been in recent contact with the atmosphere such as the surface water in the subtropical gyre of the North Atlantic. The ocean effect on the atmospheric ^{14}C gradient between the northern and southern hemispheres has been modeled [*Stuiver and Braziunas*, 1998; *Levin et al*., 1985; *Braziunas et al*., 1995] and the relative depletion of ^{14}C in the southern hemisphere atmosphere has been attributed to ocean circulation and CO_2 exchange between the ocean and atmosphere [*McCormac et al*., 2002]. The southern ocean, with a surface area approximately 150% larger than that of the northern hemi-

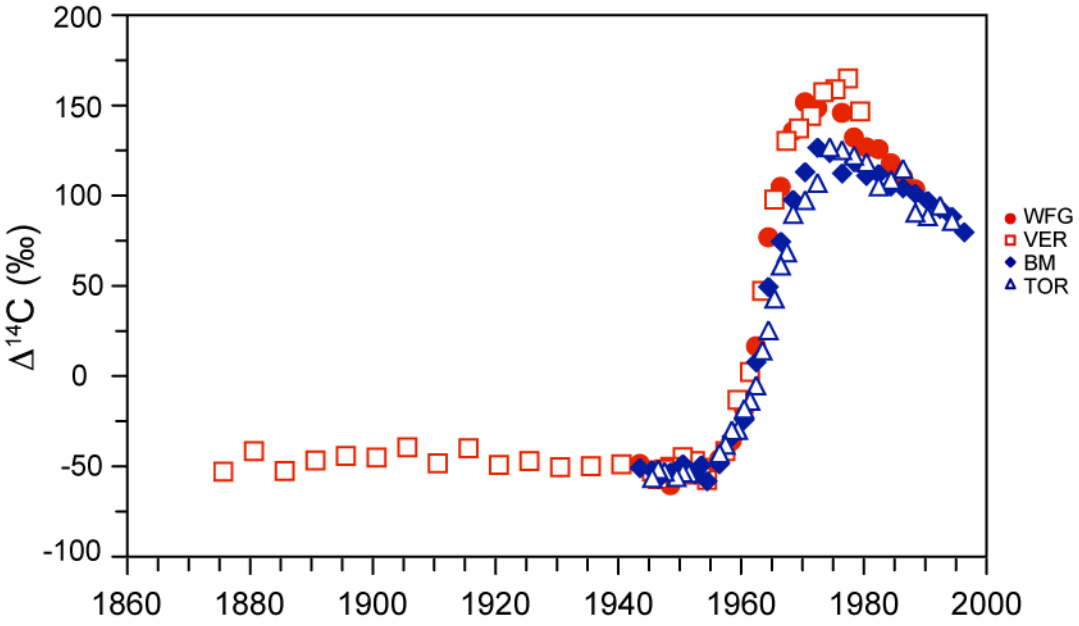

Figure 5-4. $\Delta^{14}C$ of coral samples analyzed in this study (WFG – West Flower Garden Bank; VER – Veracruz, Mexico, BM – Boca de Medio, Cariaco Basin, TOR – Isla Tortuga, Cariaco Basin).

sphere, is depleted in ^{14}C reflecting older, deeper waters at the surface in the southern hemisphere.

The difference between the Gulf of Mexico corals and those sampled from the Cariaco Basin was not expected. However, while atmospheric equilibration is significantly important during this time period, the influence of surface advection and source waters cannot be disregarded. The South Equatorial Current originates off the west coast of Africa and travels across the Atlantic at approximately 10°S. It reaches the coast of Brazil and diverges to the south as the Brazil Current and northward as the North Brazil Current and into the Caribbean. Therefore, the origin of the water that is entering the Cariaco Basin is primarily from the southern hemisphere [*Stramma and Peterson*, 1989; *Fratantoni*, 2001; *Centurioni and Niiler*, 2003]. To test this hypothesis, the data collected here were compared to $\Delta^{14}C$ results from a coral off the coast of Brazil at Abrolhos Bank. This coral exhibits a similar post-bomb sequence as that seen in the Cariaco corals. The maximum $\Delta^{14}C$ of 137.8 ± 2.3‰ is reached between 1974 and 1975. The maximum $\Delta^{14}C$ at Cariaco Basin is 127.1 ± 2.5‰. Figure 5-5 shows the differences in the timing and amplitude of the $\Delta^{14}C$ of the four corals analyzed for this study in addition to the other coral $\Delta^{14}C$ data previously published.

SUMMARY AND CONCLUSIONS

Estimates of the surface water radiocarbon concentration in the Caribbean Sea and Gulf of Mexico are presented. Prior to the effects of atmospheric nuclear weapons testing in the 1950s and 1960s, the average $\Delta^{14}C$ for the region is -52.9 ± 0.5‰. This yields an average reservoir age of 238 ± 10 years and ΔR of -32 ± 25 years. These values are close to previously published reservoir ages and ΔR ages for the Caribbean. The relatively small ΔR ages compared to the marine 1-D model suggest the internationally ratified Marine04 curve is a reasonable approximation for this region for the modern oceanographic regime. This may not be the case during the past when significantly different oceanographic and climatic regimes existed. The smaller reservoir age compared to the marine model is consistent with short residence times in

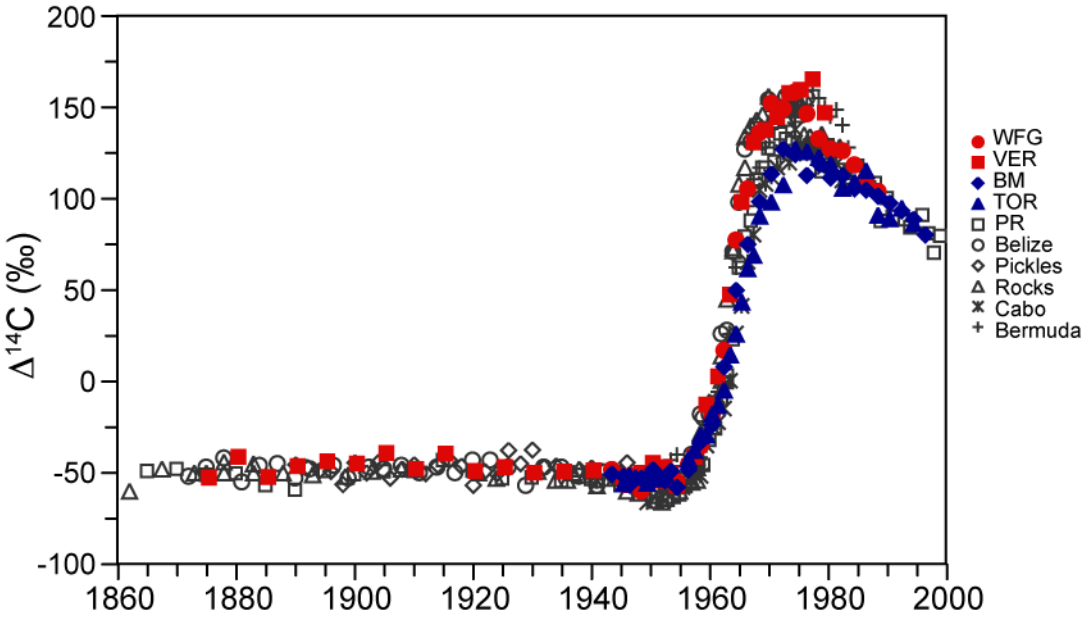

Figure 5-5. $\Delta^{14}C$ of all coral samples used in this study. Solid, colored symbols are from this study (WFG – West Flower Garden Bank; VER – Veracruz, Mexico, BM – Boca de Medio, Cariaco Basin, TOR – Isla Tortuga, Cariaco Basin). Open, black symbols are previously published data (PR – Puerto Rico [*Kilbourne et al*., 2007], Belize [*Druffel*, 1980], Pickles Reef, Florida [*Druffel*, 1997], Rocks Reef, Florida [*Druffel and Linick*, 1978; *Druffel*, 1982], Cabo Albrohos, Brazil [*Druffel*, 1996], Bermuda [*Druffel*, 1989; *Druffel*, 1997]).

the Caribbean and Gulf of Mexico and high rates of air-sea exchange of CO_2. There is little to no Suess Effect apparent in the Gulf of Mexico $\Delta^{14}C$ values, which implies a relatively small amount of ^{14}C-depleted atmospheric CO_2 being mixed into the surface waters.

The amplitude of the post-bomb radiocarbon peak seen in the coral cores from Veracruz, Mexico and Flower Garden Banks are consistent with that seen in radiocarbon records from corals in the Florida Keys and Belize. The amplitude of the post-bomb radiocarbon peak in the Cariaco Basin coral cores is nearly 30‰ lower than found in the Veracruz and Flower Garden Banks cores. However, the amplitude closely resembles that from a coral core off the coast of Brazil. It is suggested that this is due to the difference in the atmospheric $\Delta^{14}C$ between the northern and southern hemispheres and the advection of surface water from the southern hemisphere into the south Caribbean and Cariaco Basin. The data do not support an upwelling-induced reduction, as prior to the introduction of nuclear weapons testing into the atmosphere the $\Delta^{14}C$ of the corals were not significantly different from each other. Following the post-bomb peak in coral $\Delta^{14}C$, the values have begun to decrease toward pre-bomb concentrations.

CHAPTER VI

CONCLUSIONS

SUMMARY

This dissertation sought to characterize natural climate variability in the Gulf of Mexico and Caribbean Sea over the last few centuries. Four primary research questions were addressed through the use of isotope geochemistry and coral growth analysis in an attempt to better understand the climate variability in this region. Below is a summary of the conclusions to these questions.

1. Using salinity and stable oxygen isotope values, can the relative contributions of the freshwater sources to the northern Gulf of Mexico be identified and determined? What is the open-ocean end member oxygen isotope value in the northern Gulf of Mexico?

Understanding the relative contributions of the fresh water sources is crucial to understanding the circulation and mixing on the shelf. Using river and shelf salinity-$\delta^{18}O$ data, this study has shown that the relative contributions of the major rivers flowing into the Texas-Louisiana shelf area, the Mississippi and Atchafalaya Rivers, have a large amount of seasonal and annual variability. In addition to variability in the percent contribution of each river, the oxygen isotope values of the rivers also vary seasonally because of changes in the $\delta^{18}O$ of the river sources. However, seawater samples analyzed for salinity and oxygen isotopic composition from two cruises along the Louisiana continental shelf during two different times of the year (August 2005 and May 2006) did indicate the ability to estimate the sources and relative contributions of the different freshwater sources on the northern Gulf of Mexico shelf. During the summer, it is suggested that there is a strong influence of Atchafalaya River water on the shelf. In contrast, during the spring, when river runoff is at its greatest, there is more of an influence of Mississippi River water.

From seawater samples collected at the Flower Garden Banks, the open ocean end member $\delta^{18}O$ value for the northern Gulf of Mexico shelf has been established to be

1.1‰. Knowledge of this value is important when trying to understand the mixing of fresh river water and open ocean seawater along the northern Gulf of Mexico shelf, and in particular the Texas-Louisiana shelf and slope.

2. Can a decadal pattern in coral growth rates of long-lived hermatypic corals collected at the Flower Garden Banks be identified? If so, is the pattern related to changes in local and regional climate? Does a relationship exist between changes in coral growth and broader atmospheric patterns such as the Pacific/North American pattern?

Coral growth (as annual extension rates) derived from long-lived corals at the Flower Garden Banks show a clear relationship to local and regional climate conditions, particularly winter air temperature (Figure 4-8). A clear feature seen in the new coral cores from this study, in addition to those from previous studies [*Hudson and Robbin*, 1980; *Dodge and Lang*, 1983; *Deslarzes*, 1992; *Slowey and Crowley*, 1995], is a significant decrease in the extension rate of the corals at the Flower Garden Banks in between 1956-57 and 1957-58. This event is correlated with an unusually cold winter in the southeastern U.S. and a positive phase of the PNA pattern. This event is shown to extend beyond just the southeast U.S., as a coral core from Veracruz, Mexico also shows a decrease in extension rate at 1957-58. This relationship suggests a correlation between the winter flow of the North American jet stream (associated with the PNA pattern) and coral growth at the Flower Garden Banks.

3. What is the reservoir age of surface ocean water in the Gulf of Mexico and Caribbean Sea based on coral radiocarbon measurements?

Estimates of the surface water radiocarbon concentration based on coral radiocarbon measurements yields an average reservoir age of 238 ± 10 years and ΔR of -32 ± 25 years for the Gulf of Mexico/Caribbean Sea. These values are close to previously published reservoir ages and ΔR ages for the Caribbean. The relatively small

ΔR ages compared to the marine 1-D model suggest the Marine04 curve is a reasonable approximation for this region for the modern oceanographic regime.

4. How does oceanic radiocarbon measured in coral skeletons differ between Gulf of Mexico and Caribbean sites? What are the possible mechanisms for these differences?

The amplitude of the post-bomb radiocarbon peak seen in the coral cores from Veracruz, Mexico and Flower Garden Banks is consistent with that seen in radiocarbon records from corals in the Florida Keys and Belize. The amplitude of the post-bomb radiocarbon peak in the Cariaco Basin coral cores is nearly 30‰ lower than that found in the Veracruz and Flower Garden Banks cores. However, the value closely resembles the amplitude from a coral core off the coast of Brazil. It is suggested that this is due to the difference in the atmospheric $\Delta^{14}C$ between the northern and southern hemispheres and that the advection of surface water from the southern hemisphere into the south Caribbean and Cariaco Basin. The data do not support an upwelling-induced reduction, as prior to the introduction of nuclear weapons testing into the atmosphere, the $\Delta^{14}C$ of the corals were not significantly different from each other. Following the peak in coral $\Delta^{14}C$, the values have begun to recover to pre-bomb concentrations.

IMPLICATIONS

The results reported in this dissertation provide valuable information for understanding the marine environment when using carbonate proxies to study and reconstruct past climate in the Gulf of Mexico and Caribbean. Understanding the seasonal and annual variability of the different sources of fresh water on the northern Gulf of Mexico continental shelf is important in the interpretation of results from stable isotope analyses on calcium carbonate materials from this region and the potential magnitude of past climate events. In a similar fashion, the knowledge of the $\Delta^{14}C$ marine reservoir age for the Gulf of Mexico and Caribbean is important in calibrating marine samples for paleographic studies. Previously, this value had not been established for the Gulf of Mexico.

REFERENCES

Adams, R. M., C. C. Chen, B. A. McCarl, and R. F. Weiher (1999), The economic consequences of ENSO events for agriculture, *Clim. Res.*, *13*, 165-172.

Antonov, J. I., R. A. Locarnini, T. P. Boyer, A. V. Mishonov, and H. E. Garcia (2006), *World Ocean Atlas 2005,* Volume 2, *Salinity*, *NOAA Atlas NESDIS 62*, edited by S. Levitus, 182 pp., U.S. Government Printing Office, Washington, D.C.

Astor, Y., F. Muller-Karger, and M. I. Scranton (2003), Seasonal and interannual variation in the hydrography of the Cariaco Basin: Implications for basin ventilation, *Cont. Shelf Res.*, *23*, 125-144.

Barber, R. T., and F. P. Chavez (1986), Ocean variability in relation to living resources during the 1982-83 El Niño, *Nature*, *319*, 279-285.

Barnes, D. J., and J. M. Lough (1989), The nature of skeletal density banding in scleractinian corals: Fine banding and seasonal patterns, *J. Exp. Mar. Biol. Ecol.*, *126*, 119-134.

Barnston, A. G., and R. E. Livezey (1987), Classification, seasonality, and persistence of low-frequency atmospheric circulation patterns, *Mon. Weather Rev.*, *115*, 1083-1126.

Boicourt, W. C., W. J. Wiseman, A. Valle-Levinson, and L. P. Atkinson (1998), The continental shelf of the southeastern United States and Gulf of Mexico: In the shadow of the Western Boundary Current, in *The Sea, Volume 11, The Global Coastal Ocean: Regional Studies and Syntheses*, edited by A. R. Robinson and K. Brink, pp. 135-182, Harvard University Press, Cambridge, MA.

Bowen, G. J., and B. Wilkinson (2002), Spatial distribution of $\delta^{18}O$ in meteoric precipitation, *Geology, 30*, 315-318.

Bratkovich, A., S. P. Dinnel, and D. A. Goolsby (1994), Variability and prediction of freshwater and nitrate fluxes for the Louisiana-Texas shelf: Mississippi and Atchafalaya River source functions, *Estuaries*, *17*, 766-778.

Braziunas, T. F., I. Y. Fung, and M. Stuiver (1995), The preindustrial atmospheric $^{14}CO_2$ latitudinal gradient as related to exchanges among atmospheric, oceanic, and terrestrial reservoirs, *Global Biogeochem. Cycles*, *9*, 565-584.

Broecker, W. S., and E. A. Olson (1961), Lamont radiocarbon measurements VIII, *Radiocarbon, 3*, 176-204.

Broecker, W. S., and T.-H. Peng (1982), *Tracers in the Sea*, 690 pp., Eldigio Press Lamont-Doherty Geological Observatory, Palisades, NY.

Buck, C. E., and P. G. Blackwell (2004), Formal statistical models for estimating radiocarbon calibration curves, *Radiocarbon*, *46*, 1093-1102.

Buddemeier, R.W. and R.A. Kinzie (1976), Coral growth, *Oceanographic and Marine Annual Reviews, 10*, 183-225.

Buddemeier, R. W., J. E. Maragos, and D. W. Knutson (1974), Radiographic studies of reef coral exoskeletons: Rates and patterns of coral growth, *J. Exp. Mar. Biol. Ecol.*, *14*, 179-200.

Carricart-Ganivet, J. P. (2004), Sea surface temperature and the growth of the West Atlantic reef-building coral *Montastraea annularis*, *J. Exp. Mar. Biol. Ecol.*, *302*, 249-260.

Centurioni, L. R., and P. P. Niiler (2003), On the surface currents of the Caribbean Sea, *Geophys. Res. Lett., 30*, 1279, doi:10.1029/2002GL016231.

Clark, I., and P. Fritz (1997), *Environmental Isotopes in Hydrogeology*, 352 pp., Lewis Publishers, Boca Raton, FL.

Cochrane, J. D., and F. J. Kelly (1986), Low-frequency circulation on the Texas-Louisiana continental shelf, *J. Geophys. Res.*, *91*, 645-659.

Cole, J.E., R.G. Fairbanks, and G.T. Shen (1993), Recent variability in the Southern Oscillation: Isotopic results from a Tarawa Atoll coral, *Science, 260*, 1790-1793.

Coplen, T. B., and C. Kendall (2000), Stable hydrogen and oxygen isotope ratios for selected sites of the U.S. Geological Survey's NASQAN and benchmark surface-water networks, *Open File Rep. 00-160*, 424 pp, U.S. Geol. Surv., Reston, VA.

Craig, H. (1961), Isotopic variations in meteoric waters, *Science, 133*, 1702-1703.

Craig, H., and L. I. Gordon (1965), Deuterium and oxygen-18 variations in the ocean and marine atmosphere, in *Proc. Stable Isotopes in Oceanographic Studies and Paleotemperatures*, 1965, Spoleto, Italy, edited by E. Tongiogi, pp. 9-130, V. Lishi e F., Pisa, Italy.

Crowley, T. J. (2000), Causes of climate change over the past 1000 years, *Science*, *289*, 270-277.

Cruz-Piñón, G., J. P. Carricart-Ganivet, and J. Espinoza-Avalos (2003), Monthly skeletal extension rates of the hermatypic corals *Montastraea annularis* and *Montastraea faveolata*: Biological and environmental controls, *Mar. Biol.*, *143*, 491-500.

Dansgaard, W. (1964), Stable isotopes in precipitation, *Tellus, 16*, 436-468.

Darnell, R. M., and R. E. Defenbaugh (1990), Gulf of Mexico: Environmental overview and history of environmental research, *American Zoologist*, *30*, 3-6.

Davis, J. C., I. D. Proctor, J. R. Southon, M. W. Caffee, D. W. Heikkinen, et al. (1990), LLNL/UC AMS facility and research program, *Nucl. Instrum. Methods Phys. Res., Sect. B, 52*, 269-272.

Deslarzes, K. (1992), Long-term monitoring of reef corals at the Flower Garden Banks (Northwest Gulf of Mexico): Reef coral population changes and historical incorporation of barium in *Montastrea annularis*, Ph.D. dissertation, 170 pp, Texas A&M University, College Station, TX.

Dickson, R. R., and J. Namias (1976), North American influences on the circulation and climate of the North Atlantic sector, *Mon. Weather Rev.*, *104*, 1255-1265.

Dodge, R. E., and J. C. Lang (1983), Environmental correlates of hermatypic coral (*Montastrea annularis*) growth on the East Flower Gardens Bank, northwest Gulf of Mexico, *Limnology and Oceanography, 28*, 228-240.

Dodge, R. E., and J. Thomson (1974), The natural radiochemical and growth records in contemporary hermatypic corals from the Atlantic and Caribbean, *Earth Planet. Sci. Lett.*, *23*, 313-322.

Dodge, R.E. and J.R. Vaisnys (1980), Skeletal growth chronologies of recent and fossil corals, in *Skeletal Growth of Aquatic Organisms*, edited by D. C. Rhoads and R. A. Lutz, pp. 493-517, Plenum Press, New York, NY.

Downton, M. W., and K. A. Miller (1993), The freeze risk to Florida citrus. Part II: Temperature variability and circulation patterns, *J. Clim.*, *6*, 364-372.

Druffel, E. R. M. (1980), Radiocarbon in annual coral rings of Belize and Florida, *Radiocarbon, 22*, 363-371.

Druffel, E. R. M. (1982), Banded corals: Changes in oceanic carbon-14 during the little ice age, *Science, 218*, 13-19.

Druffel, E. R. M. (1987), Bomb radiocarbon in the Pacific: Annual and seasonal timescale variations, *J. Mar. Res., 45*, 667-698.

Druffel, E. R. M. (1989), Decade time scale variability of ventilation in the North Atlantic: High-precision measurements of bomb radiocarbon in banded corals, *J. Geophys. Res., 94*, 3271-3285.

Druffel, E. R. M. (1996), Post-bomb radiocarbon records of surface corals from the Tropical Atlantic Ocean, *Radiocarbon, 38*, 563-572.

Druffel, E. R. M. (1997), Pulses of rapid ventilation in the North Atlantic surface ocean during the past century, *Science, 275*, 1454-1457.

Druffel, E. R. M., and T. W. Linick (1978), Radiocarbon in annual coral rings of Florida, *Geophys. Res. Lett., 5*, 913-916.

Druffel, E. R. M., S. Griffin, J. Hwang, T. Komada, S. R. Beaupre, et al. (2004), Variability of monthly radiocarbon during the 1760's in corals from the Galapagos Islands, *Radiocarbon*, *46*, 627-631.

Dunbar, R.B. and J.E. Cole (1993), Coral records of ocean-atmosphere variability: Report from the workshop on coral paleoclimate reconstruction, *NOAA Climate and Global Change Program Special Report No. 10,* 38 pp., University Corporation for Atmospheric Research, Boulder, CO.

Dunbar, R. B., G. M. Wellington, M. W. Colgan, and P. W. Glynn (1994), Eastern Pacific sea surface temperature since 1600AD: The $\delta^{18}O$ record of climate variability in Galapagos corals, *Paleoceanography*, *9*, 291-315.

Dunn, D. D. (1996), Trends in nutrient inflows to the Gulf of Mexico from streams draining the conterminous United States, 1972-93, *Water Resources Investigations Rep. 96-4113*, 68 pp, U.S. Geol. Surv., Austin, TX.

Dutton, A., B. H. Wilkinson, J. M. Welker, G. J. Bowen, and K. C. Lohmann (2005), Spatial distribution and seasonal variation in $^{18}O/^{16}O$ of modern precipitaiton and river water across the conterminous USA, *Hydrol. Process., 19*, 4121-4126.

Epstein, S., and T. Mayeda (1953), Variation of ^{18}O content of waters from natural sources, *Geochim. Cosmochim. Acta, 4*, 213-224.

Erhardt, R. D. J. (1990), Reconstructed annual minimum temperatures for the Gulf States, 1799-1988, *J. Clim.*, *3*, 678-684.

Fairbanks, R. G. (1982), The origin of continental shelf and slope water in the New York Bight and Gulf of Maine: Evidence from $H_2{}^{18}O/H_2{}^{16}O$ ratio measurements, *J. Geophys. Res., 87*, 5796-5808.

Fairbanks, R. G., and R. E. Dodge (1979), Annual periodicity of the $^{18}O/^{16}O$ and $^{13}C/^{12}C$ ratios in the coral *Montastrea annularis*, *Geochim. Cosmochim. Acta*, *43*, 1009-1020.

Fratantoni, D. M. (2001), North Atlantic surface circulation during the 1990's observed with satellite-tracked drifters, *J. Geophys. Res., 106*, 22,067-22,093.

Garzoli, S. L., and A. L. Gordon (1996), Origins and variability of the Benguela Current, *J. Geophys. Res., 101*, 897-906.

Gentry, D. K., S. Sosdian, E. L. Grossman, Y. Rosenthal, D. Hicks, et al. (2008), Stable isotope and Sr/Ca profiles from the marine gastropod *Conus ermineus*: Testing a multiproxy approach for inferring paleotemperature and paleosalinity, *Palaios*, *23*, 195-209.

Glynn, P. W. (1990), *Global Ecological Consequences of the 1982-83 El Niño Southern Oscillation*, 584 pp., Elsevier, New York, NY.

Goñi, M. A., R. C. Thunell, M. P. Woodworth, and F. E. Muller-Karger (2006), Changes in wind-driven upwelling during the last three centuries: Interocean teleconnections, *Geophys. Res. Lett.*, *33*, L15604, doi:10.1029/2006FL026415.

Gordon, A. L., R. F. Weiss, W. M. Smethie, and M. J. Warner (1992), Thermocline and intermediate water communication between the South Atlantic and Indian Oceans, *J. Geophys. Res.*, *97*, 7223-7240.

Gore, R. H. (1992), *The Gulf of Mexico*, 384 pp., Pineapple Press, Inc., Sarasota, FL.

Goreau, T. F. (1959), The ecology of Jamaican coral reefs. I. Species composition and zonation, *Ecology, 40*, 67-90.

Goreau, T. F., and N. I. Goreau (1959), The physiology of skeleton formation in corals. II. Calcium deposition by hermatypic corals under various conditions in the reef, *Biol. Bull.*, *117*, 239-250.

Grossman, E. L., and T. L. Ku (1986), Oxygen and carbon isotope fractionation in biogenic aragonite: Temperature effects, *Chemical Geology*, *59*, 59-74.

Grumet, N. S., N. J. Abram, J. W. Beck, R. B. Dunbar, M. K. Gagan, et al. (2004), Coral radiocarbon records of Indian Ocean water mass mixing and wind-induced upwelling along the coast of Sumatra, Indonesia, *J. Geophys. Res.*, *109*, C05003, doi:10.1029/2003JC002087.

Guilderson, T. P., and D. P. Schrag (1999), Reliability of coral isotope records from the western Pacific warm pool: A comparison using age-optimized records, *Paleoceanography, 14*, 457-464.

Guilderson, T. P., D. P. Schrag, M. Kashgarian, and J. Southon (1998), Radiocarbon variability in the western equatorial Pacific inferred from a high-resolution coral record from Nauru Island, *J. Geophys. Res.*, *103*, 24,641-24,650.

Guilderson, T. P., D. P. Schrag, E. Goddard, M. Kashgarian, G. M. Wellington, et al. (2000), Southwest subtropical Pacific surface water radiocarbon in a high-resolution coral record, *Radiocarbon*, *42*, 249-256.

Guilderson, T. P., J. E. Cole, and J. Southon (2005), Pre-bomb $\Delta^{14}C$ variability and the Suess Effect in Cariaco Basin surface waters as recorded in hermatypic corals, *Radiocarbon*, *47*, 57-65.

Hagman, D.K. and S.R. Gittings (1992), Coral bleaching on high latitude reefs at the Flower Garden Banks, NW Gulf of Mexico, in *Proceedings of the 7th International Coral Reef Symposium*, edited by R. H. Richmond, pp. 38-43, University of Guam Press, UOG Station, Guam.

Hardy J.W. and K.G. Henderson (2003), Cold front variability in the southern United States and the influence of atmospheric teleconnection patterns, *Physical Geography, 24*, 120-137.

Hastenrath, S. (1990), Diagnostics and prediction of anomalous river discharge in northern South America, *J. Clim., 3*, 1080-1096.

Helmle, K. P., K. E. Kohler, and R. E. Dodge (2002), Relative optical densitometry and the coral X-radiograph densitometry system: CoralXDS, paper presented at Int. Soc. Reef Studies 2002 European Meeting, Cambridge, England, Sept 4-7.

Highsmith, R. C. (1979), Coral growth rates and environmental control of density banding, *J. Exp. Mar. Biol. Ecol.*, *37*, 105-125.

Horta-Puga, G. (2003), Condition of selected reef sites in the Veracruz Reef System (Stony corals and algae), in *Status of Coral Reefs in the Western Atlantic: Results of Initial Surveys, Atlantic and Gulf Rapid Reef Assessment (AGRRA) Program*, edited by J. C. Lang, pp. 360-369, Smithsonian Institution, Washington, D.C.

Hudson, J.H. (1981), Growth rates in *Montastraea annularis*: A record of environmental change in Key Largo Coral Reef Marine Sanctuary, Florida, *Bulletin of Marine Science, 31*, 444-459.

Hudson, J. H., and D. M. Robbin (1980), Effects of drilling mud on the growth rate of the reef-building coral, *Montastrea annularis*, in *Marine Environmental Pollution, 1 Hydrocarbons*, edited by R. A. Geyer, pp. 455-470, Elsevier, New York, NY.

Hudson, J. H., E. A. Shinn, R. B. Halley, and B. Lidz (1976), Sclerochronology: A tool for interpreting past environments, *Geology*, *4*, 361-364.

Hughen, K. A., M. Baillie, E. Bard, J. W. Beck, C. J. H. Bertrand, et al. (2004a), Marine04 marine radiocarbon age calibration, 0-26 cal kyr bp, *Radiocarbon*, *46*, 1059-1086.

Hughen, K. A., J. Southon, C. J. H. Bertrand, B. Frantz, and P. Zermeno (2004b), Cariaco Basin calibration update: Revisions to calendar and ^{14}C chronologies for core PL07-58PC, *Radiocarbon*, *46*, 1161-1187.

Hurrell, J. W. (1995), Decadal trends in the North Atlantic Oscillation: Regional temperatures and precipitation, *Science*, *269*, 676-679.

Hurrell, J. W., Y. Kushnir, M. Visbeck, and G. Ottersen (2003), An Overview of the North Atlantic Oscillation, in *The North Atlantic Oscillation: Climate Significange and Environmental Impact, Geophys. Monogr. Ser.*, vol. 134, edited by J. W. Hurrell, et al., pp. 1-35, AGU, Washington, D.C.

Hyeong, K., and J. R. Lawrence (2003), Hydrology of the Gulf intra-coastal waterway in the San Bernard - Brazos river estuaries, Texas, USA: Oxygen isotopic ratio and salinity, *Geosciences Journal, 7*, 27-35.

Kalnay, E., M, Kanamitsu, R. Kistler, W. Collins, D. Deaven, et al. (1996), The NCEP/NCAR 40-year reanalysis project, *Bull. Am. Met. Soc.*, *77*, 437-470.

Kendall, C., and T. B. Coplen (2001), Distribution of oxygen-18 and deuterium in river waters across the United States, *Hydrological Processes*, *15*, 1363-1393.

Khim, B.-K., B.-K. Park, and H. I. Yoon (1997), Oxygen isotopic compositions of seawater in the Maxwell Bay of King George Island, West Antarctica, *Geosciences Journal*, *1*, 115-121.

Kilbourne, K. H., T. M. Quinn, T. P. Guilderson, R. S. Webb, and F. Taylor (2007), Decadal- to interannual-scale source water variations in the Caribbean Sea recorded by Puerto Rican coral radiocarbon, *Clim. Dyn., 29*, 51-62.

Kiladis, G. N., and H. F. Diaz (1986), An analysis of the 1877-78 ENSO episode and comparison with 1982-83, *Mon. Weather Rev.*, *114*, 1035-1047.

Knutson, D. W., R. W. Buddemeier, and S. V. Smith (1972), Coral chronometers: Seasonal growth bands in reef corals, *Science*, *177*, 270-272.

Lawrence, J. R. (1993), Hydrology of the Texas coastal bend estuaries 1987: $^{18}O/^{16}O$ and salinity, in *Proceedings of the Texas Academy of Science (96th Annual Meeting)*, pp. 133-139, Texas Academy of Science, Austin, TX.

Leathers, D.J., B. Yamal, and M.A. Palecki (1991), The Pacific/North America teleconnection pattern and United States climate. Part I: Regional temperature and precipitation associations, *J. Clim., 4*, 517-528.

Levin, I., and B. Kromer (1997), Twenty years of atmospheric $^{14}CO_2$ observations at Schauinsland Station, Germany, *Radiocarbon, 39*, 205-218.

Levin, I., B. Kromer, H. Schoch-Fischer, M. Bruns, M. Munnich, et al. (1985), 25 years of tropospheric ^{14}C observations in central Europe, *Radiocarbon*, *27*, 1-19.

Li, Y., W. D. Nowlin Jr., and R. O. Reid (1997), Mean hydrographic fields and their interannual variability over the Texas-Louisiana continental shelf in spring, summer, and fall, *J. Geophys. Res.*, *102*, 1027-1049.

Lighty, R. G., I. G. Macintyre, and R. Stuckenrath (1982), *Acropora Palmata* reef framework: A reliable indicator of sea level in the western Atlantic for the past 10,000 years, *Coral Reefs*, *1*, 125-130.

Linsley, B.K., L. Ren, R.B. Dunbar, and S.S. Howe (2000), El Niño Southern Oscillation (ENSO) and decadal-scale climate variability at 10°N in the eastern Pacific from

1893 to 1994: A coral-based reconstruction from the Clipperton Atoll, *Paleoceanography, 15*, 322-335.

Mahadevan, A. (2001), An analysis of bomb radiocarbon trends in the Pacific, *Mar. Chem., 73*, 273-290.

Manning, M. R., D. C. Lowe, W. H. Melhuish, R. J. Sparks, G. Wallace, et al. (1990), The use of radiocarbon measurements in atmospheric studies, *Radiocarbon*, *32*, 37-58.

McCormac, F. G., P. J. Reimer, A. G. Hogg, T. F. G. Higham, M. G. L. Baillie, et al. (2002), Calibration of the radiocarbon time scale for the southern hemisphere: AD 1850-950, *Radiocarbon*, *44*, 641-651.

McCormac, F. G., A. G. Hogg, P. G. Blackwell, C. E. Buck, T. F. G. Higham, et al. (2004), SHCal04 southern hemisphere calibration, 0-11.0 cal kyr BP, *Radiocarbon*, *46*, 1087-1092.

McPhee, J. (1989), *The Control of Nature*, 272 pp., Farrar, Straus, and Giroux, New York.

Molinari, R. L., and J. D. Cochrane (1972), The effect of topography on the Yucatan Current, in *Contributions on the Physical Oceanography of the Gulf of Mexico*, edited by L. R. A. Capurro and R. O. Reid, pp. 149-155, Houston, TX.

Molinari, R. L., and J. Morrison (1988), The separation of the Yucatan Current from the Campeche Bank and the intrusion of the Loop Current into the Gulf of Mexico, *J. Geophys. Res., 93*, 10,645-10,654.

Molinari, R. L., S. Baig, D. W. Behringer, G. A. Maul, and R. Legeckis (1977), Winter intrusions of the Loop Current, *Science*, *198*, 505-507.

Moody, C. L. (1967), Gulf of Mexico distributive province, *AAPG Bulletin*, *51*, 179-199.

Muller-Karger, F. E., and R. A. Castro (1994), Mesoscale processes affecting phytoplankton abundance in the southern Caribbean Sea, *Continental Shelf Research, 14*, 199-221.

Muller-Karger, F. E., C. R. McClain, and P. L. Richardson (1988), The dispersal of the Amazon's water, *Nature*, *333*, 56-59.

Muller-Karger, F., R. Varela, R. C. Thunell, M. I. Scranton, R. Bohrer, et al. (2001), Annual cycle of primary production in the Cariaco Basin: Response to upwelling and implications for vertical export, *J. Geophys. Res., 106*, 4527-4542.

Murray, S. P. (1997), An observational study of the Mississippi-Atchafalaya coastal plume, in *OCS Study MMS 98-0040*, edited by M. M. S. U.S. Department of the Interior, New Orleans, LA.

Niebauer, H. J. (1988), Effects of El Niño-Southern Oscillation and North Pacific weather patterns on interannual variability in the subarctic Bering Sea, *J. Geophys. Res.*, *93*, 5051-5068.

Nobre, P., and J. Shukla (1996), Variations of sea surface temperature, wind stress, and rainfall over the tropical Atlantic and South America, *J. Clim., 9*, 2464-2479.

Nowlin Jr., W. D., and C. A. Parker (1974), Effects of a cold-air outbreak on shelf waters of the Gulf of Mexico, *J. Phys. Oceanogr.*, *4*, 467-486.

Nozaki, Y., D.M. Rye, K.K. Turekian, and R.E Dodge (1978), 200-year record of C-13 and C-14 variations in a Bermuda coral, *Geophys. Res. Lett., 5*, 825-828.

Nydal, R. (2000), Radiocarbon in the ocean, *Radiocarbon, 42*, 81-98.

Nydal, R., and K. Lovseth (1983), Tracing bomb ^{14}C in the atmosphere 1962-1980, *J. Geophys. Res.*, *88*, 3621-3642.

Oeschger, H., U. Siegenthaler, U. Schotterer, and A. Gugelmann (1975), A box diffusion model to study the carbon dioxide exchange in nature, *Tellus*, *27*, 168-192.

Peterson, R. G., and L. Stramma (1991), Upper-level circulation in the South Atlantic Ocean, *Progress In Oceanography, 26*, 1-73.

Philander, S. G. H. (1990), *El Niño, La Niña, and the Southern Oscillation*, 293 pp., Academic Press, Inc., San Diego, CA.

Poore, R. Z., T. M. Quinn, and S. Verardo (2004), Century-scale movement of the Atlantic Intertropical Convergence Zone linked to solar variability, *Geophys. Res. Lett.*, *31*, L12214, doi:10.1029/2004GL019940.

Rabalais, N. N., R. E. Turner, and W. J. Wiseman (2001), Hypoxia in the Gulf of Mexico, *J. Environ. Qual.*, *30*, 320-329.

Reimer, P. J., M. Baillie, E. Bard, A. Bayliss, J. W. Beck, et al. (2004), IntCal04 terrestrial radiocarbon age calibration, 0-26 cal kyr BP, *Radiocarbon*, *46*, 1029-1058.

Rezak, R., and T. J. Bright (1981), Seafloor instability at East Flower Garden Bank, northwest Gulf of Mexico, *Geo-Marine Letters*, *1*, 97-103.

Richards, F. A. (1975), The Cariaco Basin (Trench), in *Oceanography and Marine Biology Annual Review*, edited by H. Barnes, pp. 11-67, George Allen and Unwin Ltd., London.

Roberts, H. H. (1998), Delta switching: Early responses to the Atchafalaya River diversion, *J. Coast. Res.*, *14*, 882-899.

Rodgers, K.B., D.P. Schrag, M.A. Cane, and N.H. Naik (2000), The bomb ^{14}C transient in the Pacific Ocean, *J. Geophys. Res., 105*, 8489-8512.

Rogers, J. C., and R. V. Rohli (1991), Florida citrus freezes and polar anticyclones in the Great Plains, *J. Clim.*, *4*, 1103-1113.

Ropelewski, C. F., and M. S. Halpert (1986), North American precipitation and temperature patterns associated with the El Niño/Southern Oscillation (ENSO), *Mon. Weather Rev.*, *114*, 2352-2362.

Ropelewski, C. F., and P. D. Jones (1987), An extension of the Tahiti-Darwin Southern Oscillation Index, *Mon. Weather Rev.*, *115*, 2161-2165.

Rowe, G. T. (2001), Seasonal hypoxia in the bottom water off the Mississippi River delta, *J. Environ. Qual.*, *30*, 281-290.

Rozanski, K., L. Araguas-Araguas, and R. Gonfiantini (1993), Isotopic Patterns in Modern Global Precipitation, in *Climate Change in Continental Isotopic Records, Geophys. Monogr. Ser.*, vol. 78, edited by P. K. Swart, et al., pp. 1-36, AGU, Washington, D.C.

Schubert, C. (1982), Origin of Cariaco Basin, southern Caribbean Sea, *Marine Geology, 47*, 345-360.

Slowey, N. C., and T. J. Crowley (1995), Interdecadal variability of Northern Hemisphere circulation recorded by Gulf of Mexico corals, *Geophys. Res. Lett.*, *22*, 2345-2348.

Smith, J., (2001), Temperature calibration of Gulf of Mexico corals, M.S. thesis, 52 pp., Texas A&M University, College Station, TX.

Sosdian, S., D. K. Gentry, C. H. Lear, E. L. Grossman, D. Hicks, et al. (2006), Strontium to calcium ratios in the marine gastropod *Conus ermineus*: Growth rate effects and temperature calibration, *Geochem. Geophys. Geosyst.*, *7*, Q11023, doi:11010.11029/12005GC001233.

Southon, J., M. Kashgarian, M. Fontugne, B. Metivier, and W. W. S. Yim (2002), Marine reservoir corrections for the Indian Ocean and southeast Asia, *Radiocarbon*, *44*, 167-180.

Stramma, L., and R. G. Peterson (1989), Geostrophic transport in the Benguela Current region, *J. Phys. Oceanography, 19*, 1440-1448.

Stuiver, M., and T. F. Braziunas (1993), Modeling atmospheric ^{14}C influences and ^{14}C ages of marine samples to 10,000 BC, *Radiocarbon, 35*, 137-189.

Stuiver, M., and H. A. Polach (1977), Discussion and reporting of ^{14}C data, *Radiocarbon, 19*, 355-363.

Stuiver, M., and P. D. Quay (1981), Atmospheric ^{14}C changes resulting from fossil fuel CO_2 release and cosmic ray flux variability, *Earth Planet. Sci. Lett., 53*, 349-362.

Stuiver, M., G. W. Pearson, and T. F. Braziunas (1986), Radiocarbon age calibration of marine samples back to 9000 Cal yr bp, *Radiocarbon*, *28*, 980-1021.

Stuiver, M., P. J. Reimer, and T. F. Braziunas (1998), High-precision radiocarbon age calibrations for terrestrial and marine samples, *Radiocarbon*, *40*, 1127-1151.

Sturges, W., and J. P. Blaha (1976), A western boundary current in the Gulf of Mexico, *Science, 192*, 367-369.

Sturges, W., and J. C. Evans (1983), On the variability of the Loop Current in the Gulf of Mexico, *J. Mar. Res., 41*, 639-653.

Suess, H. E. (1955), Radiocarbon concentration in modern wood, *Science, 122*, 415-417.

Surge, D. M., and K. C. Lohmann (2002), Temporal and spatial differences in salinity and water chemistry in SW Florida estuaries: Effects of human-impacted watersheds, *Estuaries, 25*, 393-408.

Sweeney, C., E. Gloor, A. R. Jacobson, R. M. Key, G. McKinley, et al. (2007), Constraining global air-sea gas exchange for CO_2 with recent bomb ^{14}C measurements, *Global Biogeochem. Cycles*, *21*, GB2015, doi:10.1029/ 2006GB002784.

Torgersen, T. (1979), Isotopic composition of river runoff on the U.S. East Coast: Evaluation of stable isotope versus salinity plots for coastal water mass identification, *J. Geophys. Res., 84*, 3773-3775.

Trenberth, K. E. (1984), Signal versus noise in the Southern Oscillation, *Mon. Weather Rev.*, *112*, 326-332.

Tunnell, J. W. (2007), Reef distribution, in *Coral Reefs of the Southern Gulf of Mexico*, edited by J. W. Tunnell, et al., pp. 14-22, Texas A&M University Press, College Station, TX.

Turner, R. E. (2003), Coastal ecosystems of the Gulf of Mexico and climate change, in *Integrated Assessment of the Climate Change Impacts on the Gulf Coast Region*, edited by Z. H. Ning, et al., pp. 85-103, Gulf Coast Climate Change Assessment Council and Louisiana State University, Baton Rouge, LA.

Urban, F. E., J. E. Cole, and J. T. Overpeck (2000), Influence of mean climate change on climate variability from a 155-year tropical Pacific coral record, *Nature*, *407*, 989-993.

Vega, A. J., R. V. Rohli, and K. G. Henderson (1998), The Gulf of Mexico mid-tropospheric resonse to El Niño and La Niña forcing, *Clim. Res.*, *10*, 115-125.

Vogel, J. S., J. R. Southon, and D. E. Nelson (1987), Catalyst and binder effects in the use of filamentous graphite for AMS, *Nucl. Instrum. Methods Phys. Res., Sect. B*, *29*, 50-56.

Wallace, J. M., and D. S. Gutzler (1981), Teleconnections in the geopotential height field during the Northern Hemisphere winter, *Mon. Weather Rev.*, *109*, 784-812.

Weber, J. N., E. W. White, and P. H. Weber (1975), Correlation of density banding in reef coral skeletons with environmental parameters: The basis for interpretation of chronological records preserved in the coralla of corals, *Paleobiology*, *1*, 137-149.

Williams, C. N., M. J. Menne, R. S. Vose, and D. R. Easterling (2007), United States Historical Climatology Network Monthly Temperature and Precipitation Data, http://cdiac.ornl.gov/epubs/ndp/ushcn/usa_monthly.html, Carbon Dioxide Information Analysis Center, Oak Ridge, TN.

Wilson, W. D., and W. E. Johns (1997), Velocity structure and transport in the Windward Islands Passages, *Deep Sea Research, 44*, 487-520.

Zerai, B. (2001), Spatial and temperature variability in the stable isotope compositions of waters of the Gulf of Mexico: Louisiana-Texas shelf and upper slope, M.S. thesis, 160 pp, University of Akron, Akron, OH.

APPENDIX A

Seawater oxygen isotope and salinity data.

Flower Garden Banks Samples

Bottle #	Date Collected	Bank	Collection Depth (ft)	Salinity	$\delta^{18}O$ (‰)
2	8/16/2004	WFG	79	36.314	1.10
3	5/24/2005	EFG	60	36.366	1.14
4	5/25/2005	WFG	70	36.278	1.09
5	10/19/2005	WFG	40	36.446	1.11
6	10/19/2005	WFG	30	36.464	1.11
7	7/26/2005	WFG	75	35.967	1.09
9	8/26/2005	EFG	70	36.079	1.07
10	8/25/2005	WFG	70	36.040	1.10
12	2/23/2005	WFG	80	36.345	1.13
14	2/23/2005	EFG	70	36.461	1.10
16	9/4/2004	WFG	80	36.360	1.11
18	5/11/2005	EFG	67	35.997	1.05
19	5/10/2005	WFG	90	35.705	1.03
20	5/10/2005	WFG	90	35.736	1.04
21	10/19/2005	WFG	surface	36.448	1.12
22	10/18/2005	EFG	30	36.073	1.07
23	10/18/2005	EFG	40	36.405	1.10
24	10/19/2005	WFG	60	36.510	1.08
25	10/19/2005	WFG	50	36.489	1.15
26	10/19/2005	WFG	70	36.507	1.11
29	10/19/2005	WFG	20	36.453	1.15
30	10/19/2005	WFG	10	36.485	1.15
31	10/11/2005	WFG	80	36.550	1.15
32	10/11/2005	WFG	80	36.509	1.16
35	8/9/2005	EFG	70	35.844	1.05
37	10/18/2005	EFG	surface	36.396	1.10
38	10/18/2005	EFG	60	36.219	1.08
39	10/18/2005	EFG	20	36.392	1.09
40	10/18/2005	EFG	50	36.413	1.10
41	5/14/2005	WFG	80	35.733	1.09
43	9/20/2004	EFG	70	36.181	1.08
46	5/14/2005	EFG	60	36.107	1.04
51	11/20/2004	WFG	80	35.905	1.10
100	5/13/2006	WFG	surface	35.758	1.02
101	5/13/2006	WFG	surface	35.759	0.99
102	5/13/2006	WFG	80	35.952	1.04
103	5/13/2006	WFG	80	35.952	1.02

Bottle #	Date Collected	Bank	Collection Depth (ft)	Salinity	$\delta^{18}O$ (‰)
104	5/13/2006	WFG	70	35.924	1.04
105	5/13/2006	WFG	60	35.799	0.96
106	5/13/2006	WFG	40	35.759	1.02
107	5/13/2006	WFG	20	35.754	1.00
108	5/13/2006	WFG	30	35.758	0.99
109	5/13/2006	WFG	10	35.758	1.01
110	5/17/2006	EFG	69	36.161	1.06
111	5/17/2006	EFG	69	36.159	1.05
112	5/18/2006	WFG	76	36.107	1.08
113	5/18/2006	WFG	76	36.097	1.05
114	5/13/2006	EFG	surface	35.819	1.02
115	5/13/2006	EFG	60	35.853	1.01
117	5/13/2006	EFG	20	35.808	1.01
118	5/13/2006	EFG	10	35.819	0.99
119	5/13/2006	EFG	40	35.836	1.01
120	5/13/2006	EFG	60	35.848	1.13
121	5/13/2006	EFG	50	35.847	1.12
122	5/13/2006	EFG	surface	35.818	1.02
123	5/13/2006	EFG	30	35.816	1.01
125	7/7/2006	EFG	73	36.460	1.20
126	7/8/2006	EFG	95	36.529	1.20
KD0	11/14/2005	EFG	surface	36.548	1.19
KD1	11/14/2005	EFG	surface	36.344	1.20
KD2	11/14/2005	EFG	70	36.414	1.21
KD3	11/14/2005	EFG	70	36.617	1.19

R. Long Cruise – May 2006

Bottle #	Latitude	Longitude	Collection Depth (ft)	Salinity	$\delta^{18}O$ (‰)
51	28.76	-89.59	5	34.092	0.72
52	28.76	-89.59	78	36.395	1.03
53	28.84	-89.51	2	27.122	-0.80
54	28.84	-89.51	48	36.337	1.09
55	28.95	-89.63	5	34.654	0.76
56	28.95	-89.63	40	36.335	1.12
57	28.96	-89.49	4	26.535	-0.88
58	28.96	-89.49	23	36.342	1.08
59	29.10	-89.66	2	27.718	-0.64
60	29.10	-89.66	15	34.351	0.73
61	29.11	-89.54	2	24.526	-1.31
62	29.11	-89.54	10	31.394	0.10
63	29.17	-89.63	2	26.374	-0.94

Bottle #	Latitude	Longitude	Collection Depth (ft)	Salinity	$\delta^{18}O$ (‰)
64	29.17	-89.63	9	32.778	0.39
65	29.14	-89.76	2	27.551	-0.52
66	29.14	-89.76	18	35.813	1.01
67	28.83	-89.74	2	30.471	0.00
68	28.83	-89.74	64	36.392	1.03
69	28.96	-89.74	2	29.025	-0.28
70	28.96	-89.74	45	36.311	1.07
71	29.06	-89.81	2	27.654	-0.54
72	29.06	-89.81	27	36.157	1.03
73	28.96	-90.14	2	30.519	0.01
74	28.96	-90.14	19	36.065	1.06
75	28.95	-90.41	2	29.437	-0.22
76	28.95	-90.41	11	34.918	0.71
77	28.88	-90.38	2	30.097	-0.10
78	28.88	-90.38	17	35.900	0.95
79	28.74	-90.41	4	34.844	0.75
80	28.74	-90.41	17	36.015	0.99
81	28.56	-90.41	36	36.385	1.02
82	28.56	-90.41	2	34.451	0.68
83	28.72	-90.55	2	32.306	0.30
84	28.72	-90.55	15	35.969	0.98
85	28.84	-90.55	2	29.675	-0.23
86	28.84	-90.55	17	35.789	0.97
88	28.96	-90.55	10	34.467	0.71
89	28.84	-90.68	3	30.053	-0.06
90	28.84	-90.68	16	35.753	0.96
91	28.72	-90.68	3	31.424	0.05
92	28.72	-90.68	14	35.540	0.91
93	28.88	-91.73	2	35.889	1.01
94	28.88	-91.73	20	36.333	1.07
95	28.84	-91.92	2	36.237	1.08
96	28.84	-91.92	25	36.285	1.02
97	28.90	-92.07	2	35.878	1.05
98	28.90	-92.07	24	36.133	1.06

S. DiMarco Cruise – August 2005

Bottle #	Latitude	Longitude	Collection Depth (ft)	Salinity	$\delta^{18}O$ (‰)
261	29.63	-93.64	surface	28.437	-0.07
257	29.44	-93.63	surface	28.343	-0.10
141	29.3	-93.7	surface	29.803	0.14
367	29.12	-93.7	surface	30.225	0.19

Bottle #	Latitude	Longitude	Collection Depth (ft)	Salinity	$\delta^{18}O$ (‰)
323	29.12	-93.5	surface	30.313	0.18
72	29.3	-93.5	surface	28.915	-0.01
214	29.44	-93.5	surface	28.092	-0.10
223	29.66	-93.5	surface	27.771	-0.12
225	29.65	-93.28	surface	27.684	-0.13
41	29.49	-93.27	surface	27.697	-0.15
164	29.3	-93.3	surface	28.806	-0.01
288	29.11	-93.3	surface	29.858	0.13
207	29.12	-93.11	surface	31.549	0.31
190	29.3	-93.09	surface	29.416	0.06
218	29.58	-92.9	surface	27.842	-0.10
26	29.5	-92.9	surface	27.750	-0.08
71	29.3	-92.9	surface	29.723	0.05
311	29.16	-92.9	surface	28.822	0.25
275	29.1	-92.8	surface	30.581	0.23
217	29.2	-92.7	surface	29.963	0.11
138	29.3	-92.63	surface	29.388	0.040
133	29.4	-92.6	surface	29.117	0.00
137	29.3	-92.46	surface	28.653	-0.11
267	29.06	-92.65	surface	30.403	0.12
269	28.92	-92.46	surface	30.221	0.14
343	29.06	-92.37	surface	28.910	-0.05
385	29.17	-92.33	surface	26.716	-0.06
178	29.14	-92.11	surface	26.415	-0.36
63	29.02	-92.17	surface	29.904	0.10
146	28.93	-92.23	surface	30.214	0.11
220	28.8	-92.14	surface	29.568	0.21
144	28.9	-92.07	surface	29.715	0.06
263	29	-92	surface	27.847	-0.17
201	29.12	-91.91	surface	25.805	-0.45
34	29.06	-91.77	surface	25.220	-0.54
184	28.94	-91.87	surface	29.674	0.06
202	28.88	-91.73	surface	27.141	-0.37
388	29.01	-91.65	surface	24.744	-0.61
183	28.98	-91.52	surface	25.137	-0.58
169	28.81	-91.5	surface	29.005	-0.04
78	28.7	-91.35	surface	31.001	0.23
376	28.67	-91.25	surface	29.251	0.13
764G	28.64	-91.12	surface	28.690	-0.13
291	28.58	-90.78	surface	29.977	0.20
209	28.6	-90.68	surface	29.977	0.08
387	28.62	-90.56	surface	29.742	0.25
65	28.69	-90.49	surface	30.849	0.19
37	28.74	-90.41	surface	30.187	0.25

Bottle #	Latitude	Longitude	Collection Depth (ft)	Salinity	$\delta^{18}O$ (‰)
259	28.87	-90.37	surface	30.695	0.23
143	28.88	-90.32	surface	25.172	-0.67
290	28.98	-90.32	surface	23.756	-0.95
122	28.98	-90.41	surface	24.427	-0.84
43	28.96	-90.55	surface	26.605	-0.43
219	28.84	-90.56	surface	25.124	-0.65
216	28.72	-90.68	surface	28.278	-0.10
280	28.84	-90.78	surface	28.141	-0.10
278	28.72	-90.9	surface	28.883	0.02
265	28.8	-91	surface	27.283	0.01
44	28.75	-91.12	surface	29.070	-0.15
381	28.83	-91.25	surface	27.749	-0.21
123	28.87	-91.3	surface	27.749	-0.29
306	28.9	-91.5	surface	25.278	-0.52
208	28.9	-91.6	surface	25.522	-0.53
355	28.95	-91.8	surface	27.790	-0.23
210	28.95	-91.95	surface	29.691	0.14
282	28.95	-91.95	surface	29.451	0.09
200	28.95	-91.95	surface	29.225	0.04
250	28.95	-91.95	surface	28.989	-0.06

APPENDIX B

Extension rates (mm/year) of *Montastraea faveolata* corals from the Flower Garden Banks and Veracruz, Mexico. EFG1 and EFG2 are from the East Flower Garden Bank, Gulf of Mexico; WFG1 is from the West Flower Garden Bank, Gulf of Mexico; VC5 is from Chopas Reef, Veracruz, Mexico; VC7 is from Santaguillo Reef, Veracruz, Mexico.

Year	EFG1	EFG2	WFG1	VC5	VC7
2004	7.67	8.16	7.12		
2003	9.99	11.32	7.12		
2002	9.88	8.68	7.05		
2001	10.91	8.95	7.31		
2000	10.01	10.53	8.42		
1999	11.04	8.95	8.21		
1998	9.22	9.21	6.03		
1997	13.51	11.32	8.38		
1996	11.17	9.21	7.26		
1995	9.09	8.95	6.26		
1994	9.87	11.58	9.02		
1993	9.74	9.47	6.41		
1992	11.70	10.26	8.29		
1991	10.66	9.21	6.97		
1990	10.90	8.16	7.88	7.58	7.42
1989	11.95	10.26	7.82	6.79	7.83
1988	10.91	10.79	7.69	6.79	8.17
1987	12.07	8.68	7.76	5.75	7.33
1986	7.80	9.21	6.99	10.67	9.08
1985	10.13	9.21	6.79	8.50	6.67
1984	8.04	7.63	6.35	9.33	8.08
1983	13.66	10.00	7.95	8.58	8.50
1982	10.01	9.21	7.95	11.00	8.75
1981	8.05	9.47	7.12	9.67	8.00
1980	10.13	8.16	6.15	9.17	7.17
1979	11.16	8.16	5.83	9.33	8.92
1978	9.10	10.00	7.56	9.17	8.75
1977	8.32	9.47	7.31	7.00	6.67
1976	10.51	10.00	6.79	9.83	6.83
1975	8.97	8.16	5.51	8.67	7.83
1974	9.09	8.68	5.00	10.08	8.17
1973	9.09	7.63	5.96	7.75	7.75
1972	11.65	12.63	8.53	8.61	7.58

Year	EFG1	EFG2	WFG1	VC5	VC7
1971	9.09	9.47	6.41	9.60	8.92
1970	8.82	7.63	6.22	8.29	6.67
1969	8.57	8.42	5.06	8.87	9.25
1968	11.04	8.95	7.63	9.30	7.92
1967	11.17	9.21	8.50	8.67	6.33
1966	8.05	10.00	5.73	7.13	8.56
1965	9.48	8.68	7.05	8.50	9.94
1964	9.88	9.21	7.24	8.00	9.56
1963	8.32	8.68	8.40	9.08	10.39
1962	7.93	9.47	4.87	9.75	9.67
1961	9.88	8.16	6.41	8.33	7.92
1960	8.06	6.32	4.49	9.08	7.44
1959	10.14	10.53	8.97	8.75	7.11
1958	7.95	7.63	5.13	10.39	8.06
1957	12.71	10.92	8.21	11.00	11.00
1956	11.96	11.97	10.06	8.42	8.90
1955	11.57	11.05	8.97	8.42	10.00
1954	12.62	12.37	9.49	10.00	9.41
1953	11.31	10.26	7.82	10.83	11.61
1952	10.27	11.05	7.88	8.67	8.39
1951	12.61	7.75	7.50	9.92	10.08
1950	11.18	11.00	8.50	6.00	9.66
1949	11.68	9.75	8.68	7.00	10.17
1948	13.51	12.00	9.36	7.00	10.00
1947	8.70	9.25	7.24	7.17	8.56
1946	11.67	8.50	8.53	8.75	10.42
1945	10.65	10.00	8.78	6.83	9.49
1944	12.60	9.00	9.17	6.50	9.49
1943	12.59	10.75	8.78	7.92	8.81
1942	10.91	9.00	8.46	7.08	8.81
1941	9.49	11.75	8.08	6.56	10.00
1940	11.42	10.00	9.49	6.94	8.73
1939	11.03		9.10	7.94	9.66
1938	10.52		8.65	7.06	11.10
1937	12.86		8.40	6.33	9.49
1936	8.70		8.33	7.08	9.58
1935	11.29		8.91	8.25	10.93
1934	12.99		7.69	7.00	9.15
1933	9.48		8.14	6.89	9.75
1932	11.16		7.44	9.00	10.76
1931	8.83		7.76	6.67	8.67
1930	8.96		6.67	6.67	8.50

Year	EFG1	EFG2	WFG1	VC5	VC7
1929	10.00		7.76	8.00	9.33
1928	11.17		8.01	7.83	10.33
1927	9.48		7.05	6.50	9.25
1926	10.78		9.02	5.75	9.50
1925	10.39		9.55	6.94	9.17
1924	10.65		9.36	6.72	8.83
1923	9.22		7.82	8.17	10.00
1922	10.13		7.95	9.58	10.67
1921	9.88		8.53	7.42	10.39
1920	9.09		7.18	7.50	10.42
1919	9.09		9.81	9.25	11.17
1918	9.62		7.82	7.50	10.08
1917	9.30		10.51	6.67	9.42
1916	11.04		10.19	7.75	11.17
1915	8.44		8.72	7.58	9.25
1914	8.96		8.38	8.00	9.58
1913	8.57		9.08	7.00	11.08
1912	8.96		7.87	5.17	8.67
1911	8.70		9.22	10.67	8.08
1910	10.00		6.81	8.78	9.92
1909	9.74		9.30	9.17	7.58
1908	10.77		8.80	9.42	9.25
1907	10.91		10.46	8.83	9.08
1906	9.88		7.28	9.50	7.92
1905	10.26		8.38	6.92	9.08
1904	9.09		9.22	8.50	9.42
1903	12.86		9.87	7.75	8.83
1902	10.66		7.01	7.11	8.58
1901	11.05		8.31	9.50	9.42
1900	10.39		8.57	7.00	10.13
1899	11.18		8.06	9.50	7.38
1898	10.65		8.44	8.67	10.21
1897	13.25		9.88	8.25	8.22
1896	10.65		7.86	8.42	9.33
1895	10.79		8.90	9.17	9.25
1894	12.09		10.46	8.33	10.42
1893	10.09		7.99	9.25	11.25
1892	10.87		8.52	8.83	8.50
1891	11.57		9.02	8.00	12.00
1890	11.39		7.32	9.42	7.42
1889	8.54		7.67	7.92	9.75
1888	10.28		8.38	8.50	9.17

Year	EFG1	EFG2	WFG1	VC5	VC7
1887	8.69		7.53	9.75	10.83
1886	10.12		9.78	9.08	10.08
1885	8.29		5.58	8.42	10.58
1884	11.05		9.52	9.17	9.00
1883	10.26		5.76	8.75	9.08
1882	10.86		7.55	8.75	9.42
1881	7.66		8.21	8.50	7.50
1880	11.95		7.96	9.75	7.83
1879	7.90		6.70	9.67	7.92
1878	6.76		6.48	10.75	9.00
1877	10.64		7.39	8.39	8.83
1876	9.62		8.60	7.22	10.25
1875	10.13		7.52	8.78	9.08
1874	11.15		8.80	9.78	7.75
1873	10.53		7.88	6.92	8.92
1872	9.86		7.56	7.25	8.58
1871	13.52		10.33		9.00
1870	10.91		8.55		7.75
1869	9.48		8.68		9.75
1868	11.22		7.83		7.58
1867	8.95		8.49		6.91
1866	9.48		9.74		8.32
1865	12.22		7.24		7.52
1864	11.02		8.95		8.57
1863	12.73		7.80		8.39
1862	12.48		9.34		7.80
1861	8.81		9.21		7.03
1860	10.03		8.16		6.78
1859	13.54		9.67		6.95
1858	12.21		9.28		6.19
1857	12.31		8.88		6.69
1856	9.89		7.24		5.76
1855	9.61		8.36		6.78
1854	11.03		9.47		5.17
1853	11.30		8.68		10.68
1852	9.63		9.14		6.19
1851	10.17		8.90		8.05
1850	10.89		8.88		8.90
1849	12.47		8.29		9.83
1848	11.06		9.21		8.90
1847	8.96		7.83		8.22
1846	12.34		8.16		7.20

Year	EFG1	EFG2	WFG1	VC5	VC7
1845	13.37		7.37		9.49
1844	11.44		7.89		9.10
1843	8.83				10.68
1842	12.62				8.31
1841	9.59				10.00
1840	13.88				8.08
1839	10.26				6.48
1838					8.91
1837					10.16
1836					8.91
1835					9.89
1834					9.34
1833					6.50
1832					8.52
1831					8.52
1830					9.78
1829					9.02
1828					11.39
1827					10.16
1826					7.13
1825					9.92
1824					10.82
1823					9.56
1822					6.56
1821					10.41
1820					10.00
1819					8.52
1818					9.43
1817					11.80
1816					11.16
1815					12.31
1814					7.96
1813					9.00
1812					9.58
1811					8.92
1810					9.83
1809					8.58
1808					10.42
1807					8.94
1806					6.78
1805					10.06
1804					11.33

Year	EFG1	EFG2	WFG1	VC5	VC7
1803					9.33
1802					10.25
1801					9.83
1800					7.83
1799					12.00
1798					10.17
1797					10.17
1796					9.83
1795					9.17
1794					11.42
1793					9.33
1792					9.11
1791					10.72
1790					9.38
1789					13.46
1788					10.61
1787					9.06
1786					12.17
1785					10.00

APPENDIX C

Coral Radiocarbon data.

Site	Year	^{14}C age (conventional)	+/-	Fraction Modern (absolute)	+/-	$\Delta^{14}C$ (‰) (age-corrected)	+/-
West Flower Gardens							
	1989	>Modern		1.1039	0.0036	103.9	3.6
	1987	>Modern		1.1106	0.0039	110.6	3.9
	1985	>Modern		1.1184	0.0037	118.4	3.7
	1983	>Modern		1.1261	0.0037	126.1	3.7
	1981	>Modern		1.1270	0.0037	127.0	3.7
	1979	>Modern		1.1326	0.0037	132.6	3.7
	1977	>Modern		1.1463	0.0035	146.3	3.5
	1975	>Modern		1.1584	0.0035	158.4	3.5
	1973	>Modern		1.1490	0.0035	149.0	3.5
	1971	>Modern		1.1521	0.0035	152.1	3.5
	1969	>Modern		1.1362	0.0032	136.2	3.2
	1967	>Modern		1.1053	0.0031	105.3	3.1
	1965	>Modern		1.0772	0.0032	77.2	3.2
	1963	>Modern		1.0168	0.0031	16.8	3.1
	1961	135	25	0.9818	0.0029	-18.2	2.9
	1959	285	25	0.9644	0.0029	-35.6	2.9
	1957	370	25	0.9544	0.0026	-45.6	2.6
	1955	450	30	0.9450	0.0031	-55.0	3.1
	1954	430	25	0.9476	0.0028	-52.4	2.8
	1953	445	30	0.9460	0.0031	-54.0	3.1
	1952	405	25	0.9506	0.0027	-49.4	2.7
	1951	415	25	0.9495	0.0028	-50.5	2.8
	1949	500	25	0.9399	0.0028	-60.1	2.8
	1948	440	30	0.9472	0.0031	-52.8	3.1
	1947	435	35	0.9475	0.0036	-52.5	3.6
	1946	435	30	0.9480	0.0032	-52.0	3.2
	1944	405	25	0.9516	0.0028	-48.4	2.8
Veracruz, Mexico							
	1980	>Modern		1.1470	0.0041	147.0	4.1
	1978	>Modern		1.1653	0.0044	165.3	4.4
	1976	>Modern		1.1594	0.0041	159.4	4.1
	1974	>Modern		1.1578	0.0041	157.8	4.1

Site	Year	^{14}C age (conventional)	+/-	Fraction Modern (absolute)	+/-	Δ^{14}C (‰) (age-corrected)	+/-
	1972	>Modern		1.1446	0.0041	144.6	4.1
	1970	>Modern		1.1376	0.0047	137.6	4.7
	1968	>Modern		1.1306	0.0040	130.6	4.0
	1966	>Modern		1.0982	0.0039	98.2	3.9
	1964	>Modern		1.0475	0.0041	47.5	4.1
	1962	>Modern		1.0026	0.0035	2.6	3.5
	1960	95	30	0.9871	0.0035	-12.9	3.5
	1958	335	30	0.9586	0.0035	-41.4	3.5
	1955	470	30	0.9428	0.0032	-57.2	3.2
	1954	415	30	0.9495	0.0033	-50.5	3.3
	1953	385	35	0.9531	0.0036	-46.9	3.6
	1952	445	35	0.9458	0.0036	-54.2	3.6
	1951	365	30	0.9554	0.0033	-44.6	3.3
	1950	440	30	0.9469	0.0032	-53.1	3.2
	1949	415	30	0.9500	0.0033	-50.0	3.3
	1948	425	30	0.9486	0.0035	-51.4	3.5
	1947	475	30	0.9432	0.0032	-56.8	3.2
	1946	440	30	0.9473	0.0032	-52.7	3.2
	1941	410	30	0.9513	0.0031	-48.7	3.1
	1936	420	30	0.9505	0.0030	-49.5	3.0
	1931	430	35	0.9499	0.0041	-50.1	4.1
	1926	410	30	0.9531	0.0035	-46.9	3.5
	1921	430	30	0.9510	0.0033	-49.0	3.3
	1916	360	35	0.9604	0.0040	-39.6	4.0
	1911	435	30	0.9521	0.0034	-47.9	3.4
	1906	365	35	0.9608	0.0041	-39.2	4.1
	1901	420	30	0.9550	0.0034	-45.0	3.4
	1896	415	30	0.9561	0.0034	-43.9	3.4
	1891	440	30	0.9536	0.0033	-46.4	3.3
	1886	495	30	0.9476	0.0033	-52.4	3.3
	1881	405	35	0.9587	0.0036	-41.3	3.6
	1886	510	30	0.9472	0.0033	-52.8	3.3
Boca de Medio							
	1997	>Modern		1.0802	0.0033	80.2	3.3
	1995	>Modern		1.0887	0.0041	88.7	4.1
	1993	>Modern		1.0933	0.0038	93.3	3.8
	1991	>Modern		1.0976	0.0034	97.6	3.4
	1989	>Modern		1.1015	0.0034	101.5	3.4

Site	Year	^{14}C age (conventional)	+/-	Fraction Modern (absolute)	+/-	Δ^{14}C (‰) (age-corrected)	+/-
	1987	>Modern		1.1046	0.0034	104.6	3.4
	1985	>Modern		1.1055	0.0034	105.5	3.4
	1983	>Modern		1.1125	0.0034	112.5	3.4
	1981	>Modern		1.1114	0.0034	111.4	3.4
	1979	>Modern		1.1190	0.0034	119.0	3.4
	1977	>Modern		1.1128	0.0040	112.8	4.0
	1975	>Modern		1.1243	0.0038	124.3	3.8
	1973	>Modern		1.1270	0.0034	127.0	3.4
	1971	>Modern		1.1135	0.0034	113.5	3.4
	1969	>Modern		1.0982	0.0040	98.2	4.0
	1967	>Modern		1.0750	0.0032	75.0	3.2
	1965	>Modern		1.0499	0.0035	49.9	3.5
	1963	>Modern		1.0081	0.0030	8.1	3.0
	1961	185	30	0.9762	0.0036	-23.8	3.6
	1959	260	25	0.9669	0.0029	-33.1	2.9
	1957	390	25	0.9517	0.0028	-48.3	2.8
	1955	475	25	0.9421	0.0026	-57.9	2.6
	1954	400	25	0.9510	0.0028	-49.0	2.8
	1953	445	30	0.9458	0.0034	-54.2	3.4
	1952	430	35	0.9478	0.0039	-52.2	3.9
	1951	400	35	0.9516	0.0037	-48.4	3.7
	1950	435	30	0.9475	0.0031	-52.5	3.1
	1949	440	30	0.9471	0.0031	-52.9	3.1
	1948	445	25	0.9466	0.0029	-53.4	2.9
	1947	470	30	0.9433	0.0030	-56.7	3.0
	1946	430	30	0.9483	0.0032	-51.7	3.2
	1944	425	25	0.9494	0.0029	-50.6	2.9
Isla Tortuga							
	1995	>Modern		1.0863	0.0038	86.3	3.8
	1993	>Modern		1.0948	0.0033	94.8	3.3
	1991	>Modern		1.0889	0.0037	88.9	3.7
	1989	>Modern		1.0909	0.0037	90.9	3.7
	1987	>Modern		1.1153	0.0038	115.3	3.8
	1985	>Modern		1.1091	0.0038	109.1	3.8
	1983	>Modern		1.1056	0.0037	105.6	3.7
	1981	>Modern		1.1189	0.0031	118.9	3.1
	1979	>Modern		1.1225	0.0042	122.5	4.2
	1977	>Modern		1.1256	0.0034	125.6	3.4

Site	Year	^{14}C age (conventional)	+/-	Fraction Modern (absolute)	+/-	$\Delta^{14}C$ (‰) (age-corrected)	+/-
	1975	>Modern		1.1272	0.0038	127.2	3.8
	1973	>Modern		1.1074	0.0031	107.4	3.1
	1971	>Modern		1.0980	0.0034	98.0	3.4
	1969	>Modern		1.0903	0.0029	90.3	2.9
	1968	>Modern		1.0690	0.0032	69.0	3.2
	1967	>Modern		1.0631	0.0043	63.1	4.3
	1967	>Modern		1.0600	0.0031	60.0	3.1
	1966	>Modern		1.0435	0.0031	43.5	3.1
	1965	>Modern		1.0178	0.0028	17.8	2.8
	1965	>Modern		1.0360	0.0031	36.0	3.1
	1965	>Modern		1.0320	0.0037	32.0	3.7
	1964	>Modern		1.0186	0.0031	18.6	3.1
	1964	Modern		1.0105	0.0031	10.5	3.1
	1963	Modern		0.9921	0.0033	-7.9	3.3
	1963	Modern		0.9983	0.0026	-1.7	2.6
	1963	Modern		0.9929	0.0033	-7.1	3.3
	1963	Modern		0.9970	0.0030	-3.0	3.0
	1962	175	30	0.9768	0.0036	-23.2	3.6
	1962	Modern		0.9968	0.0028	-3.2	2.8
	1961	160	25	0.9790	0.0027	-21.0	2.7
	1961	115	25	0.9849	0.0030	-15.1	3.0
	1960	235	25	0.9706	0.0029	-29.4	2.9
	1959	240	25	0.9698	0.0029	-30.2	2.9
	1959	235	25	0.9704	0.0028	-29.6	2.8
	1958	300	25	0.9624	0.0029	-37.6	2.9
	1958	310	25	0.9618	0.0029	-38.2	2.9
	1957	340	30	0.9580	0.0036	-42.0	3.6
	1957	355	30	0.9566	0.0035	-43.4	3.5
	1952	440	25	0.9468	0.0024	-53.2	2.4
	1951	440	25	0.9468	0.0026	-53.2	2.6
	1950	460	25	0.9443	0.0028	-55.7	2.8
	1948	435	30	0.9475	0.0030	-52.5	3.0
	1947	425	25	0.9486	0.0029	-51.4	2.9
	1946	465	25	0.9440	0.0029	-56.0	2.9

VITA

Name: Amy Jo Wagner

Address: Department of Oceanography, Texas A&M University, College Station, Texas 77843-3146

Email Address: amywagner98@gmail.com

Education: B.S., Marine Sciences, Texas A&M University at Galveston, 1998
M.S., Oceanography, Texas A&M University, 2002
Ph.D., Oceanography, Texas A&M University, 2009